National Library of Canada
Acquisitions and Bibliographic Services Branch
395 Wellington Street
Ottawa, Ontario
K1A 0N4

Bibliothèque nationale du Canada
Direction des acquisitions et des services bibliographiques
395, rue Wellington
Ottawa (Ontario)
K1A 0N4

Your file Votre référence

Our file Notre référence

NOTICE

The quality of this microform is heavily dependent upon the quality of the original thesis submitted for microfilming. Every effort has been made to ensure the highest quality of reproduction possible.

If pages are missing, contact the university which granted the degree.

Some pages may have indistinct print especially if the original pages were typed with a poor typewriter ribbon or if the university sent us an inferior photocopy.

Reproduction in full or in part of this microform is governed by the Canadian Copyright Act, R.S.C. 1970, c. C-30, and subsequent amendments.

AVIS

La qualité de cette microforme dépend grandement de la qualité de la thèse soumise au microfilmage. Nous avons tout fait pour assurer une qualité supérieure de reproduction.

S'il manque des pages, veuillez communiquer avec l'université qui a conféré le grade.

La qualité d'impression de certaines pages peut laisser à désirer, surtout si les pages originales ont été dactylographiées à l'aide d'un ruban usé ou si l'université nous a fait parvenir une photocopie de qualité inférieure.

La reproduction, même partielle, de cette microforme est soumise à la Loi canadienne sur le droit d'auteur, SRC 1970, c. C-30, et ses amendements subséquents.

Canada

Impulse Noise on Telephone Loops

by

Graham Keith Gowanlock, B.A.Sc.

A thesis submitted to the

School of Graduate Studies and Research

as a partial requirement for the degree of

Master of Applied Science

Ottawa-Carleton Institute for Electrical Engineering

Department of Electrical Engineering
Faculty of Engineering
University of Ottawa

© Graham Keith Gowanlock, Ottawa, Canada, 1993

National Library
of Canada

Acquisitions and
Bibliographic Services Branch

395 Wellington Street
Ottawa, Ontario
K1A 0N4

Bibliothèque nationale
du Canada

Direction des acquisitions et
des services bibliographiques

395, rue Wellington
Ottawa (Ontario)
K1A 0N4

Your file Votre référence

Our file Notre référence

The author has granted an irrevocable non-exclusive licence allowing the National Library of Canada to reproduce, loan, distribute or sell copies of his/her thesis by any means and in any form or format, making this thesis available to interested persons.

L'auteur a accordé une licence irrévocable et non exclusive permettant à la Bibliothèque nationale du Canada de reproduire, prêter, distribuer ou vendre des copies de sa thèse de quelque manière et sous quelque forme que ce soit pour mettre des exemplaires de cette thèse à la disposition des personnes intéressées.

The author retains ownership of the copyright in his/her thesis. Neither the thesis nor substantial extracts from it may be printed or otherwise reproduced without his/her permission.

L'auteur conserve la propriété du droit d'auteur qui protège sa thèse. Ni la thèse ni des extraits substantiels de celle-ci ne doivent être imprimés ou autrement reproduits sans son autorisation.

ISBN 0-315-82570-7

Canada

UNIVERSITÉ D'OTTAWA
UNIVERSITY OF OTTAWA

ABSTRACT

Impulse noise is an ever increasing impediment to successful digital data transmission in the telephone local cable plant. Two major factors have caused this to happen. Firstly, remedies have been found for nearly all the other causes of signal degradation, such as crosstalk and intersymbol interference, leaving impulse noise outstanding. Secondly, the user's demand for higher and higher data rates and the proliferation of repeaterless operation at extended loop ranges, have made the effects of impulse noise more prominent.

This thesis covers the subject of impulse noise in the local plant. It begins with experimental data obtained from field studies of the local loop segments of digital transmission systems. The theoretical aspects of impulse noise are next addressed, including the various methodologies for modeling it. Burst errors in the recovered data stream, and their relationship with impulse noise, their principal cause, are described. The methodologies for modeling burst errors are then discussed. Finally, the techniques for minimizing the harmful effects of impulse noise are examined. Included in this is a novel scheme, referred to as "Pulse Sharpening", now being introduced.

TABLE OF CONTENTS

TABLE OF ILLUSTRATIONS

FIGURES

TABLES

TABLE OF ACRONYMS

ADSL	Asymmetric digital subscriber line
AM	Amplitude modulation
AMI	Alternate mark inversion (signalling)
AT&T	American Telephone and Telegraph Company
AWGN	Additive white Gaussian noise
BCH	Bose Chaudhuri Hocquenghem (error correcting code)
BER	Bit Error Rate
BPSK	Binary Phase Shift Keying
B.S.T.J.	Bell System Technical Journal
CD	Compact Disk (recording)
C.O.	Central office (of telephone company)
CSA	Carrier serving area, 9 to 12 kft to C.O.
DAT	Digital audio tape (recording)
dBrnC	Decibels relative to reference noise level with C-message weighting
DDS	The AT&T Digital Dataphone Service data network
DFE	Decision feedback equalizer
DMS-100	Northern Telecom model software controlled voice switching machine
DSP	Digital signal processor (device)
FEXT	Far end crosstalk
FSK	Frequency shift keying

HDB3	High density bipolar line code with 3 zero substitution
HDSL	High data rate subscriber line
HF	High frequency (radio)
I&Q	In phase and quadrature (signal components)
i.i.d.	Independent identically distributed (random variables)
ISDN	Integrated services digital network
ISI	Intersymbol interference
MWAL2	Modified WAL-2 line code
NEXT	Near end crosstalk
NMS	Noise measuring set
NRZ	Non-return-to-zero (signalling)
NYNEX	Parent company of New York and New England Telephone Companies
ONE	Logic level one
PAM	Pulse amplitude modulation
PRF	Pulse repetition frequency
PRIV	Partial response class IV line code
PSK	Phase Shift Keying
QAM	Quadrature amplitude modulation
QPSK	Quadrature Phase Shift Keying
RS	Reed-Solomon (code)
RZ	Return-to-zero (signalling)
SNR	Signal-to-noise ratio, dB
SS	Spread spectrum
SSM	Stochastic sequential machine

TCM	Time compression multiplexing
TCMOD	Trellis coded modulation
WAL2	Top hat line code
ZERO	Logic level zero
ZMNL	A zero memory nonlinear device (Modestino)
2B1Q	2-binary to 1-quaternary PAM line code
3B2T	3-binary to 2-ternary PAM line code
4B3T	4-binary to 3-ternary PAM line code
6F	AT&T standard impulse NMS

CHAPTER 1

INTRODUCTION

Impulse noise is now a serious impairment to digital data transmission, using local loops. Werner [16] aptly describes the situation as follows: "In recently conducted ISDN field trials for basic access, at 144 kb/s, impulse noise in the loop plant has proved to be one of the major limiting factors in the transceiver's achievable performance. It is expected that impulse noise will be an even more severe impairment for transceivers operating at data rates that are substantially larger than ISDN's basic rate". Why this has come to pass is worthy of consideration.

The popularity of the local plant for digital data transmission has increased the exposure to impulse noise. The users' demands for improved error performance has been recognized. As well, their demands for ever increasing data rates have raised the susceptibility to the impairment. Cost savings measures by the common carriers, such as minimizing and eventually eliminating the use of digital repeaters in the local plant, have lead to increased transmission losses, again increasing noise susceptibility.

Many of the other transmission impairments have recently been dealt with successfully. ISI has been alleviated by the introduction of adaptive equalizers and coding schemes such as precoding. NEXT has

been dealt with by the creation of half duplex systems such as TCM as well as by noise prediction techniques. FEXT problems have been avoided by signal coding. Means have yet to be found to deal with impulse noise, in a practical sense.

The thesis is organized in the following manner.

Chapter 2, Experimental Observations, covers some of the practical knowledge of impulse noise gained from dealing with problems caused by this impairment. Key points are illustrated by reference to a number of photographs of oscilloscope traces of impulse noise waveforms observed in the field.

Chapter 3, Impulse Noise Models, introduces the subject and describes four different mathematical models used to represent impulse noise for analytical and simulation purposes. Section 3.1, General Comments, discusses practical aspects. Section 3.2, Background, describes the properties of impulse noise and some of the mechanisms thought to be involved in generating it. Section 3.3, The Curtis Study of Sparking Contacts, describes the electrical properties of such devices, as potential generators of a large part of the impulse noise found in local loops. The remaining sections of this chapter describe the four models in detail.

Chapter 4, Burst Error Models, describes three different models of logic errors, in the recovered received digital data stream, and

investigates their suitability for representing the effects of burst errors in practice.

Chapter 5, Impulse Noise Countermeasures, describes the ways of designing transmission equipment to reduce the impact of impulse noise and burst errors on system performance. A new technique, referred to as "Pulse Sharpening" is proposed as a means of mitigating the effects of impulse noise.

Chapter 6, Conclusions and Recommendations, completes this thesis.

The appendices contain supporting information for the main body of the thesis. Appendix A, The Commercial Environment, describes some lesser known aspects of the data communications business that exert a strong influence on engineering design in regards to impulse noise. Appendix B, Measurement of Impulse Noise, describes how the severity of impulse noise is measured both in the laboratory and in the field. Appendix C, Telephone Network Studies, lists the published results of several telephone company sponsored transmission investigations. Appendix D, Local Loop Systems, describes the operation of commonly used local loop transmission facilities. Appendix E, Computer Simulation of a Loop System, describes a model and some important conclusions drawn from it.

The section entitled References contains a list of the sources cited throughout the thesis.

CHAPTER 2

EXPERIMENTAL OBSERVATIONS

2.1 INTRODUCTION

Impulse noise was not an intractable impairment in the local loop until recent times. The situation changed, as is explained below, with the introduction of high speed extended range local loop modems. Following is a brief history of field experience with the impairment in the telephone plant environment.

Waveforms of impulse noise, in the local loop, that have been observed and documented for this thesis are presented. These experimental observations permit one to appreciate the complex and varying nature of the impairment and the limitations to digital transmission that it can impose.

Up to the early 1960's, only the D.C. printing telegraph equipment used the local loops for digital data transmission. Operation was based on on-and-off keying of a current of 60 mA from a 120 v D.C. central office (C.O.) battery. A signalling rate of 45.5 baud was commonly used. Impulse noise interference was occasionally the cause of poor performance. Nearly always the interference was caused by crosstalk, or "crossfire", as it was called, from other telegraph systems using pairs in the same cable. The problem was easily solved by placing an R-C filter, called a "waveshaper",

across the keying contacts of the offending unit. There was no equipment available at this time for measuring impulse noise (other than a telephone earpiece). Consequently, little was known about its properties.

In the mid 1960's analog digital data systems, using modems at the ends of the loops, started to appear. Frequency shift keying (FSK) of a voice frequency tone, for data rates up to 300 baud, was common. Harmful impulse noise interference in the local loop was mainly due to telegraph crossfire and again was remedied with waveshapers. Noise measuring sets (NMS's) were used to measure impulse noise as a number of "counts" in 15 minutes, for example. (Appendix B describes the NMS.)

In the early 1970's, country-wide all-digital synchronous data networks, such as the Dataroute, were put into service. The loop equipment for such systems supported operation from a data rate of 1.2 kbps up to 56 kbps using a 50 per cent duty cycle bipolar scheme. Two unloaded cable pairs, one for transmit and the other for receive, were used. Impulse noise problems were avoided by following the extremely conservative design guidelines, such as those shown below:

i) Only unloaded cable pairs with strict limits on bridged tap lengths were permitted.

ii) A cable loss of no more than 28 dB, at the Nyquist frequency, was permitted. (C.O. located regenerative repeaters were used to

extend the range in hops of up to 28 dB.)

iii) Shielded pairs, with grounded shields, were used for wiring inside the C.O.

iv) Local loops were routed around C.O.'s housing step-by-step switching machines.

The D.C. telegraph service, the major source of high level impulse noise in the local loop, was in a state of rapid decline by this time. Impulse noise from telephone pulse dialing, the remaining source of high level interference, was not strong enough to cause noticeable errors in the loop system. As was the case for the earlier services, the study of impulse noise did not have a high priority among telephone company personnel.

The local loop impulse noise situation changed radically with the recent introduction of the extended range digital loop equipment. The following major changes in design were implemented:

i) The permissable loss at the Nyquist frequency was extended from 28 to 45 dB.

ii) Regenerative repeaters were no longer to be used.

iii) The data rate was extended to 64 kbps.

Poor error performance was observed almost immediately with those systems operated near the maximum range. It was a common occurrence to find a 56 kbps system exhibiting heavy errors that would operate virtually error free, when set to operate at 19.2 kbps. The following two cases were chosen to be presented here as they represent the extremes in the range of the cases investigated.

Two non-loaded twisted pair circuits were tested; one in Brampton, Ontario and the other in Nepean, Ontario. A Tektronix model 2440 digitizing storage oscilloscope, having a bandwidth of 50 MHz, was adjusted to capture impulse events which were then recorded on film. Copies of these are included in this thesis as figures 2.A1 through 2.A17 for Brampton and 2.B1 through 2.B10 for Nepean.

2.2 BRAMPTON TESTING

The Brampton circuit was inspected because it was experiencing excessive data errors when operated at 56 kbps using the dedicated four-wire type AT&T Digital Dataphone Service (DDS) access system [1]. The circuit had always run error free at 19.2 kbps. The oscilloscope was connected to a spare pair, in the Brampton C.O. and terminated with a 135 ohm carbon resistor. The test pair was in the same binder group with the DDS circuit, which was operating at 56 kbps while oscilloscope measurements were being made. Testing was done between 11:00 A.M. and 4:00 P.M. on a Wednesday. The switching machine in the Brampton C.O. was an all electronic Northern Telecom type DMS-100. The office was acoustically quiet during the test period; no relays appeared to be keyed, electric motors running etc. Excessive data errors were not found at this time, indicating that the impulse noise level was then below its peak value.

An analysis of the figures indicates the following properties of the noise:

i) Intervals that are almost entirely noise free are observed between noise bursts. The intervals vary from 2 ms to 26 ms in duration (ref. Figs. 2.A16(b) and 2.A17(a)). There is no discernable crosstalk from any high speed data circuit, not even the active 56 kbps circuit sharing the binder group (ref. Figs. 2.A2(a) and 2.A2(b)).

ii) The noise seems to come in bursts that are 10 to 15 ms long, separated by the silent periods mentioned above (ref. Fig. 2.A17).

iii) The bursts appear to be composed of random noise signals having peak-to-peak amplitudes around 80 mv (which is near the amplitude of attenuated data signals) (ref. Fig. 2.A1). Some of the bursts contain a few cycles of an audio frequency (500 to 700 Hz, see Fig. 2.A5) sine wave with a peak-to-peak amplitude about a quarter that of the impulse noise.

iv) Nanosecond wide spikes, with amplitudes near 20 mv seem to be grouped inside the noise bursts (ref. Fig. 2.A12), although some are seen occasionally in the silent period between bursts (ref. Fig. 2.A15(a)).

v) 60 Hz powerline crosstalk, or harmonics thereof, appear to be totally absent.

vi) On several occasions, long uniform trains of ns long 20 mv spikes were observed with differing pulse repetition frequencies (PRF's):

- Figure 2.A3 shows one with a PRF of around 341 kHz

- Figure 2.A7 shows what may be crosstalk from a 20 Hz square wave. (20 Hz is the frequency of the ringing generator which is commonly implemented with saturable reactor switching elements.)
- Figure 2.A12 shows one with a PRF of 635 Hz
- Figure 2.A17(a) shows one with a PRF of 38 Hz

vii) On one occasion (Fig. 2.A10) a burst of 31 MHz sine wave, of peak-to-peak amplitude 21 mv, was found.

It would appear that we are dealing with many widely different impulse noise sources that are keyed randomly.

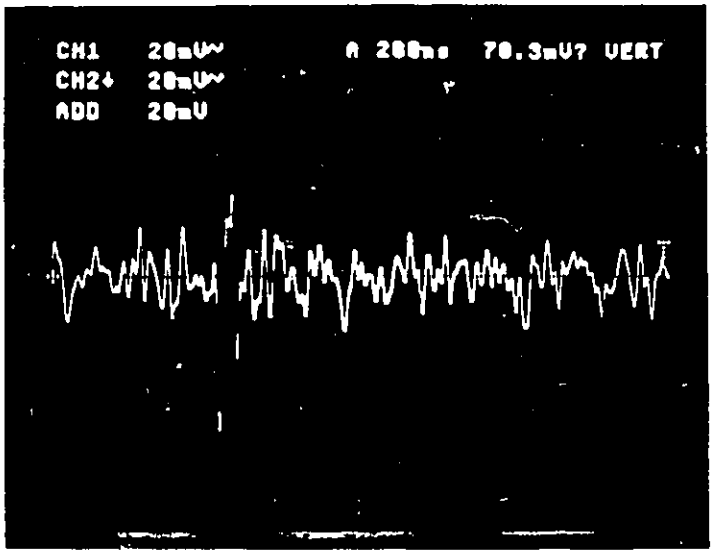

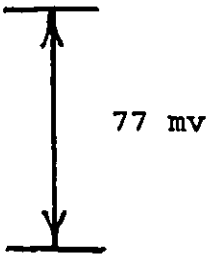

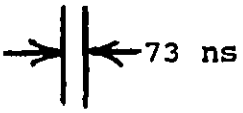

Figure 2.A1 Event A1

H: 200 ns per div.
V: 20 mv per div.
1 div. = 0.825 cm

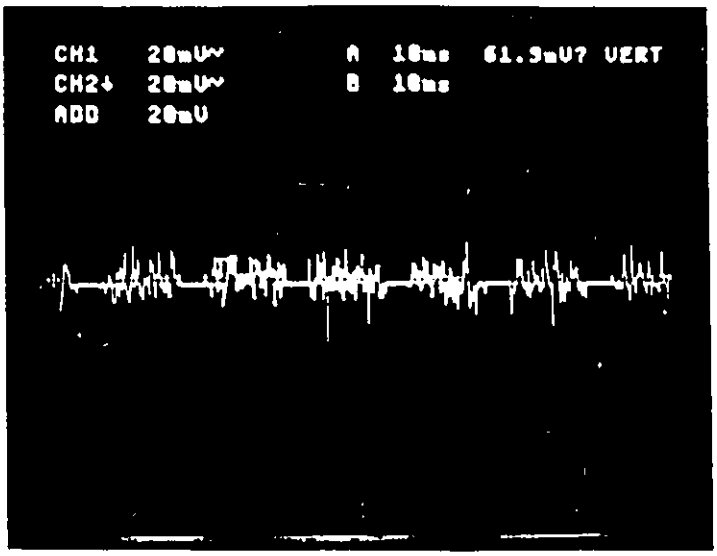

Figure 2.A2(a) Event A2

H: 10 ms per div.
V: 20 mv per div.
1 div. = 0.825 cm

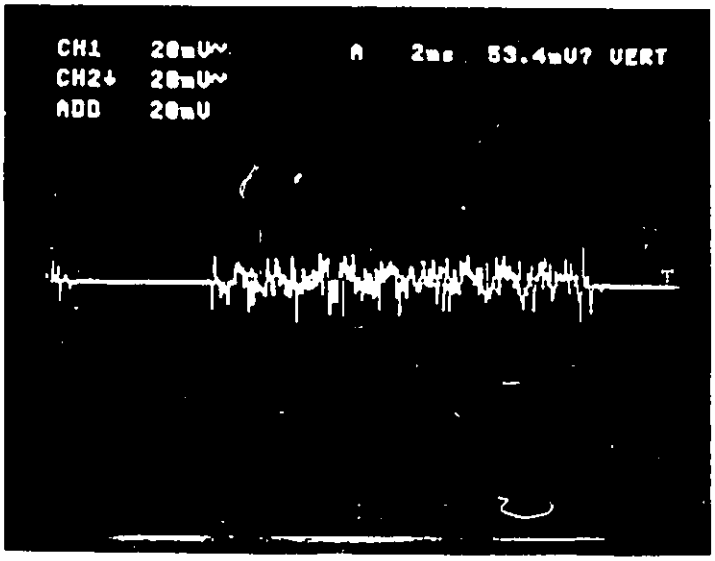

Figure 2.A2(b) Event A2

H: 2 ms per div.
V: 20 mv per div.
1 div. = 0.825 cm

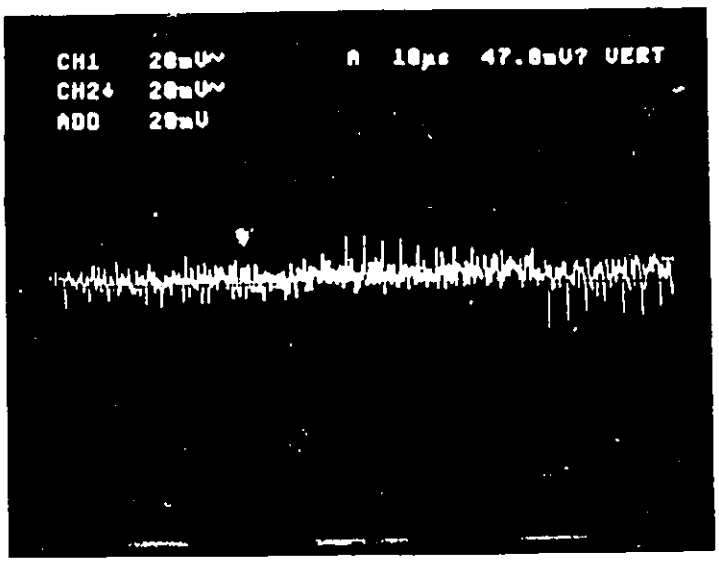

Figure 2.A3 Event A3

H: 10 µs per div.
V: 20 mv per div.
1 div. = 0.825 cm

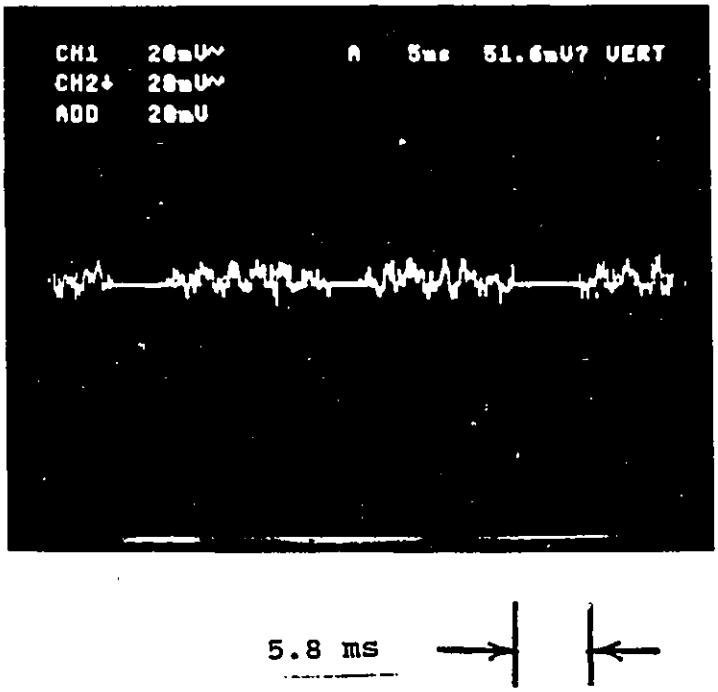

Figure 2.A4 Event A4

H: 5 ms per div.
V: 20 mv per div.
1 div. = 0.825 cm

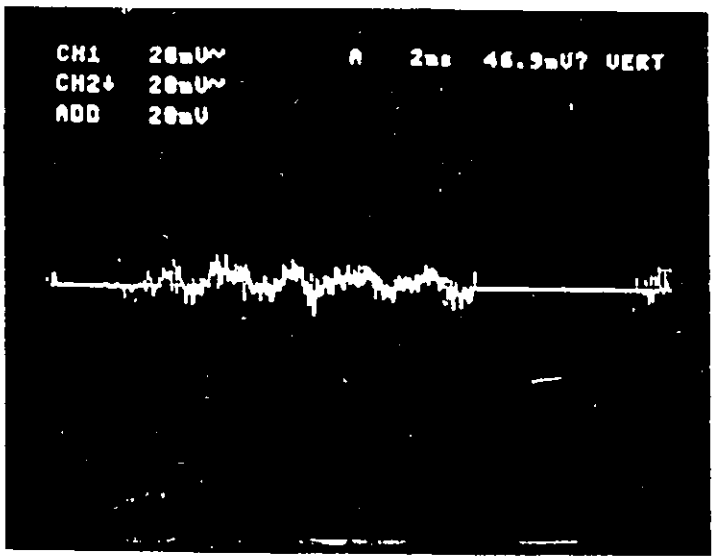

20 mv

1.9 ms (516 Hz)

5.4 ms

Figure 2.A5 Event A5

H: 2 ms per div.
V: 20 mv per div.
1 div. = 0.825 cm

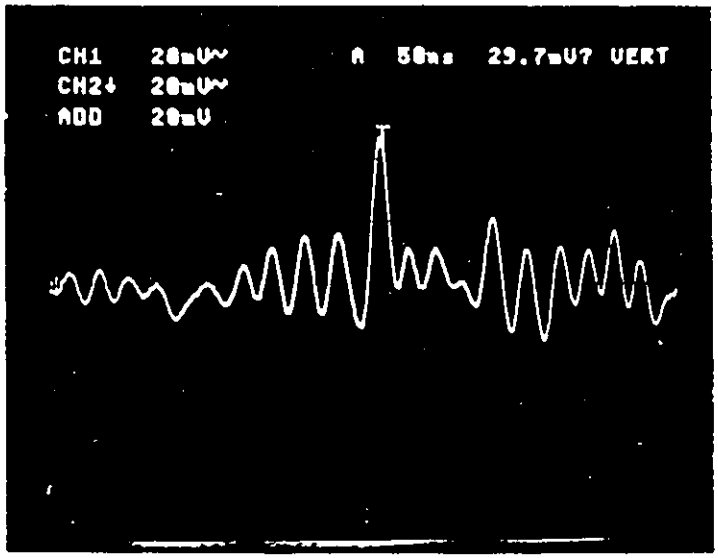

64 mv

27 ns

Figure 2.A6 Event A6

H: 50 ns per div.
V: 20 mv per div.
1 div. = 0.825 cm

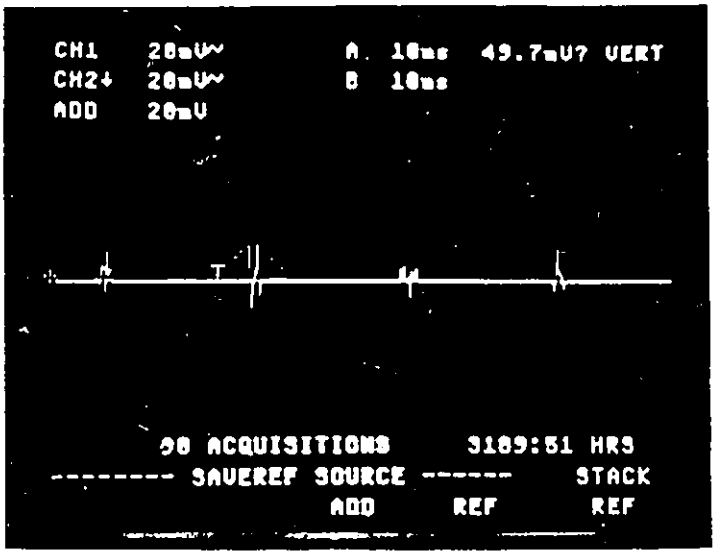

18 mv

1.8 ms

24 ms (21 Hz)

Figure 2.A7 Event A7

H: 10 ms per div.
V: 20 mv per div.
1 div. = 0.825 cm

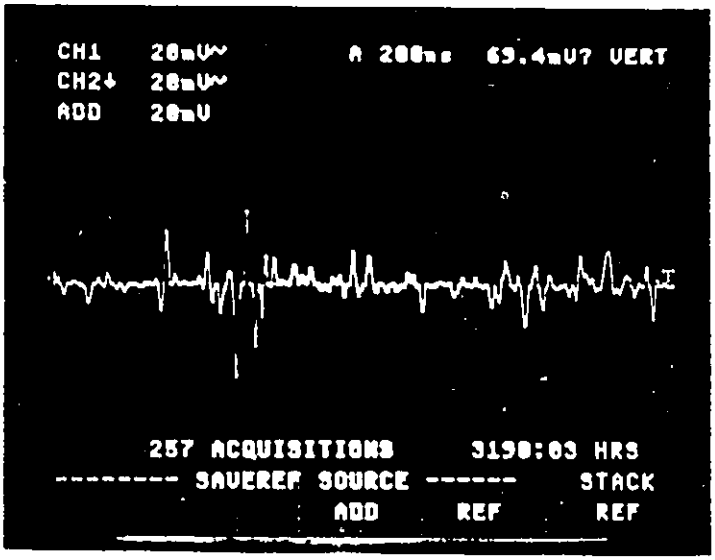

30 mv

63 ns

Figure 2.A8 Event A8

H: 200 ns per div.
V: 20 mv per div.
1 div. = 0.825 cm

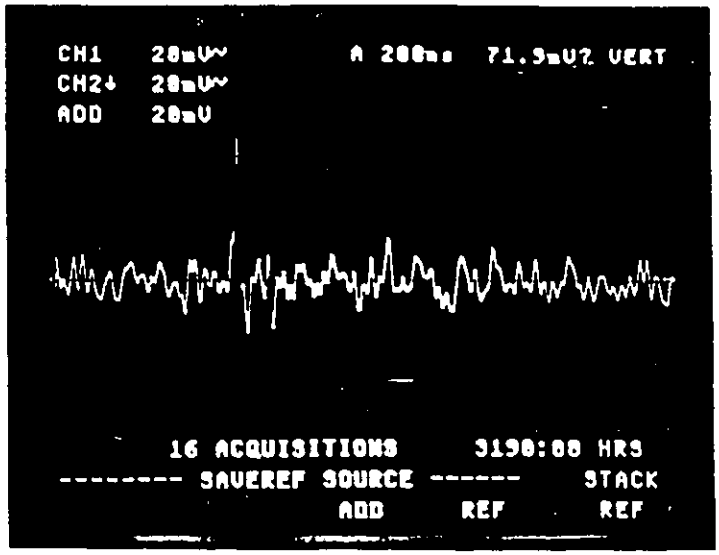

48 mv

56 ns

Figure 2.A9 Event A9

H: 200 ns per div.
V: 20 mv per div.
1 div. = 0.825 cm

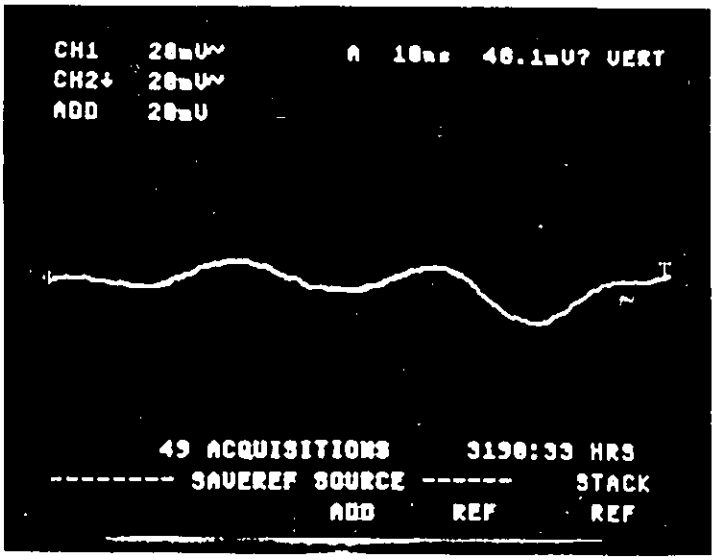

21 mv

33ns (31 MHz)

Figure 2.A10 Event A10

H: 10 ns per div.
V: 20 mv per div.
1 div. = 0.825 cm

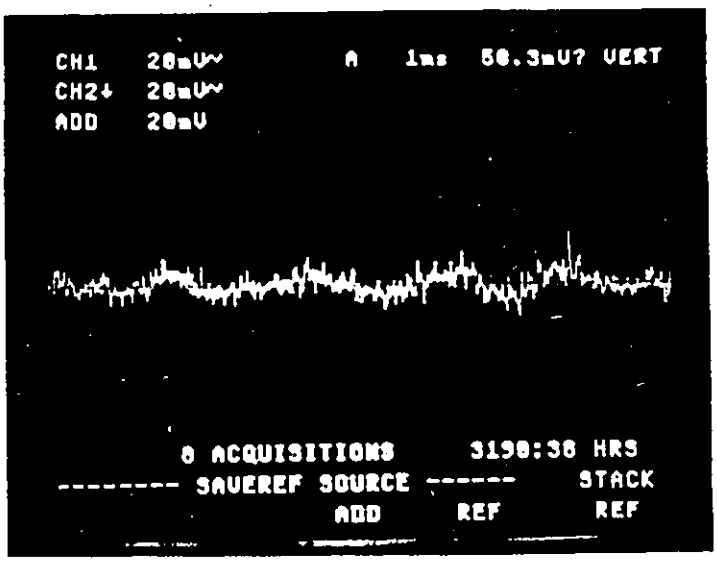

22 mv

2.4 ms (425 Hz)

Figure 2.A11 Event A11

H: 1 ms per div.
V: 20 mv per div.
1 div. = 0.825 cm

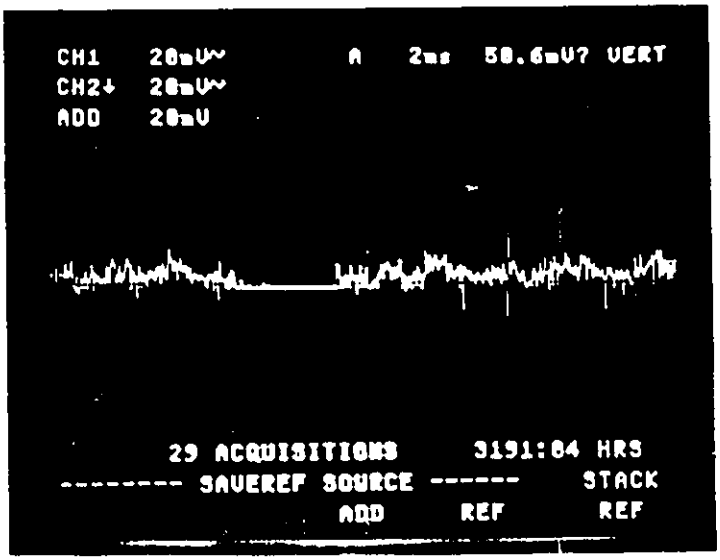

24 mv

3 ms 1.6 ms (635 Hz)

Figure 2.A12 Event A12

H: 2 ms per div.
V: 20 mv per div.
1 div. = 0.825 cm

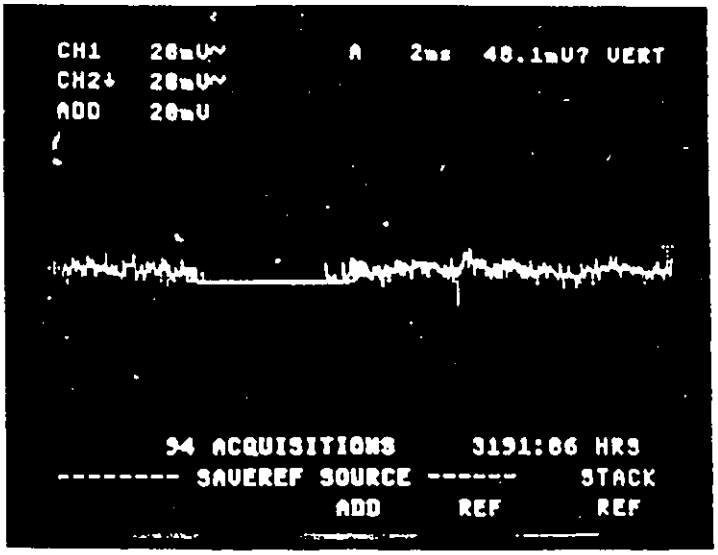

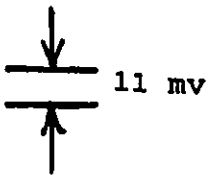

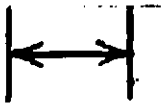

Figure 2.A13 Event A13

H: 2 ms per div.
V: 20 mv per div.
1 div. = 0.825 cm

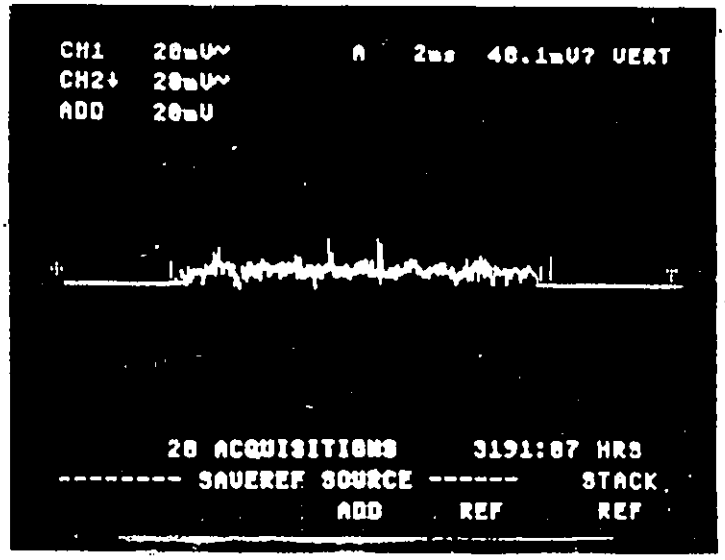

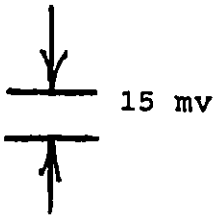

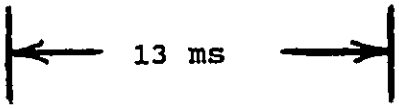

Figure 2.A14 Event A14

H: 2 ms per div.
V: 20 mv per div.
1 div. = 0.825 cm

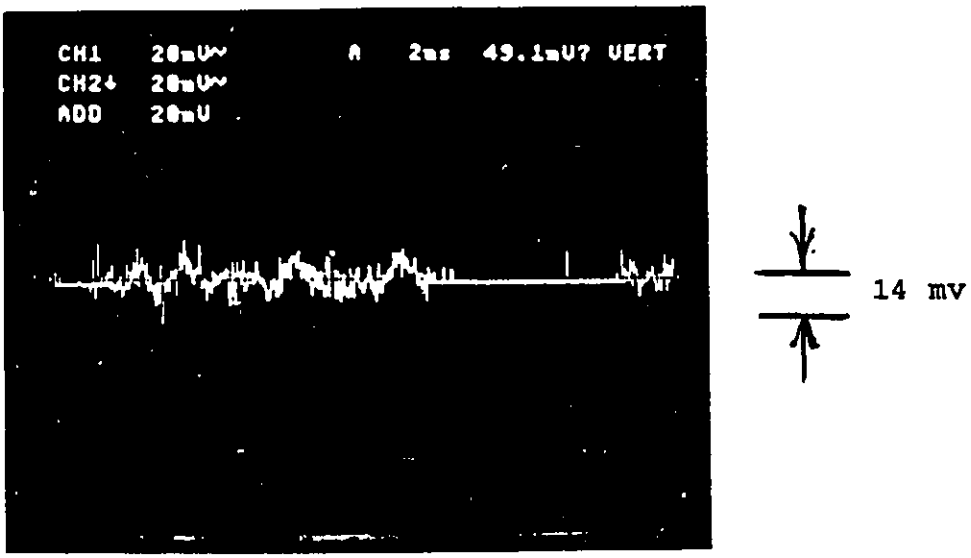

Figure 2.A15(a) Event A15

H: 2 ms per div.
V: 20 mv per div.
1 div. = 0.825 cm

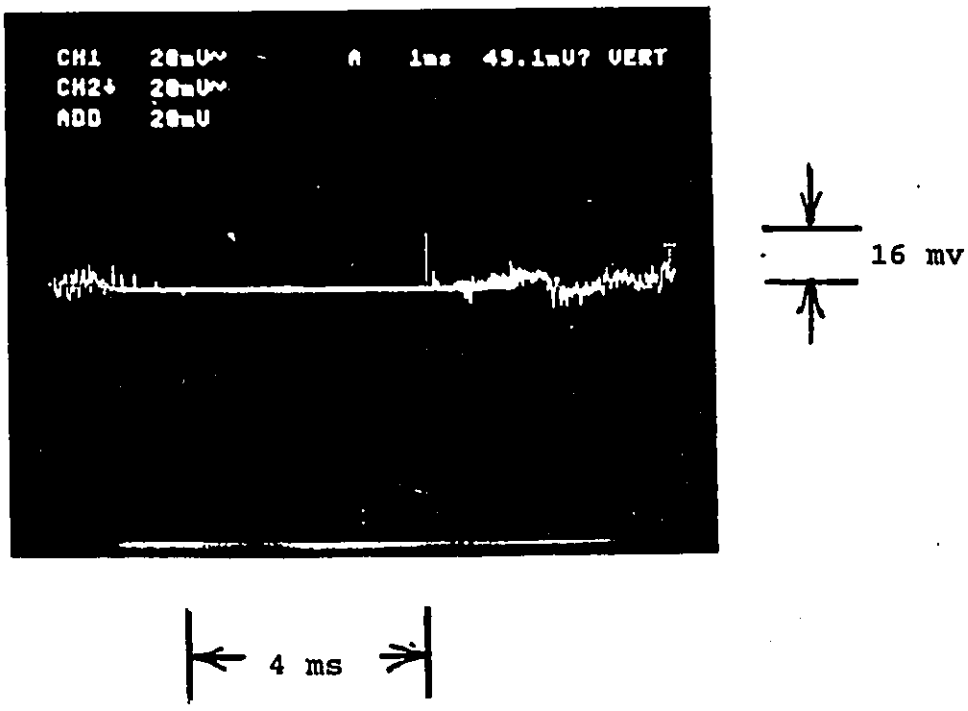

Figure 2.A15(b) Event A15

H: 1 ms per div.
V: 20 mv per div.
1 div. = 0.825 cm

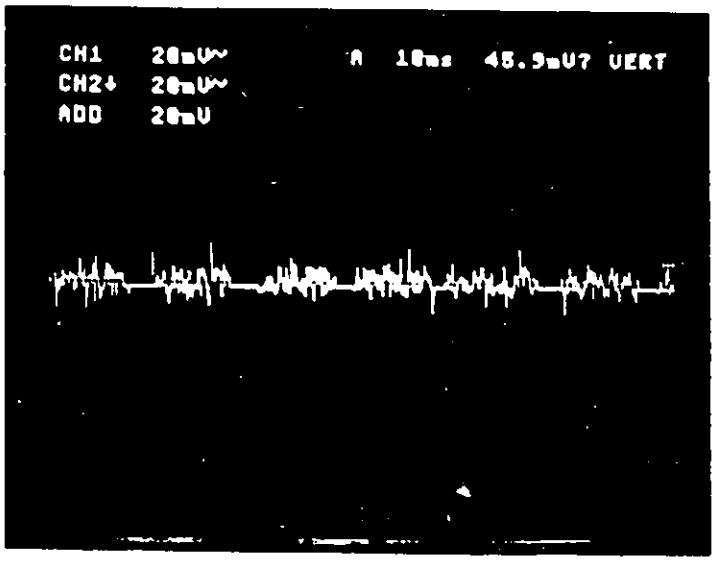

Figure 2.A16(a) Event A16

H: 10 ms per div.
V: 20 mv per div.
1 div. = 0.825 cm

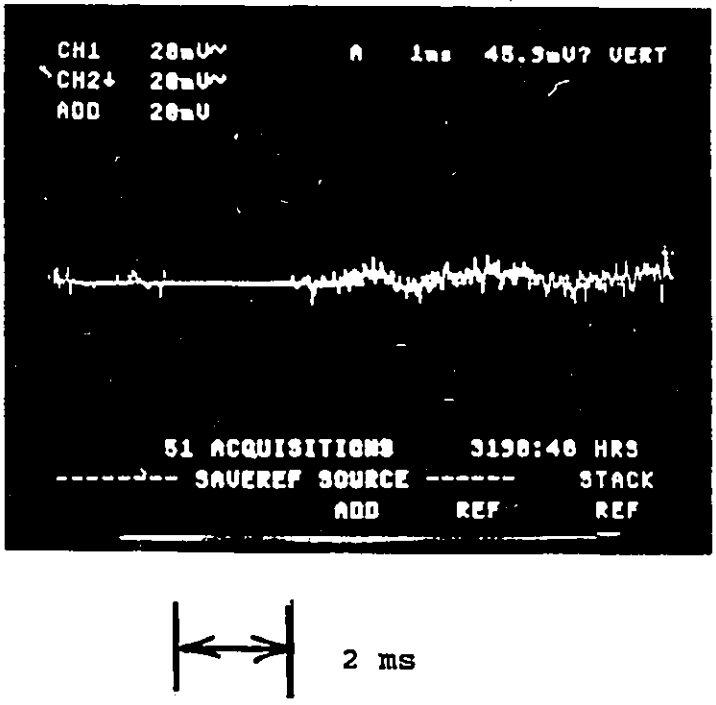

Figure 2.A16(b) Event A16

H: 1 ms per div.
V: 20 mv per div.
1 div. = 0.825 cm

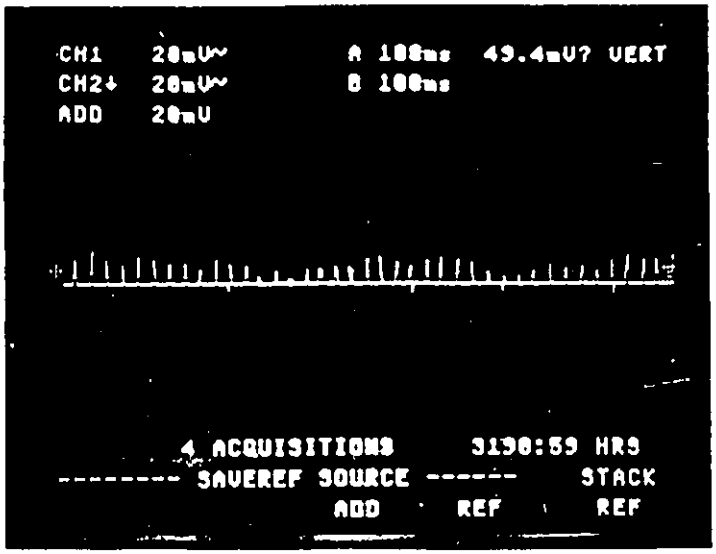

11 mv

26 ms (38 Hz)

Figure 2.A17(a) Event A17

H: 100 ms per div.
V: 20 mv per div.
1 div. = 0.825 cm

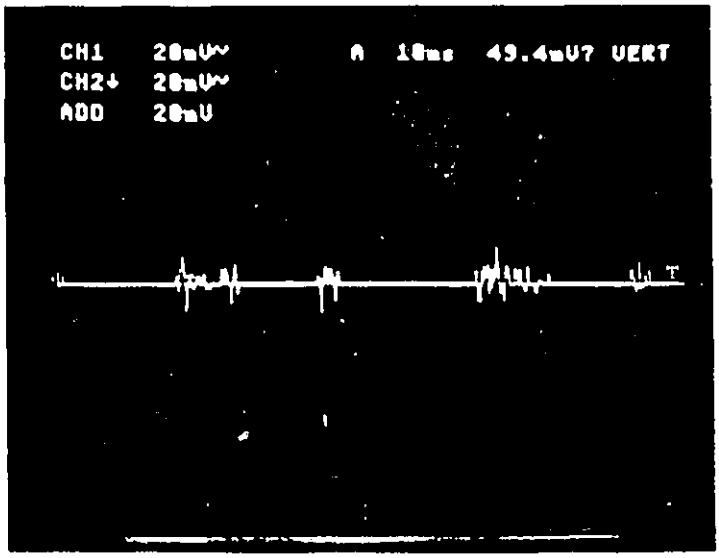

Figure 2.A17(b) Event A17

H: 10 ms per div.
V: 20 mv per div.
1 div. = 0.825 cm

2.3 NEPEAN TESTING

Testing was done at a residence on a pair, which runs nearly a cable mile, to the City View C.O. where it terminates on a DMS-100 switch. The circuit was idle during the tests, being unterminated at the premises where the measurements were taken. Work was done between 9:00 P.M. and midnight on a Thursday. This particular circuit is used to provide switched network access to the University of Ottawa timeshare computer system, via a 2400 bps modem connected to a personal computer. Over a six month period it had been observed that the system ran error free during the business day, but experienced five to ten character errors and two or three disconnections per late evening session.

An analysis of the figures indicates the following properties of the noise:

i) The noise appears mainly to arise from transients in the 60 Hz power distribution plant. (Fast spike noise or other high frequency noise appears to be totally absent.) The basic harmonic waveforms are shown as severely clipped sine waves, which in fact occur quite frequently in a power system because of transformer core saturation caused by load unbalance. Interference amplitudes are nearly a thousand times larger than those for the Brampton case. The one mystery is Figure 2.B10 which shows a clipped 30 Hz waveform.

ii) The transients occur in several forms, for example:

- Spikes are often generated at the crest of the 60 Hz waveform

(see Figs. 2.B1(a), 2.B2(a), 2.B3(a), 2.B4(a), and 2.B6(a)), which indicates either a high voltage flashover in the power network or the sudden asynchronous application or removal of a load. (Those occurring near zero-crossing do not generate large transients.) Transients are usually in the form of single spikes or short bursts of damped ringing. Peak-to-peak amplitudes are large, varying from 20 to 30 v. Rise times are generally in the ms range, indicating a frequency spectrum limited to the audio band.

- Sudden jumps in noise amplitude are noted (see Figs. 2.B5(a) and 2.B8). Peak-to-peak voltages in the 7 to 10 v range suddenly jump to the 30 to 60 v range. This increase is likely due to an abrupt load increase in the local power distribution plant. The new signals appear to be still bandlimited to the audio frequency range.

It is not quite clear why the severity of the impairment should be greater late at night rather than during the middle of the business day. Since the telephone and power cables share the same poles in the residential area and most of the photographs show 60 Hz. waveforms, then the commercial power system must be the source of the pulses. Most power company activity known to cause impulses does in fact occur early in the morning and late at night when mechanical switching devices are automatically adjusting the voltage to compensate for the rapidly increasing and decreasing user loads, respectively. During the middle of the business day the load is large but steady.

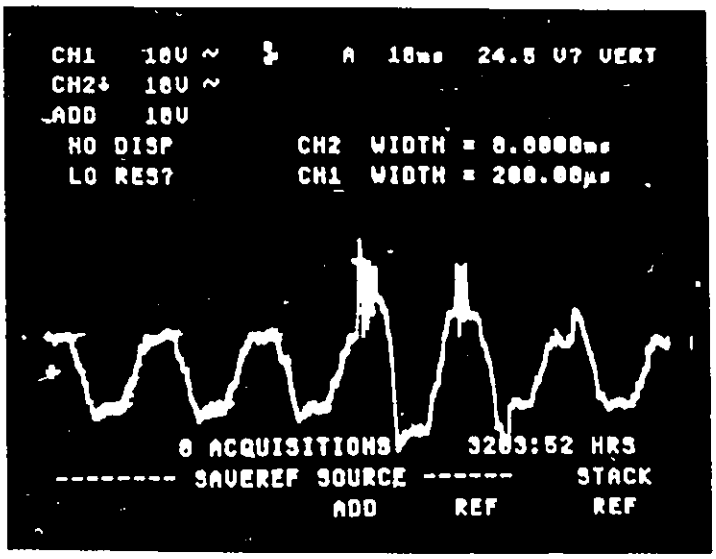

17 ms (59 Hz)

Figure 2.B1(a) Event B1

H: 10 ms per div.
V: 10 v per Div.
1 div. = 0.825 cm

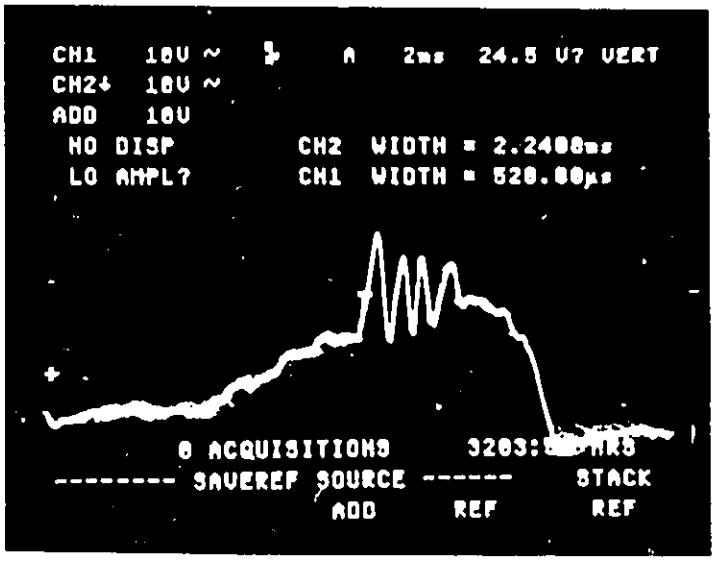

18v

1 ms

Figure 2.B1(b) Event B1

H: 2 ms per div.
V: 10 v per div.
1 div. = 0.825 cm

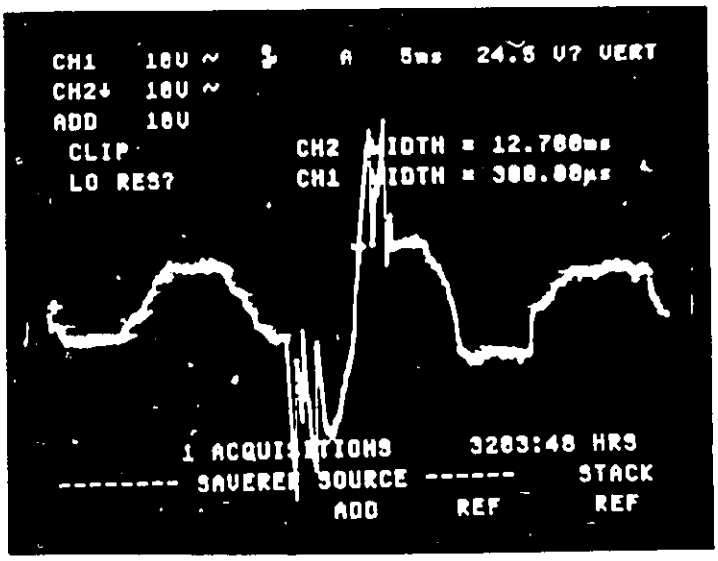

Figure 2.B2(a) Event B2

H: 5 ms per div.
V: 10 v per div.
1 div. = 0.825 cm

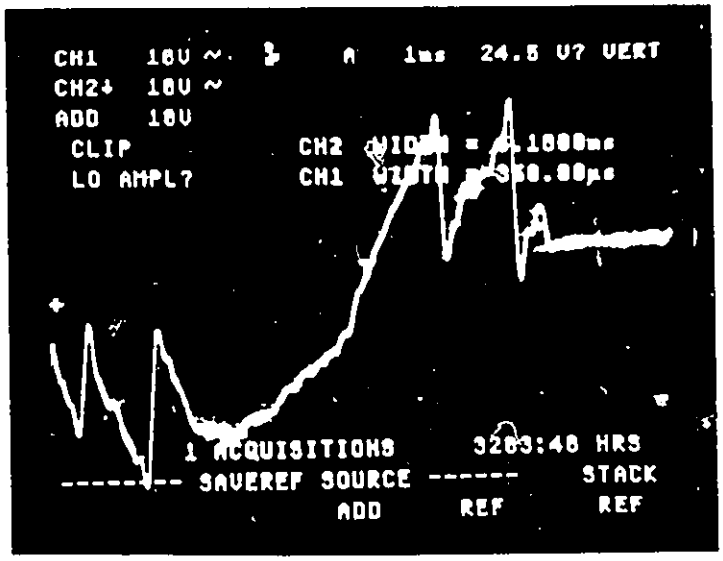

Figure 2.B2(b) Event B2

H: 1 ms per div.
V: 10 v per div.
1 div. = 0.825 cm

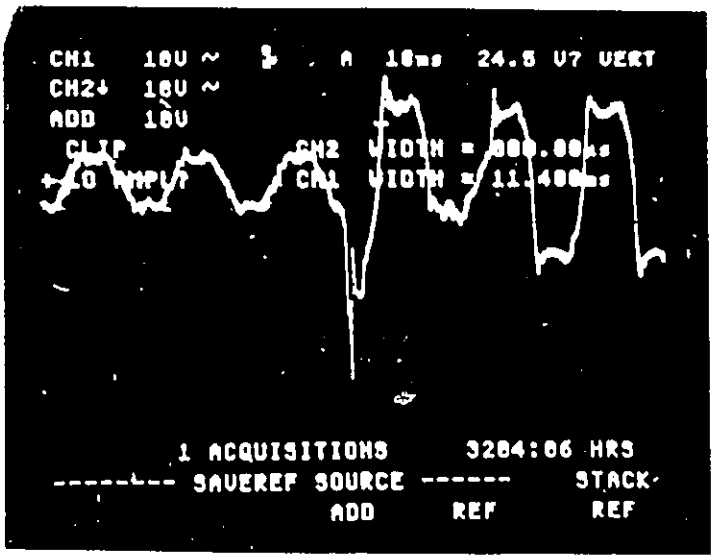

Figure 2.B3(a) Event B3

H: 10 ms per div.
V: 10 v per div.
1 div. = 0.825 cm

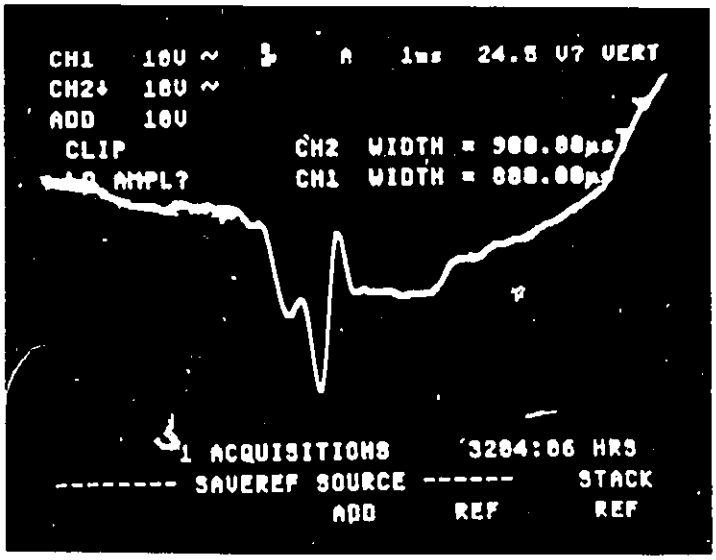

25v

0.3 ms rise

Figure 2.B3(b) Event B3

H: 1 ms per div.
V: 10 v per div.
1 div. = 0.825 cm

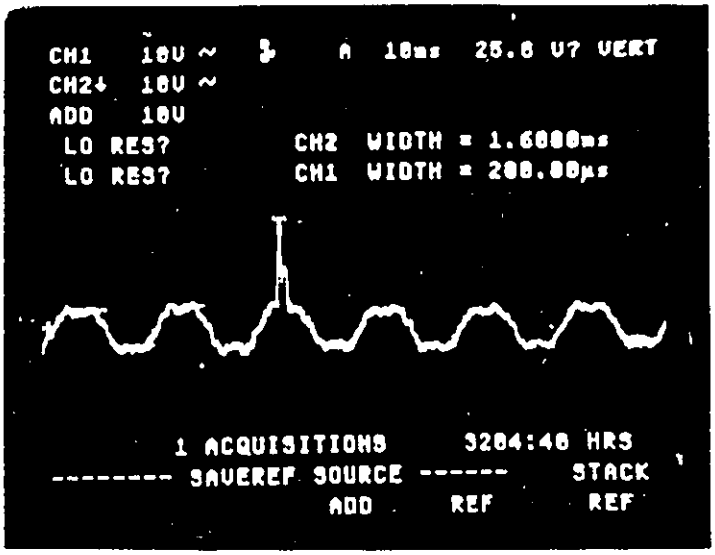

16.4 ms (61 Hz)

Figure 2.B4(a) Event B4

H: 10 ms per div.
V: 10 v per div.
1 div. = 0.825 cm

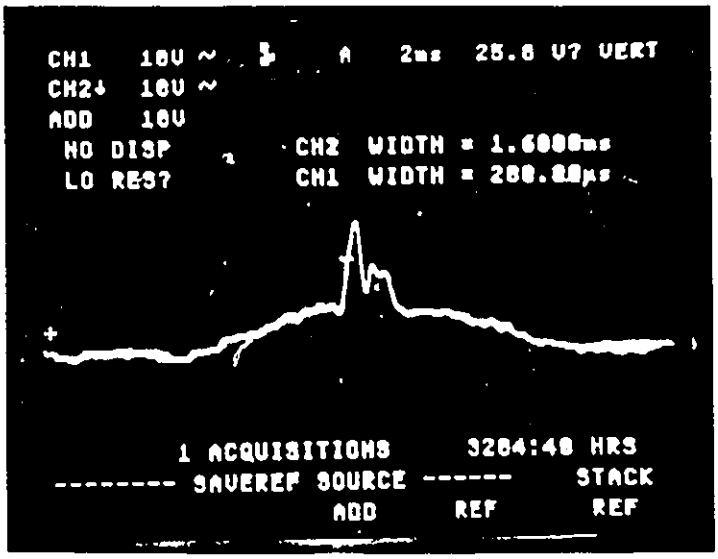

15 v

0.8 ms

Figure 2.B4(b) Event B4

H: 2 ms per div.
V: 10 v per div.
1 div. = 0.825 cm

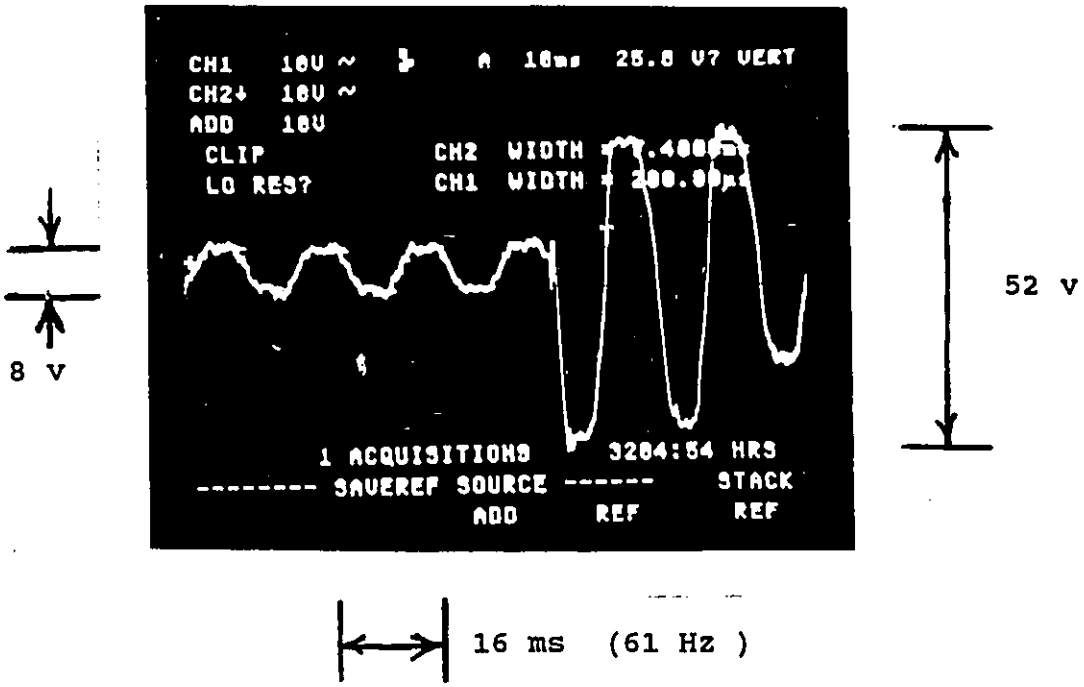

Figure 2.B5(a) Event B5

H: 10 ms per div.
V: 10 v per div.
1 div. = 0.825 cm

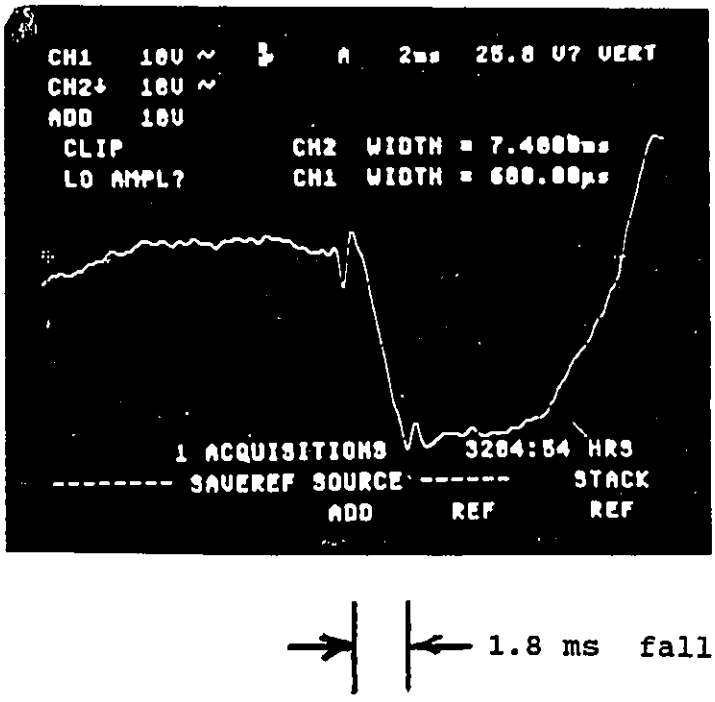

Figure 2.B5(b) Event B5

H: 2 ms per div.
V: 10 v per div.
1 div. = 0.825 cm

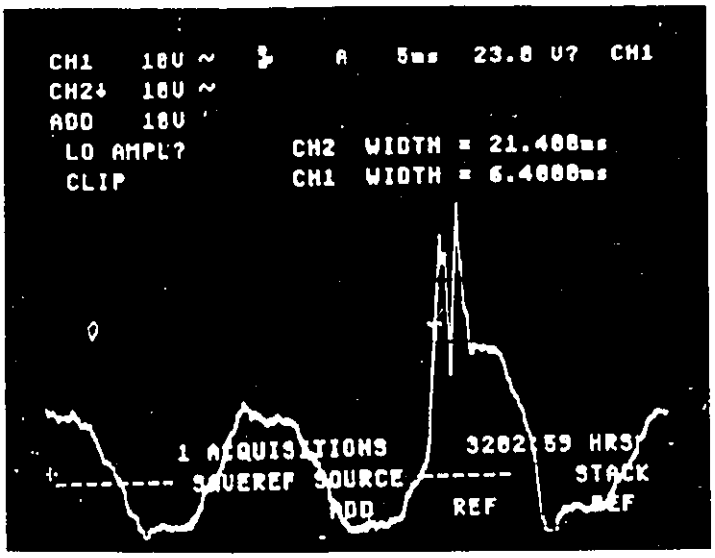

Figure 2.B6(a) Event B6

H: 5 ms per div.
V: 10 v per div.
1 div. = 0.825 cm

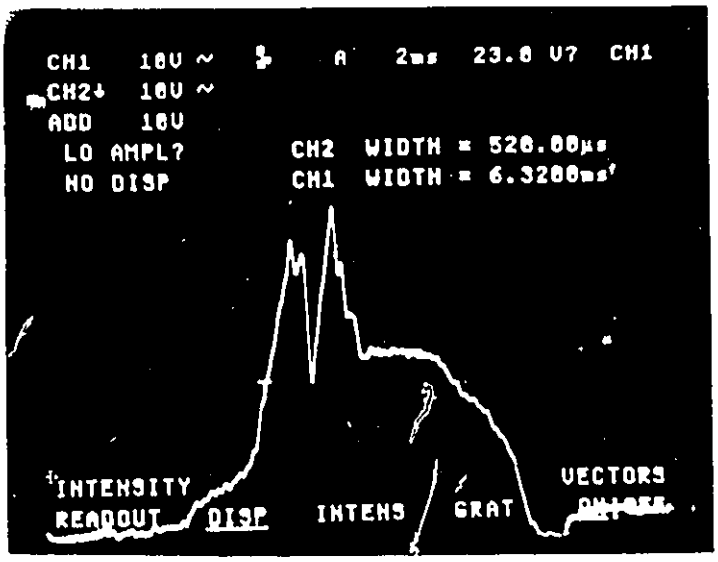

Figure 2.B6(b) Event B6

H: 2 ms per div.
V: 10 v per div.
1 div. = 0.825 cm

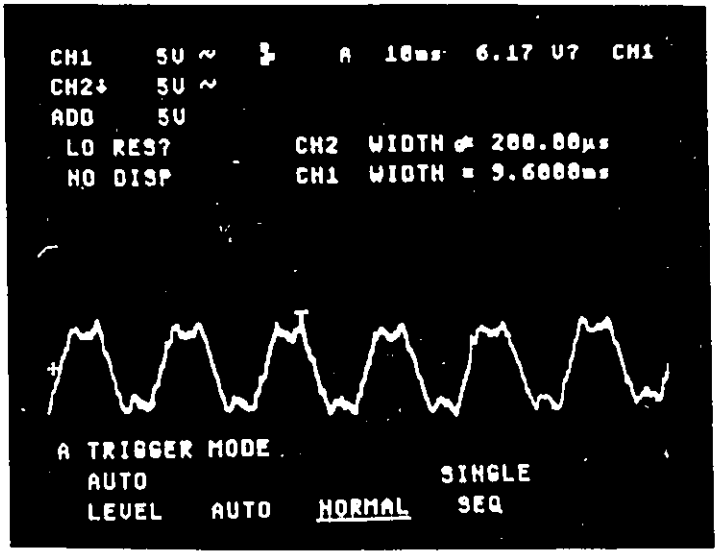

7 v

16.5 ms (61 Hz.)

Figure 2.B7 Event B7

H: 10 ms per div.
V: 5 v per div.
1 div. = 0.825 cm

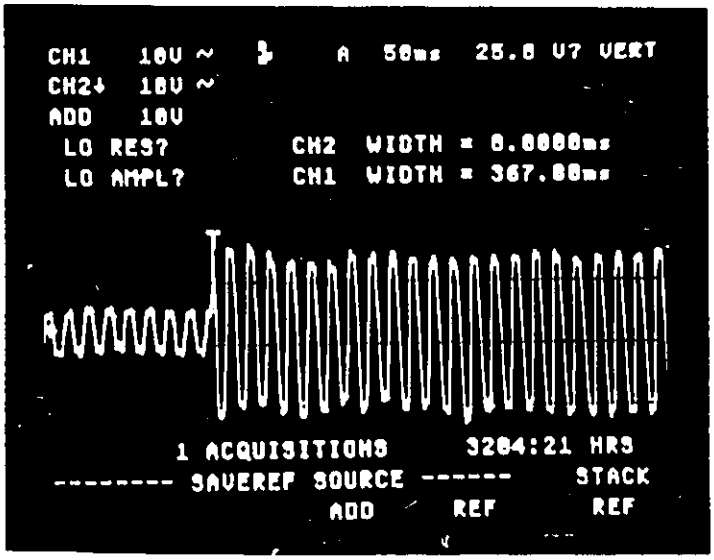

7 v

28 v

16.5 ms (61 Hz)

Figure 2.B8 Event B8

H: 50 ms per div.
V: 10 v per div.
1 div. = 0.825 cm

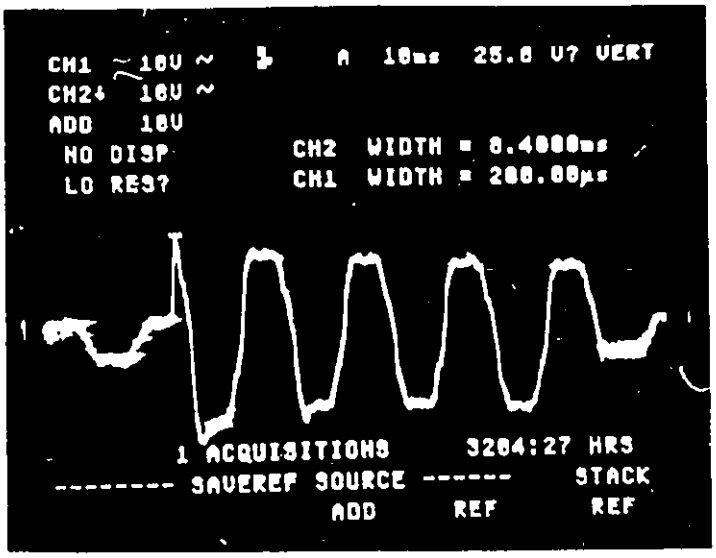

33 v

15.8 ms (63 Hz)

Figure 2.B9 Event B9

H: 10 ms per div.
V: 10 v per div.
1 div. = 0.825 cm

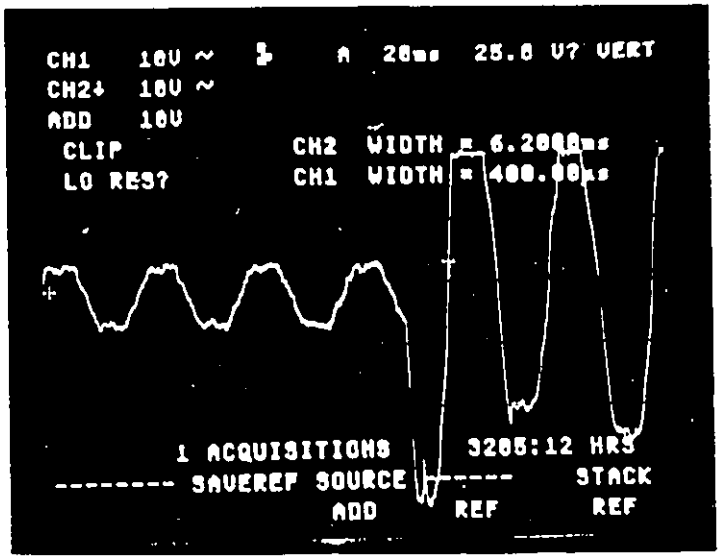

10 v

56 v

32.5 ms (31 Hz)

Figure 2.B10 Event B10

H: 20 ms per div.
V: 10 v per div.
1 div. = 0.825 cm

2.4 CONCLUSIONS

Two diverse impulse noise environments have been found. The Brampton situation is characterized by low level, high frequency and sometimes "spiky" phenomena which apparently come from many sources. The Nepean case, on the other hand, is characterized by high level, slow rise and fall times pulses associated with a low frequency background sinusoidal-like waveform. It is then almost certainly true that a single impulse noise model cannot be fitted accurately to experimental data from many local loops. Such a collection is then a striking example of a "nonergodic ensemble".

It should be noted that the photographs are not intended to represent the total noise properties of the sample loops. The trigger level of the oscilloscope was set high to capture only the "harmful" impulses. What was judged to be harmful to data transmission was based on experience. The trigger level was set to cause triggering every five to ten minutes, a value consistent with the occurrence of errors in a typical data system. The comparison between the Brampton and Nepean situations should then be made on the basis of harmful impulse noise only.

CHAPTER 3

IMPULSE NOISE MODELS

3.1 GENERAL COMMENTS

The purpose of this chapter is to explain the four most commonly used mathematical models for impulse noise.

What the researchers were trying to model was a non-stationary random voltage signal, found in a channel, that was caused by chaotic external processes. As can be seen from the photographs of the oscilloscope traces included in Chapter 2 of this thesis, impulse noise has many faces. Sometimes the channel is absolutely quiet for a period of time. Then a burst of hectic activity takes place. Single occurrences or groups of long oscillatory waves suddenly appear and then slowly fade away. Sprinkled throughout these may be extremely narrow, high amplitude, spikes that remind one of Dirac delta functions. Sometimes the spikes occur in trains or appear alone within a quiet period. There is just no way of telling what will happen next!

Fortunately, a useful model does not need to represent an impulse noise process in all its details. The essential qualities that are required are the probability distribution of the counting process initiating the events and the distribution of the peak amplitudes of the individual events.

3.2 BACKGROUND

IMPULSE NOISE DEFINED:

A rigorous and widely accepted definition of impulse noise does not seem to exist. What the recognized authorities on the subject have to say on the matter is summarized below (with detailed information following).

i) In the time domain it is characterized as being bursty with amplitudes exceeding that of the RMS value of the background Gaussian noise by more than 12.5 dB. The frequency of bursts is greatest during business hours.

ii) In the frequency domain it often tends to have a wideband flat spectrum shaped by the channel to the end-to-end frequency response of the channel. On other occasions it has components with much higher frequency.

Impulse noise is usually considered to occur in short bursts separated by long quiet periods. The amplitudes of the bursts tend to be much higher than would be predicted by a Gaussian law, according to Lucky, Salz and Weldon [2].

Freeman [3] used a more precise definition. He stated that impulse noise events are those whose peak amplitudes exceed the average power of steady background noise by more than 12.5 dB (while other authors may quote a value in the range of 12 to 13 dB). His justification was that true Gaussian noise peaks exceeding 12.5 dB were so rare (0.001 percent of the time) that they could be

ignored. He then added a statement of profound importance. Since a conventional telephone type data channel runs virtually error free at a signal-to-noise ratio of about 12 dB then, for such a system, impulse noise rather than Gaussian noise should be the major type of noise contributor to any degradation in error rate. He did not, however, address the bursty nature of the noise.

The American Telephone and Telegraph Company (AT&T) [4] took a frequency domain approach and treated impulse noise as spikes of short duration which have approximately flat spectra in the band of interest. The flat spectra are shaped by the channel response characteristics so that the average spectrum approximates the frequency response of the channel itself. Cravis and Crater [7] added to this by stating that the noise was broadband, extending to 2 MHz. (These two inconsistent claims can be reconciled by assuming that two different observation points were used. The former case describes C.O. noise as observed at the customer premises while the latter describes it at the C.O. itself. Ordinary experience indicates that the frequency spectrum of contact sparking extends up to several hundred megahertz, at least. For example, operation of a light switch may cause observable interference to a nearby television set.)

The following tentative definition is suggested:

i) Impulse noise is composed of a train of distinct ideal pulses, the strengths of which are described by a given probability distribution while the time of occurrence is described by some counting process.

ii) The ideal pulses from a certain source arrive at the point of observation via some transmission path which represents the coupling of the pulses into the contaminated circuit and their propagation thereon to the point of observation. This path can be represented by a transfer function. The transfer function is considered to be unique and time invariant for each interferer.

iii) Other forms of interference may accompany the impulses but are treated as being different from them.

Item i) includes the recognized properties of impulse noise with the additional requirement that the pulses be ideal. Item (ii) modifies the ideal pulses to general types of finite duration pulses by the inclusion of the coupling network. The nature of the pulses is then altered by the coupling path: a wideband path gives pulses with a wide spectrum; a narrow lowpass path gives ones with a low frequency spectrum. Pulses with different frequency spectra are considered to come from different sources. The time invariant property of the path is purely heuristic: pulses from a given source follow the same path of a fixed geometry of dieletrics and conductors to the point of observation. Item iii) recognizes the fact that impulses are not created in isolation but are the result

of an underlying mechanism (ie. the impulse event illustrated in Figure 2.B4(a), chapter 2, is caused by something that happened in the 60 Hz. power system). The primary event itself is treated as a different phenomenon, should its amplitude be sufficiently large so as to merit its inclusion. An important consequence of this definition is that it is easy to understand and implement mathematically.

HOW IMPULSE NOISE IS CREATED:

There are many opinions on how impulse noise is generated and injected into the local loop. The consensus seems to be that:

i) Impulse noise is generated in C.O.'s by switching activity and is coupled electromagnetically (crosstalk) into the local loops entering the office. The impulse rate is then determined by the degree of electrical activity in the office, peaking during busy hours.

ii) Impulse noise may arise from electrical events outside the C.O., such as customer dialing and power line disturbances.

iii) It may be caused by the activity of maintenance personnel.

AT&T [5] described the C.O. environment in detail. A common source of impulse noise is the transients associated with switching machine operations. Some types of machine, notably panel and step-by-step, produce so much impulse noise that it is often necessary to route data circuits around offices containing these switches. Of particular interest are alarm, bay power distribution and control

leads. These leads, and the circuits they interconnect, should be operated as balanced circuits and the leads installed as twisted pairs. Single-wire-with-ground-return operation should no longer be used in the office. Another source of impulse noise is the switching systems operations that require the transfer or reversal of battery feed connections to the telephone loops (used during connect and disconnect of a call).

Cravis and Crater [7] supported this point of view. They claimed that since impulses are caused by switching, then the error rate should depend on activity, being highest during busy hours and disappearing in the early hours of the morning. Experience shows that this is not always true. As was explained in Chapter 2 of this thesis, error performance on the one sample (Nepean) of a local loop was much better during business hours than late at night.

Komiya and associates [8] mentioned that in the Japanese environment the system of metering pulses used by cross-bar switches, to determine charges, are an additional source of noise. It is said to vary according to number and calling rate of the telephone circuits.

Werner [9] found that the most damaging type of impulse noise seemed to occur when a disturbed loop shared a common cable sheath with switched voice frequency pairs. The opening and closing of the voice loop caused sharp voltage changes to be coupled into

neighboring loops through near end (NEXT) or far end (FEXT) crosstalk coupling mechanisms.

AT&T [6] has identified cable defects that decrease immunity to impulse noise (cable shield discontinuities, unbalanced pairs, and others caused by poor maintenance housekeeping).

AT&T [4], [5] and Ungar [10] listed the following collection of external effects causing impulse noise in loops:

- lightning
- mechanical devices such as elevators
- transportation systems such as subways or railways
- power line influence
- office machines such as copiers and printers
- electronic apparatus such as terminals and computers.

It then appears that one is dealing with a multitude of causes, none of which are likely to be dominant for any random selection of loops. An ensemble of local loops should then not be treated as ergodic for impulse noise purposes. This fact should influence strongly just how one models impulse noise.

NOISE CHARACTERISTICS:

Werner [9], quoting a recent loop study by The Deutsche Bundespost, characterized impulse noise by the properties:

- occurs about 1 to 5 times per minute

- has peak amplitudes in the 5 to 20 mv range
- has most of its energy concentrated below 40 kHz
- has a time duration in the 30 to 150 μs range.

A summary of the Curtis paper, which deals with the phenomena most commonly associated with impulse noise, is given below.

3.3 THE CURTIS STUDY OF SPARKING CONTACTS

Curtis [11] investigated the electrical behaviour of metallic relay contacts used to open and close the circuit to the coil of a relay and battery located at the far end of a two-wire telephone loop. Although his motive was to study the wear-out of typical current carrying contacts, his work is valuable to the study of impulse noise. It described the characteristics of typical impulse noise found in the loop plant and how it was generated.

The Curtis paper, although over half a century old is still useful for our understanding of the underlying impulse noise phenomena. Mechanical-electrical contacts and D.C. operated relays are still commonly used with telephone cables. Commercial power distribution systems still use electromechanical switching devices. Crosstalk between pairs in the same cable as well as from nearby power lines provides a strong means for impulses to be coupled into a digital data circuit. It also provides an explanation for the fact that impulse noise tends to occur in infrequent but long bursts.

His investigation of the sparking contact was based on wideband cathode ray oscilloscope observations of the transient currents and voltages in representative telephone loops. The range of circuit designs studied was:

i) Standard 22 gauge telephone twisted pair cable with a surge impedance of 100 ohms and length ranging from 10 to 1,100 ft. One conductor of the pair was connected to ground at each end, unbalancing the pair. (It is standard practice to ground the positive terminal of the C.O. battery.)

ii) A telephone relay with D.C. coil resistance varying from 500 to 1000 ohms was connected, in series with a battery, to the far end of the loop.

iii) A low impedance battery supply, having terminal voltages ranging from 50 to 250 volts was used, giving a steady state loop current of less than 1.0 ampere.

iv) Relay contacts made of either silver, palladium or tungsten were connected to the near end of the loop.

Curtis included a selection of 27 oscillograms of contact voltages and currents which he used to support his conclusions. For our purposes they serve to illustrate the large variety of impulsive signals that can be generated by such a simple circuit arrangement.

Curtis concluded the following:

i) For steady state currents between 0.5 and 1.0 ampere, during the (bounce free) closing of the contacts, dozens to hundreds of

impulses were generated. Peak amplitudes ranged from 5 to 10 amperes and pulse widths were close to 1 μs. During the first 10 μs after closure of the contacts, a waveform somewhat resembling a damped sine wave, with a period determined by line length, was observed. This resulted because the self capacitance of the relay coil, rather than its inductance, was dominant during this interval of time. As the inductive effect of the coil took over, the current in the circuit increased more slowly. During the time that the contacts were still coming together and until they were in firm contact the following took place:

- When the contact surfaces reached a certain point, the air between them broke down and conducted electricity.
- The contact surfaces were heated by the current, causing the metal to melt and flow. A thin metal bridge was formed between the contacts, short circuiting them. The air between the contact surfaces then ceased to conduct.
- The current density was then so high in the metal bridge that it evaporated explosively, making the contacts open circuited once more.
- The air ionized again, and the cycle repeated many times until the contacts closed fully. A string of spikes, a few μs apart, was generated during these events. The above process was repeated hundreds of times as the contacts bounced (opened and closed mechanically) at about a 1 ms period. A train of distinct bursts of high amplitude impulses was thus generated by this process.

ii) In the case of lesser steady state currents, the closure of the contacts merely discharged the line causing no spiking. However, contact bouncing tended to chop the transient current, causing bursts of single spikes.

iii) For steady state currents between 0.4 and 1.0 ampere, a metallic arc (plasma) was formed on contact opening to maintain an initial voltage difference of 15 volts, rising to a final value below 30 volts. After several milliseconds, the arc went out leading to a complex transient lasting approximately one millisecond. There are many variations of this basic action, depending on initial current, contact condition and line length. The most common and destructive kind, termed the "B" transient, is illustrated in Figure 3.3.1.

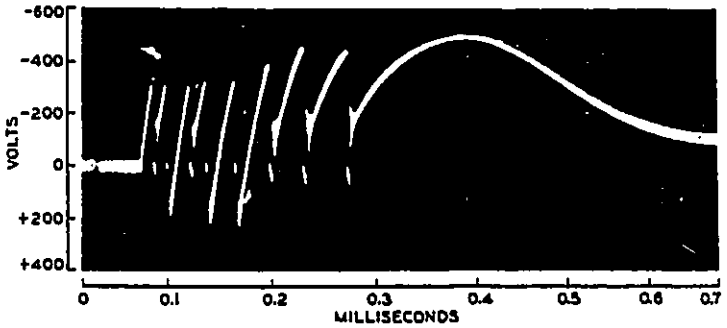

Fig. 3—Entire "B" transient (voltage).

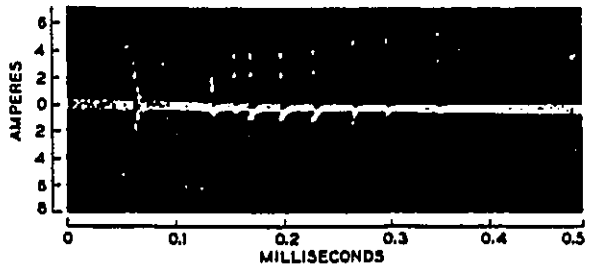

Fig. 4—Entire "B" transient (current).

(taken from Curtis [11])

Figure 3.3.1 "B" Transient Responses

The voltage and current curves were made from measurements taken at the sparking contacts. The impulse voltages reached values of nearly 800 volts, peak-to-peak. The peak-to-peak current reached nearly 10 amperes. The B transient resembles, in many respects, those which occurred during contact closure. This can be explained as follows. Imagine that the current carrying contacts are separating slowly. As they move, their area of contact decreases, until finally the metal at the point of contacts becomes overheated and explodes. The evaporated metal forms the plasma of the ensuing constant voltage arc. The molten metal then closes the gap, causing the contact voltage to go to zero. This action repeats many times, until the contact distance becomes too great to support conduction. It is apparent that this high amplitude series of impulses has the potential for interfering with a digital system.

This model of the sparking contacts should be kept in mind while an impulse noise model is being described.

3.4 THE MERTZ MODEL

The work of Mertz [12], which is now over thirty years old, is the pioneering work in creating a model for impulse noise. It was his intention to develop a model that was simple enough to be used in practice yet capable of giving reasonable accuracy.

Mertz assumed that the probability density function for impulse noise could be represented by two independent density functions, one for the amplitude of the event and another for its time of occurrence. This two distribution approach has been used by most of those who followed.

Mertz used a hyperbolic distribution to represent impulse amplitudes in the forms shown below:

$p(x)$ = the probability density function of the impulse peak voltage, x and

$P(x)$ = the cumulative probability of x.

$$p(x) = \frac{nh^n}{(x + h)^{n+1}} \quad ; \text{ where: } h \text{ and } n \text{ are positive constants and } x \geq 0$$

$$P(x) = \frac{h^n}{(x + h)^n} \quad \text{and}$$

$$\text{Variance} = \sigma^2 = \frac{2h^2}{(n-1)(n-2)}$$

Mertz said that there was experimental evidence to support his use of the distribution. (He did show that the Gaussian and Rayleigh cumulative functions track each other closely but clearly deviate from that of the hyperbolic.) Mertz stated that in practice that n is greater than 2 and as large as 5, avoiding the singularity in the variance that occurs for n = 1 or 2. He noted that this distribution is a variation of the Cauchy distribution and of

Zipf's law (also of the Pareto distribution of Mandelbrot, per Section 4.3 of this thesis).

Mertz briefly considered candidates for the impulse burst size distribution but was unable to make any headway with this problem.

He next considered modeling the quiet periods between bursts by selecting a form for Q(0,a,y), the probability of finding zero errors in a period y minutes long, for an average of a errors per minute. The Poisson model gave:

$$Q(0,a,y) = e^{-ay}.$$

He next considered a hyperbolic model which gave:

$$Q(0,a,y) = \frac{K(a)}{y - K(a)} \text{ ; where } K(a) \text{ is a function only of a.}$$

He found that the hyperbolic model did not represent the experimental data very closely, but was much better than the Poisson in this regard.

We will discuss Mertz's work on burst errors in Section 4.4.

Three years later, Fennick [13] evaluated the work of Mertz using a "vast amount of data" provided to him by the operating companies of AT&T. He found that the hyperbolic distribution, for impulse

amplitudes, was able to fit about 98% of the empirical data. Fennick verified that the quiet interval distribution of the data fit the hyperbolic distribution much more closely than did the Poisson. He used the experimental data to plot burst length probability density functions but did not attempt to develop a model. (Figure 3.4.1 shows these.) The density peaked near 1.2 ms and vanished near 10 ms.

Cases with pulses shorter than 6 ms.

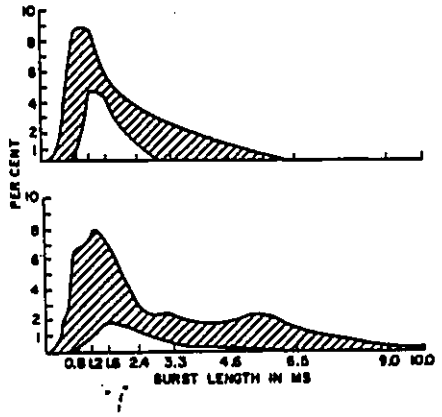

Cases with pulses longer than 6 ms.

Fig. 5. Burst-length distributions envelope of frequency functions

(taken from Fennick [13])

Figure 3.4.1 The Burst Length Distributions

Engel [14], in 1965, used the Mertz model to compare the performance of various bandpass modulation schemes. (The results of this are discussed later in Section 5.7.2.) He derived a passband impulse noise signal by using the baseband signal to amplitude

modulate a sinusoidal carrier located at channel center frequency. He considered the frequency spectrum of an impulse as that of the channel itself (which in the time domain is equivalent to treating it as an ideal impulse applied to the transmit end of the channel). Three random variables were used in the model:

i) one for baseband pulse peak amplitude

ii) one for passband pulse phase

iii) one for time of occurrence of the pulse.

He used the Mertz model for the distribution of peak amplitudes expressed in the form:

$$Pr[K > x \mid K > K_0] = (K_0/x)^{2\alpha}; \quad \text{for } x > K_0 \text{ and } \alpha > 1.$$

(This of course is the Pareto form of the distribution.)

The signal phase was treated as uniformly distributed over $[0,2\pi]$.

He stated that he did not have a reasonable choice for the probability distribution of the inter burst times. As a practical matter,he used the exponential density function and others, that he did not specify, for simulation purposes. The exponential distribution of inter burst times implied that burst arrivals were Poisson distributed.

In 1989, Széchényi [15] applied his version of the Mertz model to an investigation of the error performance of 144 kbps Integrated Services Digital Network (ISDN) access facilities, using two-wire local loops (which employ multi-level baseband transmission). He

used the results of a recent and extensive Deutsche Bundespost local loop study to support this model. (The loop study was composed of 4,392 hours of surveillance made on 150,000 impulse events on a total of 175 local loop pairs.) This data was used to provide a close fit to the peak impulse voltage cumulative distribution function of the form:

$$P(v) = (5/v)^2 \quad \text{for } 5mv \leq v \leq 40 \text{ mv}$$

$$P(v) = (0.625/v) \text{ for } \quad v \geq 40 \text{ mv.}$$

The data and the curve fitted to it are shown in Figure 3.4.2.

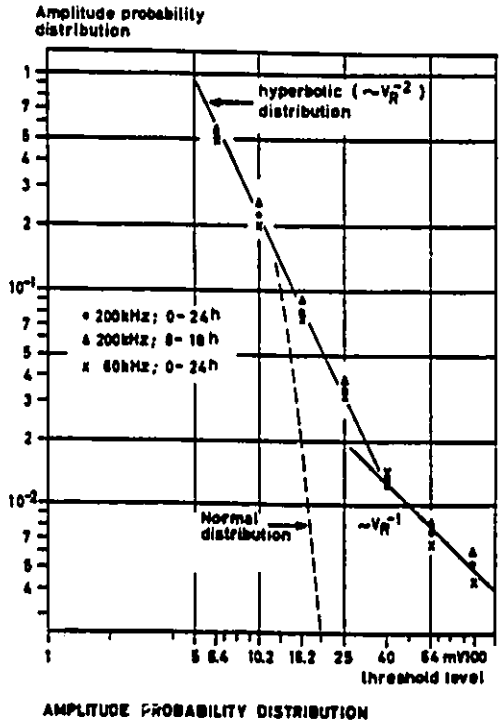

Fig. 6

Amplitude probability distribution $P_R(v_p)$ measured with different receiver-bandwidth and in different daily intervals.

(taken from Széchényi [15])

Figure 3.4.2 Amplitude Distribution of Hyperbolic Function

This is the strongest evidence yet for using the hyperbolic distribution to describe impulse amplitudes. The use of two distributions over the signal range may be indicative of two separate mechanisms for generating impulse noise, one strong and the other weak.

Széchényi showed that the arrival data of impulses does not fit a single Poisson process but fits a linear combination of several such processes very closely. This, again, is evidence of the possibility that impulse noise comes from separate processes.

Werner [16], [9], in 1991, used the Széchényi results to simulate the performance of the 1.544 Mbps High Data Rate Subscriber Line (HDSL). He found that impulse noise limited the bit error rate to slightly less than 1 in 10^7.

To summarize the contents of this section, it can be said that: The Mertz model for impulse noise in the local loop environment has been verified experimentally and refined by several users to the form:

i) The cumulative probability function for peak impulse amplitudes can be expressed as a hyperbolic function.

ii) The arrivals of impulses can be described as a linear combination of several distinct Poisson distributions, or a single one if less accuracy is acceptable.

3.5 THE FENNICK MODEL

In 1965, Fennick [17] published the results of an impulse noise study that he had performed on both radio and cable systems. He addressed only the peak amplitude distribution of impulse bursts and not their time distribution.

The study involved making analog recordings of noise bursts and analyzing them later, digitally, using a sampling rate of 15 kHz. Half hour recordings were made on each of 37 channels, 20 of which were radio based and 17 cable based. All the channels were derived from carrier systems and consequently were limited to bandwidths of 4 kHz. Caution should be exercised in applying the results to high data rate baseband cable systems.

Fennick fitted the data to the following forms:

$$p(x) = \begin{cases} 0; & x < -b \\ ce^{kx}; & -b \le x \le -a \\ q(x); & -a \le x \le a \\ ce^{-kx}; & a \le x \le b \\ 0; & x > b; \end{cases} \qquad \text{where:}$$

p(x) = probability density function of the total noise voltage (background plus impulse)

x = maximum amplitude of the impulse burst

a, b = constants (a represents the limiting amplitude of

the background noise process while b represents the channel saturation voltage)

$q(x)$ = probability density function of a zero mean Gaussian noise process with variance σ^2

c, k = constants of an exponential density function.

The experimental data, plotted in Figure 3.5.1, supports this decision. (The extremities of the curve are approximately linear, on a logarithmic scale, and so may be represented by an exponential function. Data was not available for the middle portion of the curve, so a Gaussian curve was fitted to it.)

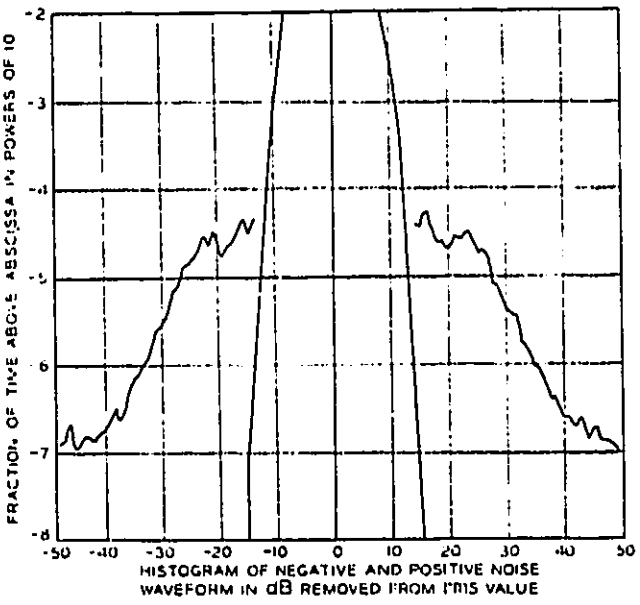

(taken from Fennick [17])

Figure 3.5.1 Noise Amplitude Histogram

This data was used to find the values for the constants:

k = 0.45 mean with an estimated standard deviation of 0.46

c = 0.0028 median value

a = 4.26σ

b = not quoted.

As a practical matter, we could simply treat the impulse noise component as being exponentially distributed and defined only for values of x exceeding a.

Fennick has contributed a useful method for accurately finding the amplitude density function of impulse noise on a cable facility.

3.6 THE MODESTINO MODEL

The Modestino model is important because of its successful application to a wide range of situations. Over seven papers, dealing with impulse noise, have been written by Modestino and his associates. (In this thesis "Modestino" will be used to refer to the work of Modestino and his many associates. The names of the others are given in the list of references.)

The Modestino model for impulse noise, which is based on the Dirac delta function, was in common use by earlier investigators (In 1974

Bender, Kneuer and Lawless [1], for example, did a rigorous analysis on the DDS access loop. They described the properties of the delta function without mentioning it by name.) Nobody, it seems, has used the delta function as extensively as Modestino has.

In 1983 Modestino [18] constructed his model as part of the noise element of a software based, general purpose, Monte Carlo simulator. This noise element was composed of a Gaussian noise process and a "low density noise process" which we know as an impulse noise process. Impulse noise was represented by:

$$u(t) = \sum_{i=0}^{N(T)} U_i \delta(T - T_i); \text{ where:}$$

U_i is a sequence of complex independent identically distributed (i.i.d.) random variables used to represent in-phase and quadrature (I&Q) components. The U_i density function is not specified but is chosen for each situation, from a range of commonly used density functions.

$\delta(T)$ is the Dirac delta function.

$\{N(T), T \geq 0\}$ is a counting process whose event times are described by the sequence $\{T_i\}$. More specifically, $\{N(T), T \geq 0\}$ undergoes a unit jump at each of the event times $\{T_i\}$. The process was not specified but was to be

chosen for each application. A Poisson process is a good example of a counting process.

He emphasized the I&Q nature of U_i by expressing it as:

$U_i = U_{ci} - jU_{si}$; $i = 0,1,2,...$; where:

$U_{ci} = R_i\cos\theta_i$; $i = 0,1,2,...$,

$U_{si} = R_i\sin\theta_i$; $i = 0,1,2,...$; where:

$\{R_i\}$ is an i.i.d. sequence possessing common probability density function f(R). An appropriate choice for this, in many applications, is said to be the Power-Rayleigh distribution, shown below.

$\{\theta(i)\}$ is an i.i.d. sequence uniformly distributed over the range $[-\pi, +\pi]$.

The peak amplitude of the impulse noise was specified by the impulse to Gaussian noise power ratio:

$$\gamma^2 T_s = \frac{E[|u(t)|^2]}{F_s N_0/2}$$; where:

$u(t)$ = the complex impulse noise signal

T_s = $1/F_s$, the data pulse width, seconds

F_s = the data signalling rate, baud

N_0 = the two-sided Gaussian noise spectral power density, w/Hz.

The Power-Rayleigh probability density function was given as:

$f(R) = \left[\frac{\alpha R^{\alpha-1}}{R_0^{\alpha}}\right] \exp -(R/R_0)^{\alpha}$ for $R \geq 0$; where:

$0 < \alpha < 2$

R_0 = a constant defined by the power ratio $\gamma^2 T_s$.

The following two tables summarize the seven Modestino papers. Table 3.6.1, Impulse Noise Characteristics, shows the parameters of the Modestino model used for different applications:

i) SOURCE is the identification number for the reference.

ii) f(R) is the probability density function for the peak amplitudes of the impulses.

iii) N(T) is the probability distribution for the impulse arrivals.

iv) PULSE SHAPE is the time waveform of the noise impulses at the data receiver threshold device. Those shown as "$\delta(t)$" represent ones having a Dirac delta waveshape while the others represent $\delta(t)$ distorted by the coupling mechanism to the threshold device.

v) DATE is the publication date of the paper.

TABLE 3.6.1

Impulse Noise Characteristics

SOURCE	f(R)	N(T)	PULSE SHAPE	DATE
[18]	Rayleigh	Poisson	Exponential	1983
[19]	Gaussian	Poisson	δt)	1984
[20]	Gaussian Laplacian	Poisson	δ(t)	1986
[21]	Rayleigh Weibull	Gamma Poisson	δ(t) Butterworth Spectrum	1987
[22]	Exponential Gaussian	Poisson	δ(t)	1987
[23]	Gaussian	Poisson	δ(t)	1988
[24]	Gaussian	Poisson	δ(t)	1990

Table 3.6.2, Application Characteristics, shows the type of application specified in each paper and the important characteristics of the system employed in each.

TABLE 3.6.2

Application Characteristics

source	APPLICATION	SYSTEM DESIGN
[18]	Universal	BPSK and QPSK
[19]	Digital access loop	2-wire, baseband, bipolar, time compression multiplexing (TCM), 200 kbps
[20]	Digital access loop	2-wire, baseband, bipolar, TCM, 200 kbps
[21]	Radio	Spatially distributed noise sources using adaptive antenna array, signal clipping, Viterbi decoder, deliberate pulse jamming
[22]	Digital access loop	2-wire, baseband, bipolar, TCM, 200 kbps
[23]	Digital access loop	2-wire, baseband, bipolar, TCM, Viterbi decoder, error correction coding, errors and erasures, 200 kbps
[24]	Digital access loop	2-wire, baseband, bipolar, TCM, Viterbi decoder, error correction coding, errors and erasures, 200 kbps

Paper [18] used the simulator to demonstrate the use of the zero memory nonlinear (ZMNL) family of devices to effectively suppress impulse noise. The ZMNL devices include peak clippers or limiters, hole punchers and Butterworth devices. Section 5.3 describes these devices.

The five papers dealing with local loop transmission have much in common in that they all dealt with 2-wire baseband transmission using bipolar signalling at 200 kbps with Time Compression Multiplexing (TCM).

Papers [19], [20] and [22] gave the results of investigations of the performance of a conventional loop transmission system (which used threshold detection without coding). Paper [19] showed that severe error performance degradation resulted from even small amounts of impulse noise in a system also subject to FEXT and additive white Gaussian noise (AWGN). Paper [20] repeated this study using impulse noise data collected during a local cable plant study. It showed that, at a data rate of 200 kbps, impulse noise causes performance to fall below acceptable limits ($P_{bit} = 10^{-6}$), at a cable length of two miles. Paper [22] showed that for data rates of 64 kbps or higher, that a bit error rate less than 10^{-6} could not be obtained with a 9 kft local loop, because of impulse noise.

Papers [23] and [24] investigated the effects of more complex schemes than those mentioned above. Error control coding, erasure decoding and Viterbi decoding were treated. The results indicated an advantage in each. Chapter 5 discusses these items in detail.

It appears that Modestino and his associates have constructed a useful model of impulse noise for use in a computer based Monte Carlo simulation system. They used this system to show how normal levels of impulse noise could severely degrade the performance of baseband local loop transmission systems and how certain special techniques could be used to remedy this.

3.7 THE POTTER AND SMITH MODEL

The Potter and Smith paper [25], published in 1985, showed how current interruptions in a cable pair could generate impulse noise in other pairs in the same cable, causing bit errors in a digital system. The next paragraph briefly describes their model.

A pulse dialing type of telephone line, originating at an analog type C.O. switching machine and terminating on a distant customer telephone set, was used as the noise source. The noise was coupled into a data pair by crosstalk and propagated along the pair to the data receiver. A conventional type receiver for alternate mark inversion (AMI) signals was used. Inside the receiver, the impulse noise was fed through the line equalizer and the receiver predetection filter to a threshold detector. The writers took pains to ensure that each element of the impulse noise path was represented by a highly realistic mathematical model. For example, the telephone and data pairs were represented by the transmission line equations. A solution to the mathematical model for an AMI data

system operating at 2,048 kbps was compared to the results from a laboratory hardware model (using real relays etc.). The theoretical results agreed with the experimental within 1 dB.

The impulse noise source was modeled by a step voltage, excluding its D.C. component, applied to a transmission line. The source contained circuit components that unbalanced the line (which usually happens in practice). The impulse was then propagated on the telephone pair in differential and common modes. It was shown that only the differential mode signal was important, the common mode signal being highly attenuated. The step voltage was generated in bursts in an attempt to match the complex contact operation described by Curtis [11]. The burst rate was set to that of pulse dialing. Dialing events were set to agree with digit size and calling rate corresponding to the busy hour of a typical telephone exchange.

The Potter and Smith model is a good example of how impulse noise can be modeled for a particular situation. The writers were successful because they chose carefully the class of events that they wished to model and then investigated their properties in detail before attempting to create the model. This approach should give valid results for representing the many other impulse noise scenarios.

CHAPTER 4

BURST ERROR MODELS

4.1 GENERAL COMMENTS

The purpose of this chapter is to explain the three most commonly used mathematical models for burst errors and discuss their suitability for representing the effects of impulse noise.

Errors show up as incorrect symbols in a discrete serial data stream. They are usually visualized as bit errors in a binary data sequence. The following representation is used to simplify matters:

$r_k = e_k \oplus s_k$, where:

s_k = the error free source data sequence

r_k = the recovered data sequence containing bit errors

"$\oplus$" = modulo 2 addition

e_k = the error sequence with ONE representing the introduction of a bit error and ZERO representing no error.

The study of transmission errors is then carried out as the more concrete task of investigating the pattern of ONE's and ZERO's in sequence e_k. Probability density as well as correlation functions are sought which can be used to represent the error patterns for a good many local loop based channels.

The following process is often used to select a probability model to represent burst errors:

i) A candidate model is chosen on theoretical grounds and adjusted to fit a set of error data from some well recognized burst error study. This is done by selecting the constants of the model to make it match the experimental values (eg. mean, variance, correlation coefficient etc.) as closely as possible (eg. by a minimum least square errors procedure).

ii) The accuracy of the model is verified by measuring its consistency with the original data (eg. by the size of least square error).

The above requirement is a necessary but not sufficient condition for evaluating the quality of a burst error model.

Other important considerations are:

i) Is the model defined by only a small number of arbitrary constants? A minimum number usually makes it easier to evaluate the constants for a given set of experimental data. From a philosophical point of view, a minimum number of constants indicates that the form of the mathematical law itself tends to describe the error generating mechanism. As the number of arbitrary parameters increases, the problem tends to become an exercise in blind curve fitting.

ii) Is the model sufficiently versatile so that it can represent differing error patterns? For a given impulse noise process, the

received error patterns are strongly influenced by the coding and modulation schemes used. It is important that the same type of error model apply to each.

The following burst error models were investigated with these factors in mind.

4.2 THE GILBERT MODEL

Gilbert proposed [26], in 1960, that burst errors be modeled by the simple two state Markov process shown in Figure 4.2.1.

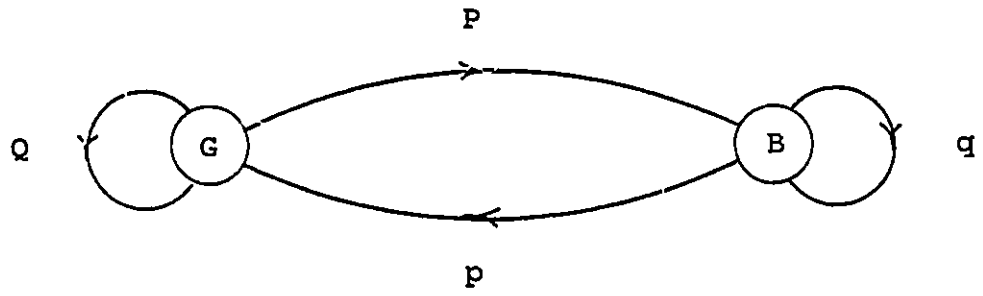

Figure 4.2.1 The Gilbert Model of Burst Errors

Two states of the system are defined:

G = the "good" state of the channel when it runs error free

B = the "bad" state of the channel when it may generate errors.

The state transition probabilities are:

P = the probability of a transition from state G to state B

p = the probability of a transition from state B to state G

Q = the probability that state G is maintained

q = the probability that state B is maintained.

Bit errors occur according to:

h = the probability that a symbol is error free (ie. $P_{bit} = 1 - h$) while the system is in state B.

It should be noted that only three independent constants are required to define the Markov process, with P, p and h being typical choices.

A change of state is permitted to occur only just before the channel outputs a symbol and remains fixed until just before the next symbol leaves.

The magnitudes of the above parameters define the nature of the error process. For example:

i) A binary symmetric memoryless channel is represented by the case with: P = 1.0 and p = 0.0, Q = 0.0 and q =1.0.

ii) An extremely bursty channel is represented by making: P very close to 0.0, p very close to 0.0, Q very close to 1.0, q very close to 1.0 and h close to 0.5.

iii) A "typical" channel was said to be described by: P =0.03, p = 0.25, Q = 0.97 , q = 0.75 and h = 0.5. Gilbert showed a pattern of 500 bits generated by this process. One, two

or three errors were separated by between four and sixty error free bits.

iv) A fit was made to the data from two voice frequency channels investigated by Alexander, Gryb and Nast [27] with the following values found: P= 0.003, p =0.034, Q = 0.997, q = 0.966 and h = 0.84.

The Gilbert model has the great advantage of clarity. Given a set of values for P, p and h, it is very easy to visualize how a system using this model would behave.

Gilbert developed an algorithm for evaluating P, p and h from experimental error data which he demonstrated with the Alexander data. He included a graph of error free run-length probabilities, as a function of run-length, showing the Alexander data and the fitted model. The two tracked each other closely over the entire run-length range.

Since the model is based on a non-degenerate Markov chain, the Shannon channel capacity is known to exist [51]. This allows one to compare the performances of local loop systems, with varying degrees of burst error impairments, on a recognized scientific basis. The following equation was derived by Gilbert:

$$C = 1 + P(1)\sum_{K=0}^{\infty} v(K)\log_2 v(K); \quad \text{where:}$$

C = channel capacity, bits per symbol

$P(1) = P_e = \frac{(1-h)P}{P+p}$

$v(K) = \frac{[1-h]}{J-L}[(qJ + p - Q)J^K - (qL + p - Q)L^K]$

$J = \frac{Q + hq + \sqrt{(Q + hq)^2 + 4h(p - Q)}}{2}$

$L = \frac{Q + hq - \sqrt{(Q + hq)^2 + 4h(p - Q)}}{2}$

Gilbert included a derivation of a formula for error covariance.

One last property of this model is that it can be used to represent either a memoryless or memory type channel, of varying degree.

In 1963, Elliott [28] showed techniques for using the original Gilbert model to find exact solutions to a number of problems. He derived an exact expression for P(m,n), the probability of m errors in a block of n bits, from values of P, p, h. He used this to derive equations representing the probability of undetected errors in linear block error correcting codes. As an example, he used the Gilbert model for the Alexander telephone channel study [27] to calculate the failure rates of 29 such codes.

Elliott also considered a more general form of the Gilbert model by allowing errors to occur while the system was in the G or "good"

state. He added a new parameter, k, which was the probability of error free operation (ie. $P_{bit} = 1 - k$) while in state G, corresponding to h for state B of the original model. He derived an expression for P(m,n).

In 1968, McCullough [29] created a modified form of the Gilbert model by making the following changes to it:

i) His model allowed for many states with transitions from any one to any other. A probability of error was defined for each state.

ii) Transitions from one state to another could occur only immediately after a bit error had occurred, which simplified the algebra involved.

McCullough used this model to achieve the following important results:

i) He derived an expression for a bound of the Shannon channel capacity of his model (but not the capacity itself).

ii) He derived expressions for error separation, block error and burst statistics for a two state Markov process.

iii) He used a three state model to represent error events recorded on three 24 mile long T-1 digital lines. Curves of the cum -ulative probability function for inter-burst intervals, in bits, are shown in Figure 4.2.2. It is apparent that the model represents the situation accurately.

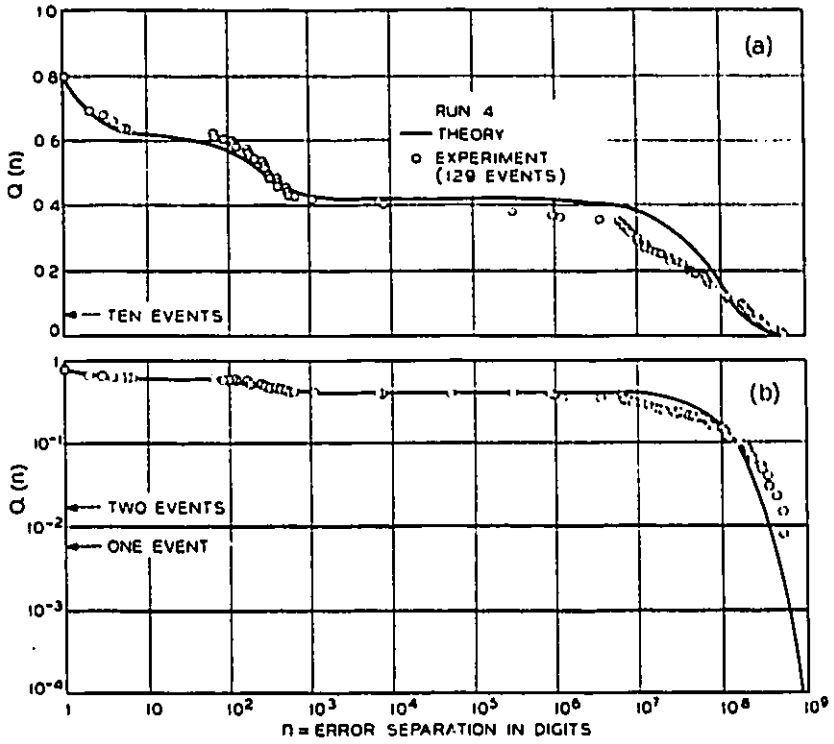

Fig. 3 — Error separation statistics for T1 digital transmission line.

(taken from McCullough [29])

Figure 4.2.2 Cumulative Probability of Error Separation

In 1973, Chao [30] extended our knowledge of the properties of the Gilbert model. He investigated the statistical properties of a random variable, equal to the number of bit errors in a block of n bits, Z_n, finding:

i) the covariance of Z_n,

ii) the closed form moment generating function for Z_n,

iii) that in the limit, for a small probability of bit error, the process $\{Z_n(t): t > 0\}$ becomes Poisson.

In 1988 William Turin [31] used the stochastic sequential machine model (SSM) as an extension of the Gilbert model to represent a most general error process. He stated that the new model could be used to simulate a manifold of characteristics and impairments in a communications system. Channel crosstalk (FEXT and NEXT), ISI, AWGN, Channel nonlinearity, burst errors, data scrambling, as well as error decoding could all be built into the one structure. The Turin approach may be an effective way of modeling a real transmission system, although it appears to be rather laborious to set up.

In 1991, Kumozaki [32] extended the Gilbert model to a three state process which he used as a burst error source to investigate the performance of a 200 kbps digital loop system. Figure 4.2.3 shows the Markov state diagram for this design.

Kumozaki tested his error model, as part of a computer type simulator, against a prototype hardware system. The model employed TCM operating at 200 kbps and 16 bit delay interleaving with a Hamming (13,9) code. The results are shown in Table 4.2.1.

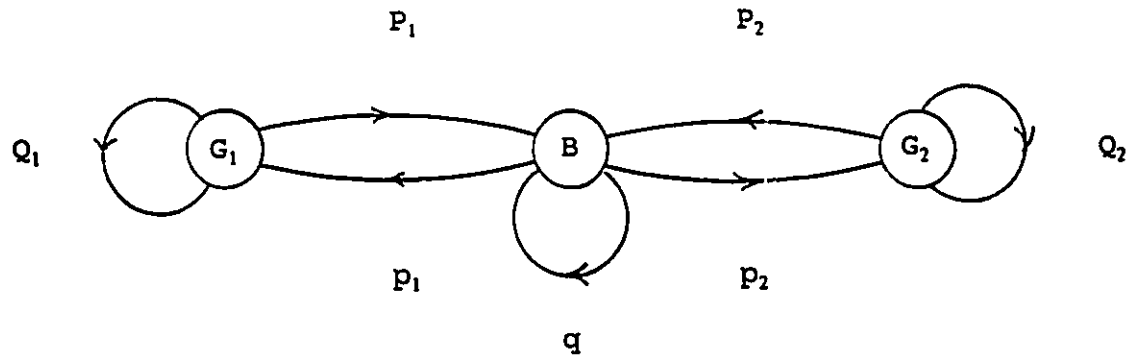

Figure 4.2.3 The Kumozaki Model of Burst Errors

Three states of the system are defined:

G_1 = the "good" state one of the channel when it runs error free

G_2 = the "good" state two of the channel when it runs error free

B = the "bad" state of the channel when it generates errors.

The state transition probabilities are:

P_1 = the probability of a transition from state G_1 to state B

p_1 = the probability of a transition from state B to state G_1

P_2 = the probability of a transition from state G_2 to state B

p_2 = the probability of a transition from state B to state G_2

Q_1 = the probability that state G_1 is maintained

Q_2 = the probability that state G_2 is maintained

q = the probability that state B is maintained

Bit errors occur according to:

h = the probability of error free operation (ie. $P_{bit} = 1 - h$) while in state B.

The model, which is based on five independent constants, was fitted to experimental error data from a T-1 digital repeatered line to give the following typical values:

$P_1 = 4.88 \cdot 10^{-4}$, $P_2 = 7.67 \cdot 10^{-9}$, $p_1 = 8.53 \cdot 10^{-2}$,

$p_2 = 2.15 \cdot 10^{-1}$ and $1 - h = 0.527$

TABLE 4.2.1

Experimental Results

	P_{bit} (Experimental)	P_{bit} (Theoretical)
without error correction	$1.1 \cdot 10^{-8}$	$1.9 \cdot 10^{-8}$
with error correction	$1.4 \cdot 10^{-10}$	$9.3 \cdot 10^{-11}$

(taken from Kumozaki [32])

It appears that the Kumozaki model was very successful in representing burst errors.

The original Gilbert model of impulse noise has evolved to more complex configurations under the influence of subsequent investigators. The newer designs appear to increase both the accuracy and versatility of the model in achieving its ends.

Nevertheless, the original model represents burst errors adequately while exhibiting structural simplicity and ease of application.

4.3 THE MANDELBROT MODEL

Berger and Mandelbrot [33], in 1963, suggested that the Pareto distribution could be used to model burst errors in a communication channel. The Pareto distribution seemed to be a good choice for this since it could be used to represent events that were tightly clustered in bursts, which in turn were separated by long periods of inactivity. The following cumulative distribution was used:

$F(t) = Pr(T_n - t_{n-1} < t)$, where:

T_n = the instant of time at which error number n is to occur

t_{n-1} = the instant of time at which error number n -1 occurred

$1 - F(t) = t^{-a}$ for t small

$1 - F(t) = Pt^{-b}$ for t large, where: a, b and P are positive constants

The following should be noted:

i) t can never be less than 1.0 to keep F(t) a real positive number less than 1.0,

ii) the constants a, b and P must be constrained to keep F(t)

continuous at the crossover point from small to large values of variable t,

iii) inter-error times are assumed to be statistically independent.

$F(t) = 1 - t^{-a}$ can be differentiated to show, for $t > 1$, that the probability density function is $f(t) = at^{-(a+1)}$. This can be used to show the following peculiarities of the Pareto distribution:

i) For $0 < a < 1$ there are no moments of any order.

ii) For $1 < a < 2$ only the first moment exists.

Mandelbrot demonstrated that the Pareto model is not consistent with Shannon information theory. For a Pareto channel, he noticed that the average number of bits in error goes to zero as the word length increases to infinity. In spite of having uncorrectable errors in the channel, the channel capacity C, becomes unity. This implied that the infinite limiting operations of information theory could not be applied to the Pareto channel.

The tail of the Pareto cumulative distribution function represents a linear function when expressed logarithmically as:

$$\log\{Pr(T_n - t_{n-1} > t)\} = -a\log\{t\}.$$

Log-log plots of the inter-error times were shown for data supplied by the German Postal Administration. This was unpublished data from a field study of error performance of frequency and phase shift

keyed (FSK and PSK) systems, operating at 1200 bps and using samples of dedicated and switched voice grade channels. The curves, shown in Figure 4.3.1, being almost linear, supported the use of the model.

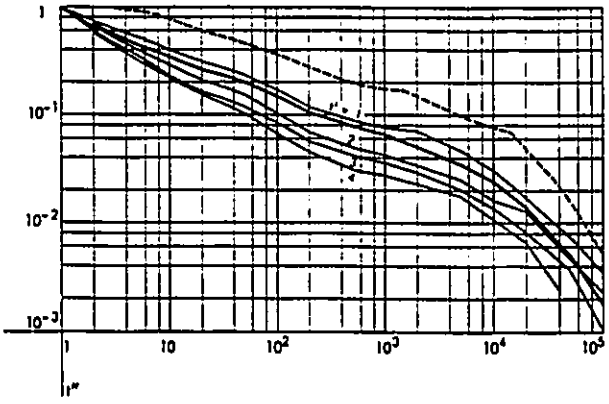

Figure 3 **Cumulated doubly logarithmic plots of empirical inter-error distributions at the transmit level of −22 dbm.** *Bold line: marginal (unconditioned) frequencies Pr* $(T_{n+1} - T_n \geq t'')$. *Dashed line: marginal frequencies* $Pr(T_{n+3} - T_n \geq t'')$. *Thin lines (looking from the top down): conditioned frequencies* $Pr(T_{n+1} - T_n \geq t'')$, *when* $T_n - T_{n-1} = t'$), *for the following values:* $t' = 1$, $t' = 2$, $t' = 3$, $t' = 4$. *The peculiar behavior for* $t' = 1$ *is discussed in the body of the paper.*

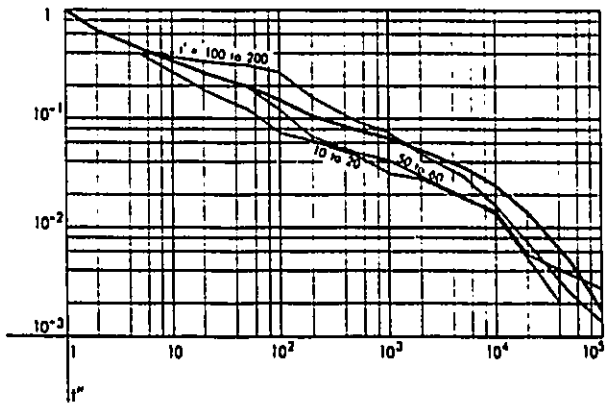

Figure 4 **Cumulated doubly logarithmic plots of empirical inter-error distribution at the transmit level of −22 dbm.** *Bold line: same as in Fig. 3. Thin lines (looking from the top down, in the region of* $t'' = 100$*): conditioned frequencies corresponding to the following ranges of values of* t' : t' *between 100 and 200,* t' *between 50 and 60,* t' *between 10 and 20.*

(taken from Berger and Mandelbrot [33])

Figure 4.3.1 Double Logarithmic Plots of Experimental Data

Sussman [34], in 1963, modified the Mandelbrot-Berger model slightly to avoid the singularity in the density function at t = 0 by using the variation:

$$G_1(t) = Pr(T_n - t_{n-1} \geq t) = 1.0; \quad \text{for } t < \delta$$
$$= (\delta/t)^a; \quad \text{for } t \geq \delta, \; a > 0$$

Setting $\delta = 1.0$ gave:

$$G_1(t) = 1.0; \quad \text{for } t < 1$$
$$= t^{-a}; \quad \text{for } t \geq 1$$
$$g_1(t) = at^{-(a+1)}; \quad \text{for } t \geq 1.$$

He said that experimental evidence showed that parameter a lies in the range (0,1), which gives the distribution a mean value of infinity. He eliminated this possibility by defining L, a positive finite constant, as the upper limit of t. This model was fitted to the data of Alexander, Gryb and Nast [27] (for 600 bps operation over telephone circuits), using the log-log format of Mandelbrot and Berger. Curves of the cumulative inter-error distribution, shown in Figure 4.3.2, indicate that a very close fit resulted. Four different values were found for constant a, which clustered around a = 0.115.

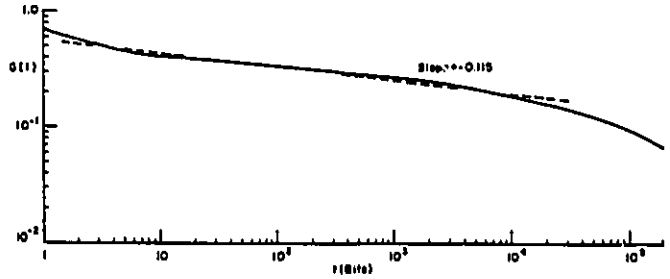

Fig. 1—$G(t)$ is the probability that the interval between successive errors exceeds t bits. (Fig. 30, All Calls [1].)

(taken from Sussman [34])

Figure 4.3.2 Double Logarithmic Plots of Experimental Data

Elliott [35], in 1965, considered a model represented by a renewal process. (A renewal process is one in which all inter-error periods are i.i.d. The Pareto process is one such process.) He represented the results of the Alexander, Gryb and Nast (AGN) [27] study as curves of P(m,n), the probability of exactly m bit errors in a block of n bits, for n the independent variable and m a parameter. He showed curves for seven values of m, all which had similar "S" type shapes. He fitted three different renewal distributions to the plotted values, one to each tail and one for the centre portion of the curve. The resulting curves matched the experimental values

extremely well, as can be seen in Figure 4.3.3. (The three fitted curves are shown by solid lines; the Alexander Gryb and Nast curve is dotted.)

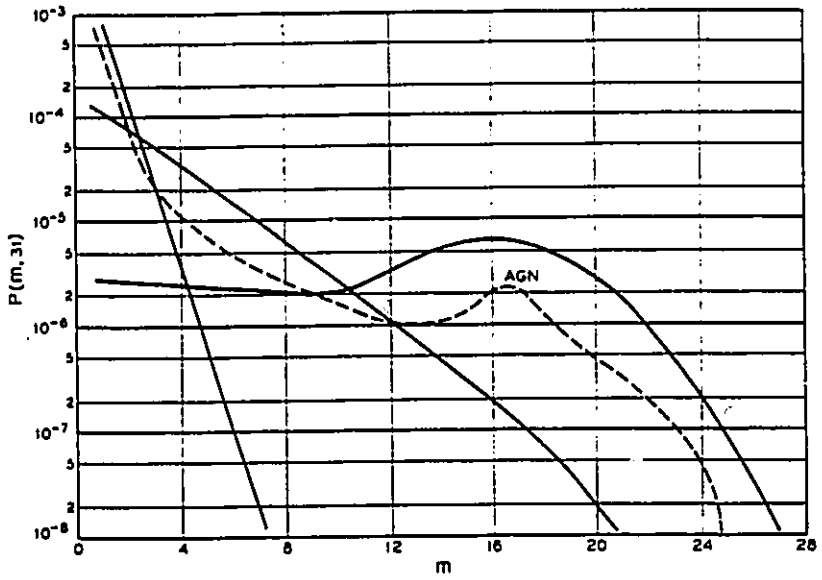

Fig. 2 — $P(m,31)$ for components of model.

(taken from Elliott [35])

Figure 4.3.3 Three-renewal Process Error Model

The Elliott procedure is a useful and practical tool for constructing burst error models. The probability function he derived, P(m,n), should be particularly useful for evaluating the performance of various error correcting codes.

In 1965, Mandelbrot [36] published a variation on the Pareto model, which he referred to as a "self-similar point process". (The self-similar designation comes from the geometric symmetry property of the family of cumulative distribution curves.) He modified his original Pareto distribution in order to improve the discontinuity behaviour of the original. The new functions were:

$P(u) = Pr\{T_n - t_{n-1} > u\}$

$P(u) = 1.0;$ for $u < \epsilon$

$= (u/\epsilon)^{-\theta};$ for $\epsilon < u < T$

$= 0,$ for $u \geq T$, where: ϵ, θ and T are constant parameters.

By setting $P(u) = 1$, in the first segment, he avoided having a value of P(u) exceeding 1, which would have resulted from using a downward continuation of the second segment. By making T a finite parameter he forced the mean value to be finite. The Shannon channel capacity also does not exist for this model.

Fano [37], while reviewing the work of his predecessors on the Pareto distribution, observed that none had found a physical mechanism for burst errors. He then showed that the Pareto model could be derived analytically from one such mechanism that existed in the switched voice telephone network. Dialing pulses from a telephone set could, through crosstalk coupling into other loops, initiate a regenerative action that would create a burst of

impulses in other cable pairs. This would cause bursts of errors in a digital transmission system using pairs in the same cable. The errors, he showed, were described by the Pareto distribution. His argument was sound but there is no physical evidence, in the modern network, to support it. The subject is thus open for further research.

The Pareto distribution of Mandelbrot appears to be an excellent choice as a model for burst errors in digital channels operating on local loops. The mathematical complexity, that had to be introduced to avoid existence problems with the distribution mean and variance, and the absence of a Shannon channel capacity, make it less desirable to use in practice. It is doubtful if this form of the Pareto model will be used, to any degree, in future research.

4.4 THE MERTZ MODEL

In 1961, Mertz [38] used the hyperbolic distribution to describe both the tendency of errors to occur in long bursts and for the bursts to be separated by long quiet intervals of time. (You may recall that Mertz also used this distribution to describe the peak amplitudes of impulse noise, which is described in Section 3.4.) The hyperbolic distribution is defined as:

$p(x)$ = the probability density function of x

$$p(x) = \frac{nh^n}{(x + h)^{n+1}} \quad ; \text{ where: n and h are positive constants and } x \geq 0.$$

$P(x) = Pr\{X \geq x\}$

$$P(x) = \frac{h^n}{(x + h)^n}$$

He then derived the mean and variance of x:

$$\text{mean} = \mu = \frac{h}{n - 1}$$

$$\text{variance} = \sigma = \frac{h}{n - 1} \cdot \sqrt{\frac{n}{n - 2}}$$

This distribution resembles the Pareto distribution discussed in Section 4.3. It also suffers from the same existence problems. That is, the mean does not exist for n = 1, nor does the variance for n = 1 or 2. Mertz solved this by defining the probability density from 0 up to z, z being finite. The value of z was defined by a quantity, A(k), which he called the k-tile. A(k) was found from the mean of the experimental data and an arbitrary parameter k.

He defined a probability function p(a,c), which he used to show that the hyperbolic distribution was a better fit, than the Poisson, to experimental data for burst errors.

p(a,c) = the probability that exactly c events happen during a period of time for which the long term average is a events.

For the Poisson distribution he showed that:

$$p(a,c) = \frac{a^c e^{-a}}{c!}$$

and for the hyperbolic, for the case n = 1:

$$p(a,c) = \frac{h}{(c + h)(c + 1 + h)} .$$

By plotting the two functions on the same graph he showed that:

1) The probability of zero events is higher for the hyperbolic than for the Poisson.
2) The probabilities for various numbers of events tend to peak more sharply, and at lower values of a, for the Poisson than for the hyperbolic.
3) For the hyperbolic law the probability of a finite number of occurrences always stays below that for zero occurrences. For the Poisson distribution they cross and for large values of a are above that for zero occurrences.

Mertz showed that the hyperbolic distribution, rather than the Poisson, was best able to fit a set of experimental data. Figure 4.4.1, which was taken from the Mertz paper, illustrates this conclusion.

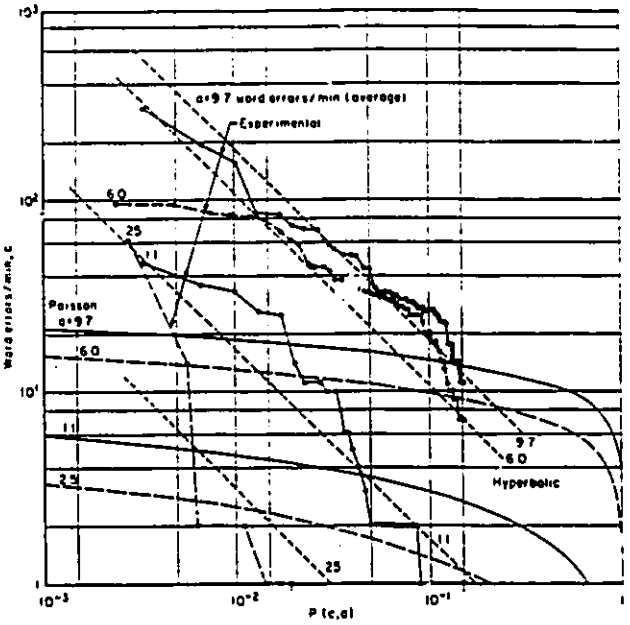

Fig. 6—Distribution of word errors per minute in long-haul private-line data circuit (Lincoln Laboratory data,[4] 1300 bits/sec). Comparison with hyperbolic and Poisson formulas.

(taken from Mertz [38])

Figure 4.4.1 The Hyperbolic Burst Error Distribution

However, Mertz used valid data from only one circuit. The 1200 bps data from the Alexander study [27], also used by Mertz, was later shown to have been corrupted by operator error (ref. Sussman [34]).

The influence of Mertz was apparent because many researchers began to use the hyperbolic rather than the Poisson distribution to represent burst errors. However, additional experimental verification should now be done to further confirm the use of the hyperbolic model for present day local loop based data systems.

CHAPTER 5

IMPULSE NOISE COUNTERMEASURES

5.1 GENERAL COMMENTS

Radio frequency/ electromagnetic interference engineers deal with impulse noise by suppressing it at its source and by installing susceptible equipment in "RF tight" enclosures. On the other hand, things are not so simple for the data transmission engineer. He cannot control the electrical environment in which his equipment operates. He does not usually know where impulse noise sources are located, and when he does may not be able to treat them. Also, it is impractical to install cables with individual pairs shielded from each other in the local loop environment. He must somehow design his communications equipment to survive in this harsh interference environment and hope for the best.

Figure 5.1.1 gives an overview of the situation. It shows the possible combination of elements that can be used to implement a baseband local loop type data transmission system. Along with this, it shows the possible techniques that can be used to minimize the effects of impulse noise in the loop. The following six sections of this chapter provide details on these techniques.

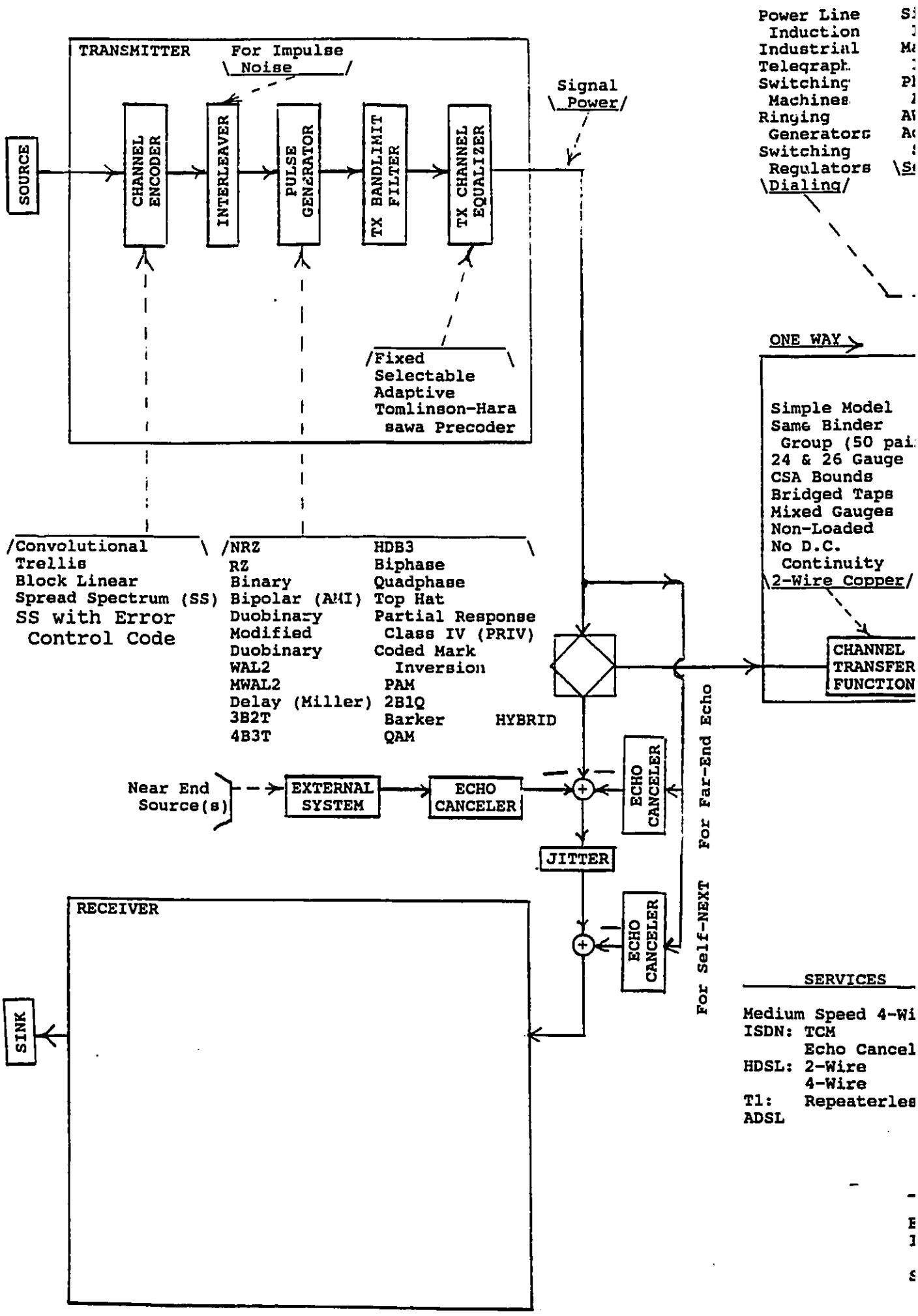
TRANSMITTER
For Impulse Noise
Signal Power
SOURCE
CHANNEL ENCODER
INTERLEAVER
PULSE GENERATOR
TX BANDLIMIT FILTER
TX CHANNEL EQUALIZER
Fixed
Selectable
Adaptive
Tomlinson-Harasawa Precoder
Convolutional
Trellis
Block Linear
Spread Spectrum (SS)
SS with Error Control Code
NRZ
RZ
Binary
Bipolar (AMI)
Duobinary
Modified Duobinary
WAL2
MWAL2
Delay (Miller)
3B2T
4B3T
HDB3
Biphase
Quadphase
Top Hat
Partial Response Class IV (PRIV)
Coded Mark Inversion
PAM
2B1Q
Barker
QAM
HYBRID
Near End Source(s)
EXTERNAL SYSTEM
ECHO CANCELER
ECHO CANCELER
JITTER
ECHO CANCELER
For Far-End Echo
For Self-NEXT
RECEIVER
SINK
Power Line
Induction
Industrial
Telegraph
Switching Machines
Ringing Generators
Switching Regulators
Dialing
ONE WAY
Simple Model
Same Binder Group (50 pai
24 & 26 Gauge
CSA Bounds
Bridged Taps
Mixed Gauges
Non-Loaded
No D.C. Continuity
2-Wire Copper
CHANNEL TRANSFER FUNCTION
SERVICES
Medium Speed 4-Wi
ISDN: TCM
Echo Cancel
HDSL: 2-Wire
4-Wire
T1: Repeaterles
ADSL

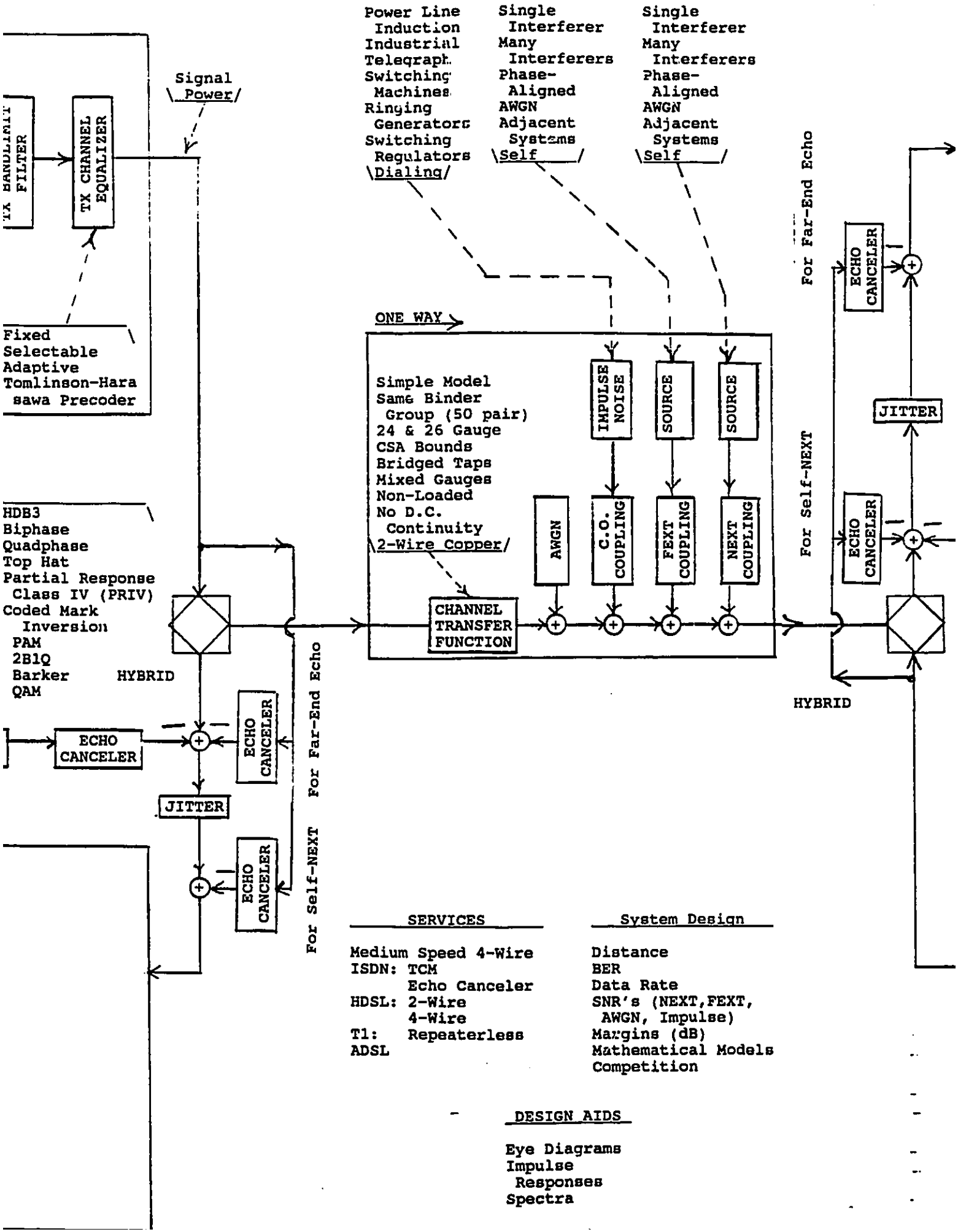

SERVICES	System Design
Medium Speed 4-Wire	Distance
ISDN: TCM	BER
Echo Canceler	Data Rate
HDSL: 2-Wire	SNR's (NEXT,FEXT,
4-Wire	AWGN, Impulse)
T1: Repeaterless	Margins (dB)
ADSL	Mathematical Models
	Competition

DESIGN AIDS

Eye Diagrams
Impulse
Responses
Spectra

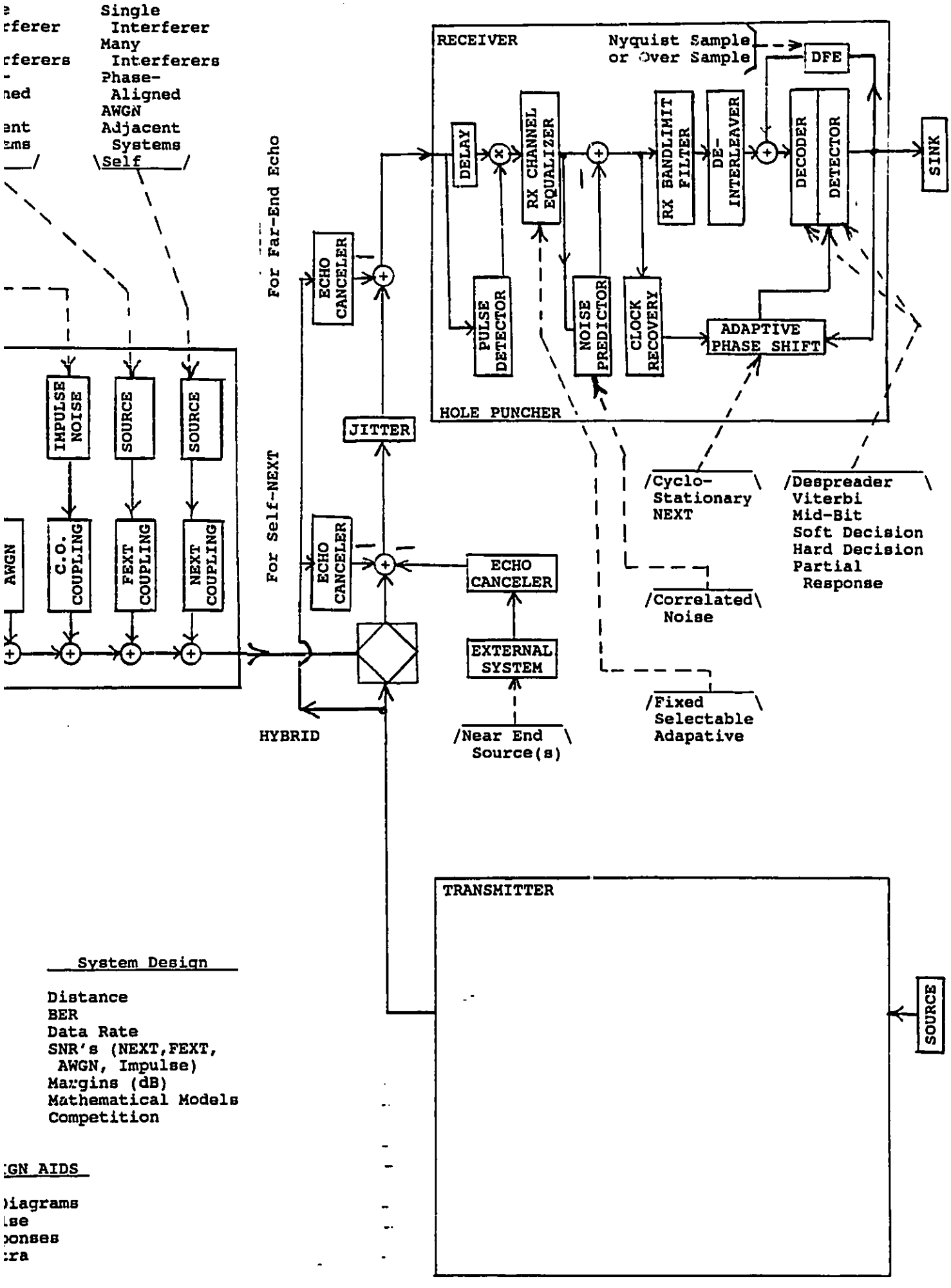
Single Interferer
Many Interferers
Phase-Aligned AWGN
Adjacent Systems
Self
For Far-End Echo
For Self-NEXT
RECEIVER
Nyquist Sample or Over Sample
DFE
DELAY
RX CHANNEL EQUALIZER
RX BANDLIMIT FILTER
DE-INTERLEAVER
DECODER
DETECTOR
SINK
ECHO CANCELER
PULSE DETECTOR
NOISE PREDICTOR
CLOCK RECOVERY
ADAPTIVE PHASE SHIFT
HOLE PUNCHER
JITTER
IMPULSE NOISE
SOURCE
SOURCE
AWGN
C.O. COUPLING
FEXT COUPLING
NEXT COUPLING
ECHO CANCELER
ECHO CANCELER
HYBRID
EXTERNAL SYSTEM
/Near End Source(s)
/Cyclo-Stationary NEXT
/Correlated Noise
/Fixed Selectable Adapative
/Despreader Viterbi Mid-Bit Soft Decision Hard Decision Partial Response
TRANSMITTER
SOURCE
System Design
Distance
BER
Data Rate
SNR's (NEXT,FEXT, AWGN, Impulse)
Margins (dB)
Mathematical Models
Competition

5.2 PULSE SMEARING AND DESMEARING

In 1961, Wainwright [39] published the results of his study of the smearing-desmearing technique for reducing the effects of impulse noise. He cited R. M. Lerner as the originator of the idea, in 1959. The figure below shows a block diagram of the scheme used.

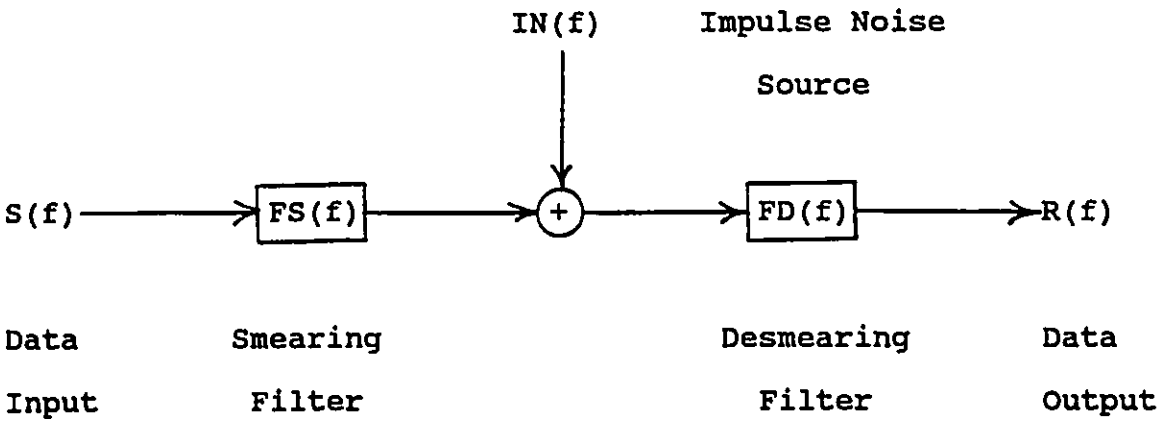

Figure 5.2.1 Smear-Desmear System For Reducing Impulse Noise

S(f) = the Fourier transform of the transmit voltage signal s(t)

FS(f) = the transfer function of the smear filter

IN(f) = the Fourier transform of the impulse noise voltage in(t), at the receiver input

FD(f) = the transfer function of the desmear filter

R(f) = the Fourier transform of the received voltage signal, r(t), just before the detector

This diagram has been reduced to its bare essentials to simplify the explanation which follows. The Smear and Desmear Filters, which are special all-pass phase-shift networks, have been added to the conventional transmission system, at the channel ends. They are intended to have no effect on the operation of the data system itself, altering only the characteristics of the impulse noise coupled into the channel. This is achieved because filter FD(f) introduces phase distortion into the impulse waveform, causing it to be extended over a much longer period of time.

There may be some confusion concerning the use of the terms "smearing filter" and "desmearing filter". Either type of filter causes pulse smearing when used alone. No pulse smearing results when two such filters, having complementary phase characteristics, are connected in tandem. The terms "smearing" and "desmearing" were used to point out this relationship. That is, FS(f) smears the data signal while FD(f) desmears it. There should be no confusion in claiming that FD(f) serves to smear the noise impulses, although the ambiguous use of the nomenclature is not very desirable.

A matched pair is achieved by ensuring that in a restricted useful passband of the system that:

i) Both filters are ideally all-pass.

ii) The filters have complementary phase shifts with frequency.

These conditions could be expressed analytically as:

$$|FS(f)| = |FD(f)| = 1$$

$$FS(f)FD(f) = 1, \text{ ignoring delay.}$$

The existence of stable Networks results if either network has its zeroes and poles only in the left hand side of the complex plane. This is apparent if the Laplace transform of the filter transfer function is expressed as the quotient of polynomials P(S) and Q(S):

$$\text{If } FS(S) = \frac{P(S)}{Q(S)} \qquad \text{then } FD(S) = \frac{Q(S)}{P(S)}.$$

It has been shown that FS(S) is stable if its poles are in the left hand complex plane [52]. For FD(S) to also be stable requires the zeroes of P(S), the poles of FD(S), to be in the left hand plane, giving the two requirements.

The impulse noise signal is given by the quantity IN(f)FD(f), at the detector of the data receiver. FD(f) should be chosen to minimize the incidence of data errors. The following appear to be important factors for achieving this result:

i) A process that causes a narrow pulse to be spread out, or "smeared" in time, can be used to reduce bit errors caused by incorrect decisions in the detector stage. The energy of a noise impulse that would ordinarily contaminate one, and sometimes two bits, would be spread over many bits. Thus the decision process would have to contend with a very small energy per bit

over the span of spreading, rather than a large energy for one bit.

ii) The span of spreading should be as large as possible, in order to minimize the probability of a bit error. An upper bound for the span is determined by the degradation caused from spreading so much that adjacent spread pulses overlap, with the amplitudes adding and building high amplitude pulses, once more.

iii) The spreading and despreading operations should be complementary for the data signals, so as to avoid generating ISI.

The spreading of a noise impulse is caused by the same phenomenon that causes ISI in data pulses. Any linear network that introduces signal distortion, by means of frequency or phase distortion, or both, could be used to accomplish this. Frequency distortion, in one network, can be eliminated by means of an equalizer network. Unfortunately, this would degrade system performance, should Gaussian noise be introduced at some point between the two networks. This leaves the all-pass type phase-shift network as the feasible alternative for the design of the spreading and despreading networks.

Wainwright [39] showed experimentally that a particular value of FD(f) does in fact reduce bit errors from impulse noise in a sample transmission system. These results are illustrated in Figure 5.2.2.

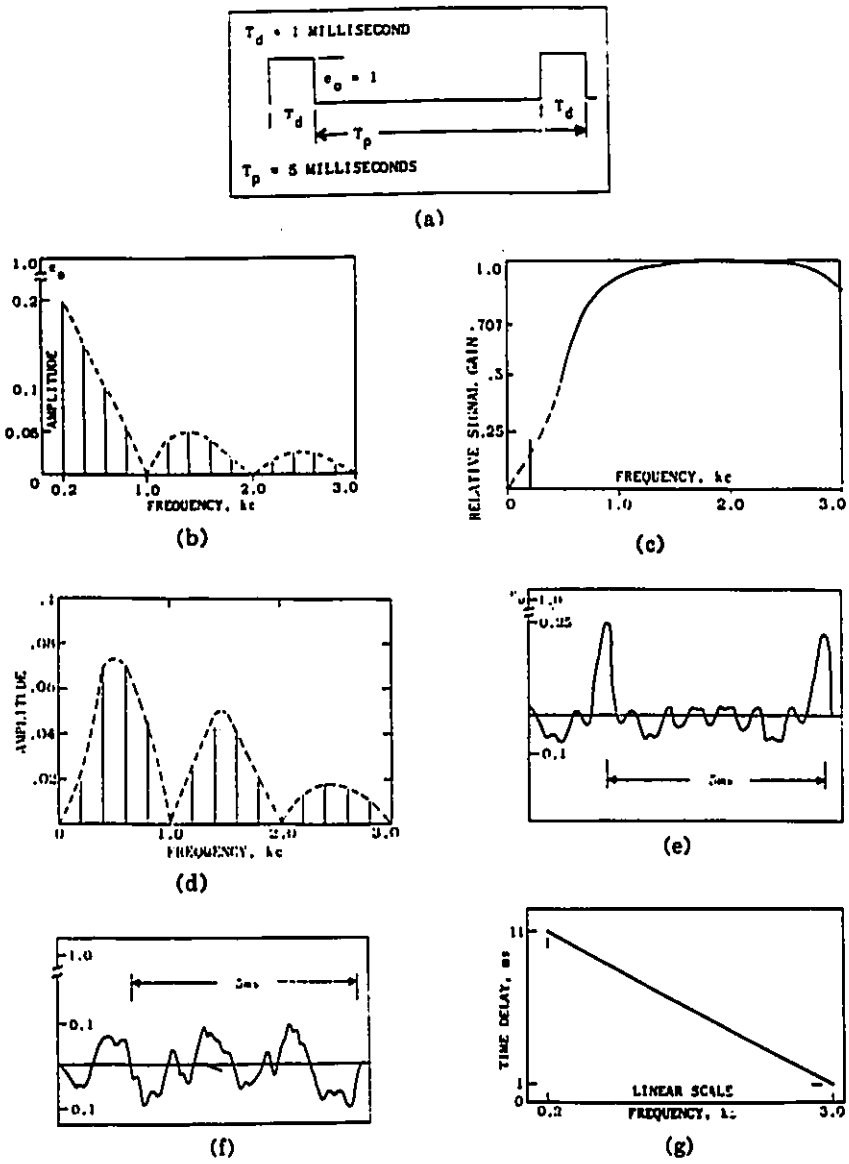

Fig. 4 (a)—Noise pulses before band limiting. (b) Spectrum-energy distribution of pulses shown in (a). (c) Relative attenuation characteristic of band-pass filter in Sebit-24. (d) Spectrum-energy distribution plot for pulses shown in (a) after band limiting per (c). (e) Effect of band limiting on pulses shown in (a). (f) Effect of band limiting and smearing of pulses shown in (a). (g) Time-delay curve of a desmear filter (see text).

(taken from Wainwright [39])

Figure 5.2.2 Noise Impulse Spreading

He used an analog passband system, bandlimited to 3 kHz, with impulse noise represented by 1 ms square pulses repeated 5 ms apart. The desmear filter was implemented with a lumped L-C network, having a linear differential time-delay-frequency characteristic of 11 ms at 200 Hz to 1 ms at 3 kHz. He found that the smearing effects of the normal 3 Khz bandlimiting filter increased the system signal-to-impulse noise margin by 12 Db. When the smearing-desmearing filters were added to the system, the margin was increased 8 Db, to a total of 20 dB. ("dB margin" or "dB improvement" means that a smeared system has the same performance as a bare system having a signal to impulse noise ratio that much larger.)

Engel [14], in 1965, investigated the effects of using various phase response functions for the spreading and despreading filters. He found that:

i) The type of phase shift function used did not influence the efficiency of the pulse smearing process significantly. The use of linear, half-cycle sinusoidal and full-cycle sinusoidal differential delays with frequency, did not make more than a 0.25 dB difference in the impulse noise improvement.

ii) The improvement could be degraded for a sufficiently strong impulse. Such a pulse could give a smeared pulse having a large enough amplitude as to cause errors over several bit intervals. Stretching of the burst length would then result.

In the same year, Bennett and Davey [40] noted that the process could be viewed more generally as a dynamic process employing frequency sweeping or "chirp", in addition to the static smearing.

The smearing-desmearing technique was further developed by Beenker, Claasen and Van Gerwen [41] in 1985. They addressed the problem of finding optimal smear-desmear filters in the discrete time domain. In particular, they were interested in a time domain filter employing a small number, N, of binary coefficients, represented by +1 and -1, to avoid the need for hardware multiplication. They were concerned with the problems of designing such filters for the smear-desmear operations, so that a maximum degree of impulse smearing was realized at a minimum cost of increased ISI. (ISI is inherently generated by the combination of filters fs_n and fd_n which are not exact complements.) In light of this, they defined two measures of smear-desmear performance, F_1 and F_2, where:

F_1 = "first merit factor"

$$= \frac{\text{maximum amplitude of impulse noise}}{\text{maximum amplitude of smeared impulse}}$$

F_2 = "second merit factor"

$$= \frac{\max|h_n| \text{ over } n}{\sqrt{\sum_n B_n^2}} \quad ; \text{ where:}$$

h_n = the time domain end-to-end transfer function, ignoring smearing-desmearing filters

B_n = the time domain transfer function of the tandem connected smear-desmear pair.

F_1 measured the capability of smearing to decrease the amplitude of the noise impulses, with large values of F1 being best. F_2 measured the extraneous introduction of ISI, caused by mismatching between smear and desmear filters; again large values of F_2 were desirable. Both F_1 and F_2 should be maximized simultaneously for the greatest improvement in impulse noise performance.

Using computer simulation they found the following:

i) F_1 and F_2 cannot be maximized simultaneously. For a low P_{bit} from ISI then F_2 should be greater than 15 dB, and may range as high as 25 dB before F_1 becomes seriously degraded.

ii) The classical frequency domain (Wainwright) method of design, using linear differential phase filters and ignoring ISI, was shown to be inferior to the new one. For a baseband system, the new design gave a value of F_1 about 1.4 times larger than that for the classical, while F_2 was much larger with the new.

iii) For a baseband system, using smearing filters of length N and desmearing filters of length M, they found the following values of F_1 and F_2.

TABLE 5.2.1

Merit Factors For A Baseband System

N	M	F_1 dB	F_2 dB
13	29	10.95	21.92
27	67	13.83	20.43
59	123	16.86	20.46

(taken from Beenker, Claasen and Van Gerwen [41])

It is apparent that a significant improvement in the Signal-to-Noise-Ratio (SNR) margin for impulse noise is realized for even modest values of N and M.

iv) For a passband system, using N = 64, for various types of bases of the arithmetic used in convolving the time sequences, the following were found:

TABLE 5.2.2

Merit Factors For A Passband System

	Binary sequences		Ternary Sequences		Real-Valued Sequences	
	F_1 dB	F_2 dB	F_1 dB	F_2 dB	F_1 dB	F_2 dB
optimum F_1	9.43	15.58	9.21	20.56	11.05	8.81
optimum F_2	8.32	17.26	8.14	21.83	8.60	47.37
large F_1 and F_2	8.75	16.92	9.18	21.40	10.00	26.45

(taken from Beenker, Claasen and Van Gerwen [41])

It is apparent that increasing the precision of the filter constants gives a sizeable improvement in the ISI situation, without changing the impulse noise margin significantly.

The smearing-desmearing technique offers a considerable improvement in the SNR margin against impulse noise, without significantly degrading performance caused by other forms of interference. The purely digital implementation offers improved performance over the original analog one [41]. In practice, it should be possible to use the digital method, at virtually no monetary cost, if digital transmit and receive filters are used in the conventional parts of the modem. The smearing-desmearing filters may be implemented by modifying the filters to incorporate these new functions.

5.3 NONLINEAR CIRCUIT ELEMENTS

In 1983, Modestino, Jung and Matis [18] described the use of amplitude limiting devices to reduce the effects of impulse noise. Figure 5.3.1 illustrates this approach. The three tandem connected elements were used in place of the pre-detection filter in the conventional data receiver.

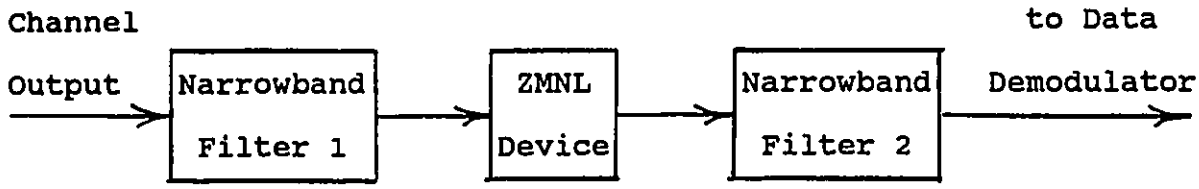

Figure 5.3.1 Generalized Impulse Noise Amplitude Limiter

Narrowband filters 1 and 2 appear to be equivalent to the normal single receive filter. The authors of the paper do not discuss criteria for assigning values to each filter individually. The ZMNL, zero memory nonlinear device, is used to represent the class of instantaneous acting amplitude limiters. Three types of these were investigated: the limiter, the hole puncher and the Butterworth nonlinearity. The first two of these devices were borrowed from radio engineering, where they were used to suppress impulse noise in high frequency (HF) receivers, according to Rhode and Bucher [42].

The limiter is designed to pass low level signals unaltered, except that it fixes the signal level (or clips it), whenever it exceeds a threshold value. The threshold is set slightly above the

amplitude of a noise free data signal, so that limiting occurs only in the presence of impulse noise. In radio engineering, it is called a "peak clipper" or "noise limiter" to avoid confusing it with the hard limiter used to suppress amplitude modulated (AM) interference in frequency modulation receivers. (Modestino uses the term "hard limiter" to describe what is often called a "soft limiter". In this thesis, the word "limiter" will be used for the name of this component.) Best noise limiting occurs when Filter 1 has a large bandwidth while Filter 2 has a small one. The wideband input filter ensures that incoming noise spikes are not stretched in time. The narrowband filter ensures that only a minimum energy, of the clipped pulse, is passed to the data demodulator.

The hole puncher has the voltage transfer function:

$g(R) = 1; \quad 0 \leq R \leq R_t$

$= 0; \quad R > R_t$; where:

R_t is the punching threshold voltage, which is set slightly above the peak amplitude of a noise free line signal. (Polarity has been ignored to simplify the definition.)

In the absence of impulse noise, the hole puncher has no effect on the signal, but effectively zeroes the signal in the presence of a noise impulse. In radio engineering, it is called a "noise blanker" and was known as the "Lamb noise silencer", when it was invented in the mid 1930's.

Personal experience with the noise blanker, used in a radio receiver, indicates that it is extremely effective in suppressing, narrow, high amplitude, impulse noise spikes. For example, the noise hits, caused by the flash-over to ground of static electricity on the antenna, during a snow storm, were made inaudible by the blanker. The blanker is of little value in suppressing some other types of noise, that from a distant thunderstorm for example.

The design of Filter 1 and Filter 2 for the hole puncher, is the same as for the limiter case.

The Butterworth nonlinearity was used by Modestino, and his associates, to represent a general form of nonlinearity. It is defined by the voltage transfer function:

$$g(R) = \frac{1}{1 + (R/R_c)^n} \quad ; \text{ for } 0 < R < \infty; \text{ where:}$$

R_c is the clip level and $n > 1$ is the order. (Polarity has been ignored to simplify the definition.)

For n close to 1, the device behaves much like a limiter. For large n, it behaves like a hole puncher. Apparently the device is intended to represent a class of impulse noise suppressing devices rather than any particular one. Because of its simple mathematical form, it is well suited for system analysis, either analytical or by computer simulation. It is this latter approach that Modestino and associates took in evaluating the devices.

Using the simulation program Interactive Communications Simulator (ICS), Modestino evaluated the effectiveness of these suppression techniques. They measured the performance of the devices in terms of the change in the signal to background Gaussian noise, to attain a fixed bit error rate, P_{bit}. They found that:

i) Figure 5.3.2 shows the error performance of the limiter, compared to the design without it. The limiter provided an 18 dB improvement in the SNR for $P_{bit} = 10^{-3}$. The improvement was even more for lower values of P_{bit}.

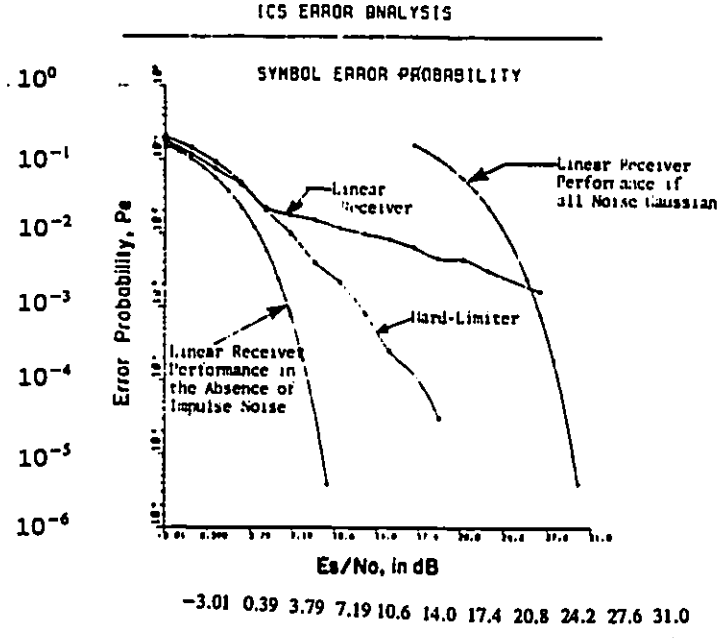

Figure 9
Simulated Performance of Linear and Hard-Limiting Receiver for QPSK Modulation in Impulsive Noise.

(taken from Modestino, Jung and Matis [18])

Figure 5.3.2 Limiter Error Performance

ii) Figure 5.3.3 shows the error performance of the hole puncher, compared to the design without it. The hole puncher provided a 7 dB improvement in SNR over the limiter for $P_{bit} = 10^{-4}$. This was for $P_f = 0.01$, the probability of false operation of the device by Gaussian background noise (the lower the value of the threshold voltage of the device, the greater the chance of a false alarm). There was however a penalty of 2.5 dB in the SNR for using the device in the absence of impulse noise.

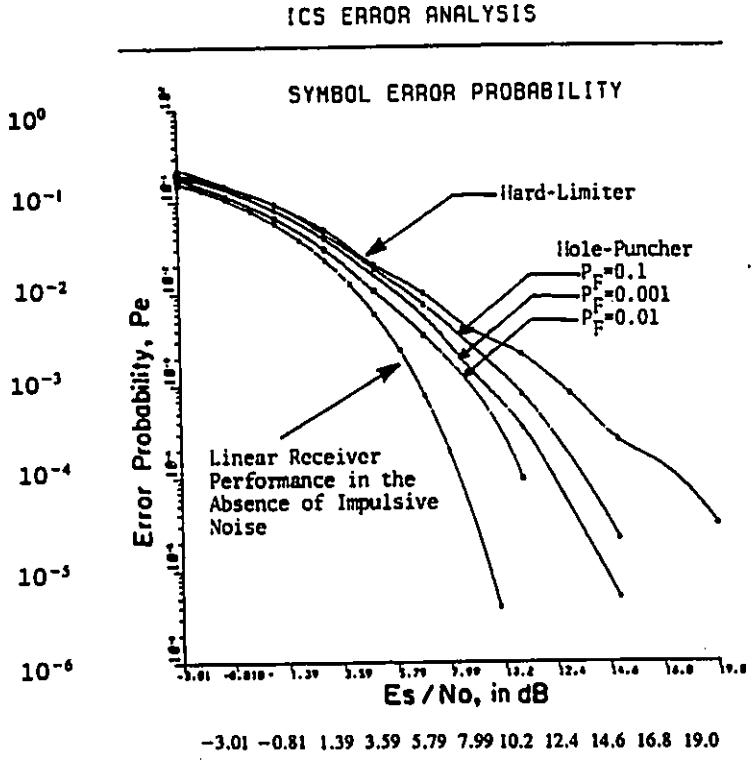

Figure 10
Simulated Performance of Hole-Puncher and Hard-Limiting Receiver for QPSK Modulation in Impulsive Noise.

(taken from Modestino, Jung and Matis [18])

Figure 5.3.3 Hole Puncher Error Performance

iii) Figure 5.3.4 shows the error performance of the Butterworth nonlinearity, for three values of parameter n compared to the design without it. The Butterworth nonlinearity showed various degrees of improvement over the linear receiver alone. A family of SNR vs. P_{bit} curves plotted for n = 1 , 3 and 6 cut across each other for various segments in the SNR range. The Butterworth, for n = 1, showed an improvement of 15 dB at $P_{bit} = 10^{-3}$. It was 1 dB better than the hole puncher at $P_{bit} = 10^{-5}$ while only 1 dB worse than the linear receiver in the absence of impulse noise.

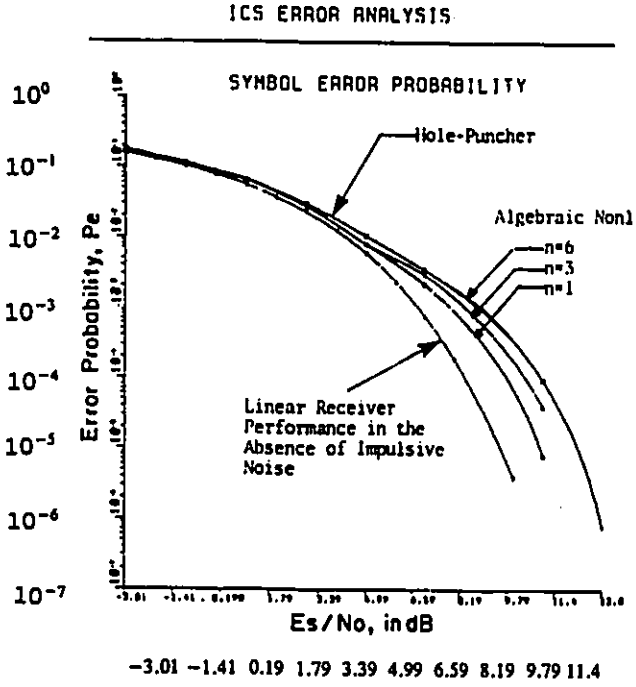

Figure 11

Simulated Performance of Algebraic Nonlinear Receiver Characteristic and Hole-Puncher Each with P_p=0.01 for QPSK Modulation in Impulsive Noise.

(taken from Modestino, Jung and Matis [18])

Figure 5.3.4 Butterworth Nonlinearity Error Performance

It would appear that nonlinear devices should merit further investigation, to verify that the above highly significant improvements in performance could be realized in the field.
A nonlinearity, the Butterworth for example, should be easily implemented in modern data receivers. It could be incorporated into the receiver filter routine in a modem employing a DSP derived filter.

5.4 ERROR CONTROL CODING

Error control coding has been suggested as a means of controlling the burst errors caused by impulse noise in the local loop. Four papers were found that dealt with this matter, one in 1965 and the others in 1991.

In 1965, Elliott [35] investigated the properties of a Bose Chaudhuri and Hocquenghem (BCH) code, using a channel model based on the error burst data of Alexander, Gryb and Nast [27], for a 600 bps FSK system. Figure 5.4.1 illustrates the error rate improvement from employing the following code. He found that the raw bit error rate of $5 \cdot 10^{-3}$ could be improved to approximately 10^{-7}, by using a (31,21) BCH code with a 300 bit interleaver. (The curves represent the probability of having m or more errors in a block of 31 symbols. The uncoded case corresponds to the curve for m = 1. The coded case corresponds to that for m = 3; the BCH code can correct 2 errors.) These favorable results may not be achieved by a present

day, local loop based system. The necessary signal bandwidths are now considerably wider, because of increased data rates, which increases crosstalk coupling and signal transmission losses. A decrease in coding gain is then almost certain to occur.

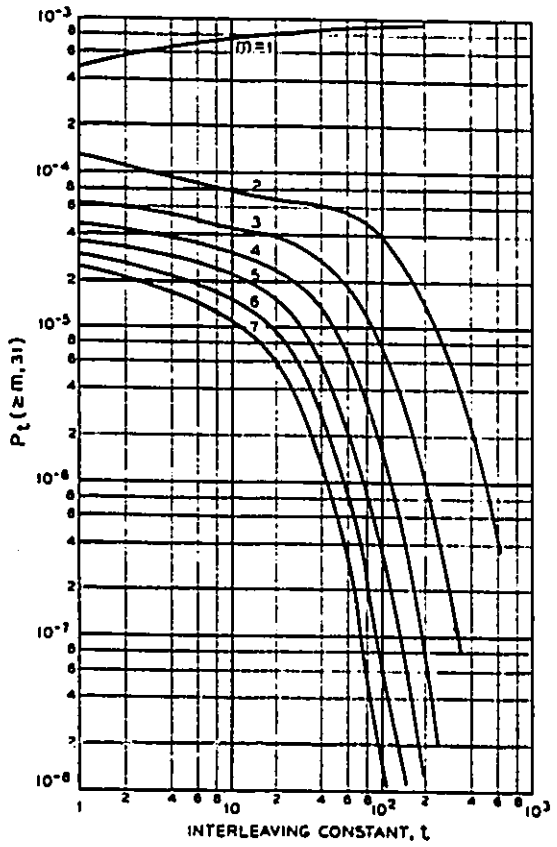

Fig. 13 — $P_t(\geq m,31)$ vs t for $m = 1, \cdots, 7$.

(taken from Elliott [35])

Figure 5.4.1 System Block Error Performance

In 1991, Kerpez [43] investigated the effectiveness of error control coding, in dealing with burst errors caused by impulse noise in an Asymmetric Digital Subscriber Line (ADSL). The ADSL operated in one direction at 1.6 Mbps, with Quadrature Amplitude Modulation (QAM), and 16 kbps in the other. Only the high speed direction was investigated. Impulse noise and FEXT were the only transmission impairments considered. (NEXT was ignored for this type of system. Appendix E discusses the effects of NEXT on a coded system.) Three codes were considered:

i) C2: A (28,24) rate 6/7 Reed-Solomon code (RS),

ii) CIRC: The interleaved RS code used for the compact disk (CD) and digital audio tape (DAT) recording systems. This is a (28,24) outer code and an (32,28) inner code, with an interleaving depth of 112, giving a (3584,2688) 3/4 rate code.

iii) Iwadare convolutional code of rates 3/4 and 6/7.

For a particular model of the impulse noise channel, he found that the C2 code reduced the uncoded block error rate by nearly 700 times, while the CIRC code reduced it approximately 500 times. Table 5.4.1 gives these results.

TABLE 5.4.1

CD Coding Performance

Table I, Block error rate (BLER), ADSL & impulse noise.

ADSL code	uncoded	C2	CIRC
rate	1	6/7	3/4
Max. correctable burst length, μS.	0	1120	960
Error threshold T_J, mV	1.111	1.026	0.672
BLER, for $H \geq T = .672$ mV	0.349	0.00050	0.00069

(taken from Kerpez [43])

The Iwadare rate 3/4 code gives the same error performance as the CD code for an Iwadare decoder, based on a 12,000 stage shift register design. The rate 6/7 code is not quite so effective as the rate 3/4 code. These points are illustrated in Figure 5.4.2.

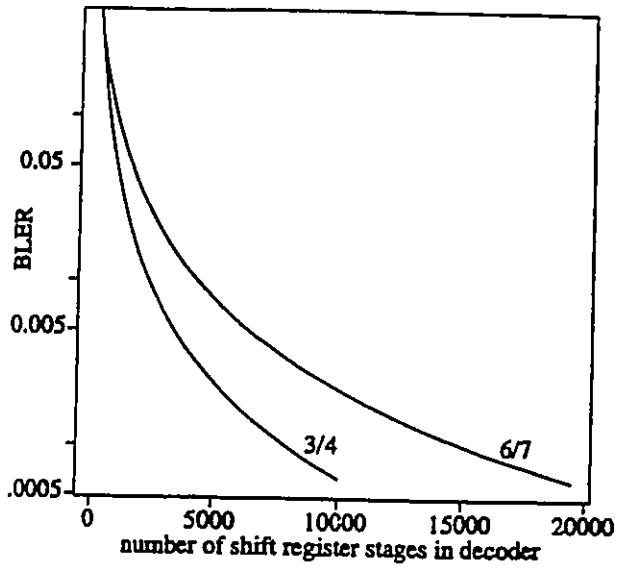

Figure 4, Block error rate, Iwadare codes, impulse noise.

(taken from Kerpez [43])

Figure 5.4.2 Iwadare Coding Performance

Kumozaki [32] investigated the performance improvement in a TCM system, when using an interleaved Hamming code. An actual local loop system was used, with impulse noise generated by telephone pulse dialing, at a fixed rate, over a pair in the same cable. The data system operated at 200 kbps and used AMI signalling. He found that a (13,9) code, with 16 bit interleaving, reduced the bit error rate from 10^{-8}, for a noncoded system, to 10^{-10} with a coded system. The bit error rate was reduced by a factor of 100 times. (Note that NEXT was ignored with the TCM mode of operation.)

Sistanizadeh and Kerpez [46] investigated the performance of trellis coded modulation (TCMOD) with HDSL's, using local loops contaminated by impulse noise. The HDSL system operated at 1.544 Mbps, full duplex, by using two cable pairs, each operating at 800 kbps, duplex, using echo cancelers. 1800 pulse noise events, recorded on magnetic tape during a NYNEX Company local loop study, were used with a hardware loop simulator, to measure code efficiency. Table 5.4.2 documents their findings. Neither four-state nor sixteen-state TCMOD produced a significant change in the error performance over the uncoded system. It should be noted that NEXT was present on the channels.

TABLE 5.4.2

HDSL Coding Gains For Impulse Noise

Table I

Percentage of 1800 NYNEX Impulses That Cause Errors

modulation	Uncoded (DFE)	Four-state TCMOD	Sixteen-state TCMOD
PAM	26%	27%	33%
QAM	18%	16%	18%

(taken from Sistanizadeh and Kerpez [46])

The suspected harmful influence of NEXT on a system using error control coding was confirmed by computer simulation studies. (Appendix E includes the results of computer simulation runs that were used to investigate the importance of NEXT interference on a system using error control coding. It is shown that such coding schemes are seldom useful when used with a local loop contaminated by strong NEXT interference.)

5.5 ERASURE DECODING

Erasure decoding is a variation of error control coding that makes use of information indicating that certain symbols in the data stream are of questionable validity. They may then be safely excluded from the subsequent hard decision decoding process. Some mechanism must exist for reliably identifying erasures. Such a process is not likely to be exact: there will be erroneous bits in the stream which cannot be identified as such. The decoder then would be required to correct bit errors as well as erasures.

In Section 5.4 it was noted that error control coding, on an impulse noisy local loop, was able to improve error performance of the system, but only under certain circumstances. Intuitively, it would appear that this situation could be improved by using erasure decoding.

The additional information, allowing unreliable symbols to be identified, should improve the accuracy of the decoding process. This will be shown to be true in this section.

Errors and erasures decoding is described by Michelson and Levesque [44]. With a block code, for example, decoding is done by excluding the doubtful bit positions when trying to find the Hamming distance to the nearest valid codeword. A doubtful bit is thus treated as one that is not information bearing. The following illustrates one method of using erasures to correct errors in a block code.

The decoder can correct t errors, where $2t + 1 = d$, with d the minimum Hamming distance for the set of codewords. One can decode the block for s erasures and an unknown number of errors as follows:

i) Set all erased bits in the received word equal to ZERO and try to correct up to t errors.

ii) Set all erased bits in the received word equal to ONE and try to correct up to t errors.

iii) If both decodings are successful, but produce different codewords, accept the one having the smaller number of errors.

The effectiveness of the receiver depends on the criterion for deciding whether or not a bit is an erasure. For a system contaminated by impulse noise, it would be necessary to identify those bits coincident with an impulse of sufficiently large amplitude.

Threshold detectors could perform this function. The threshold voltages should be set to values that balanced the risk of a false alarm (from other forms of interference) against a miss. In the Geist and Cain paper [45] and the first Modestino paper [23] an idealized erasure identification process was used. (Modestino termed this a "genie-aided" system.) In both papers, an erasure was declared whenever a noise impulse coincided with a bit. The amplitude of the impulse was not taken into account, so that some erasures resulted in the destruction of useful information. In the second Modestino paper [24], a practical design, based on multiple thresholds in the decision device, was employed. As will be seen, according to simulation results, the performance of a local loop system is highly dependent on the criterion used for declaring erasures.

In 1980, Geist and Cain [45] showed that a convolutional encoder and a Viterbi decoder operated quite effectively in a periodic burst erasure environment. Interleaving was useful only for very long burst lengths. For short burst lengths, it was found that interleaving actually caused a degradation in performance. These results were derived from an idealized model and do not necessarily apply to the real local loop environment.

In 1988 and 1990, Modestino and his associates [23], [24] investigated the performance of the Geist and Cain design on a two-wire baseband digital loop system, with impulse noise being the major

transmission impairment. They noted that on a severely bandlimited channel, such as the two-wire twisted-pair digital subscriber loop, that:

i) The increased line signalling rate, associated with channel coding, exacerbates the already severe ISI problem.

ii) The effects of channel crosstalk also increase with the line signalling rate and can likewise be expected to be more prominent with coding.

They stated that, by a careful choice of coding rate and decoding strategy, it was possible to reduce the effects of impulse noise. They supported this by demonstrating a coding gain using a computer simulation model based largely on the design treated by Geist and Cain. (A local loop channel model was added to the convolutional encoder and erasures Viterbi decoder studied by these other researchers.) The basic model that Modestino analyzed is defined by the following:

i) TCM was employed on a single loop pair. (NEXT was ignored.)

ii) AMI signalling was used.

iii) Impulse noise, FEXT and additive white Gaussian noise (AWGN) were the only transmission impairments.

iv) The impulse noise arrival rate was fixed at one pulse per hundred baud intervals ($\lambda T_s = 0.01$).

v) The FEXT level was fixed at a value corresponding to 50 similar interferers.

vi) The AWGN level, as expressed by the ratio E_b/N_0, was used as the independent variable.

vii) Data scrambling and descrambling was used to eliminate the error bias of the channel. Interleaving was used to remove the channel memory caused by ISI.

viii) One erasure was assumed to occur with each noise impulse.

A computer model was constructed, using the above information and standard models for cables (non-loaded, bridged taps, lengths to practical limits, etc.). The idealized erasure identification process was used in this model. A data rate of 200 kbps was chosen. A variety of short constraint length codes, K = 8, were tried for code rates of 1/2, 2/3, 3/4, 4/5, and 5/6. The results that they achieved with these codes is shown in Figure 5.5.1.

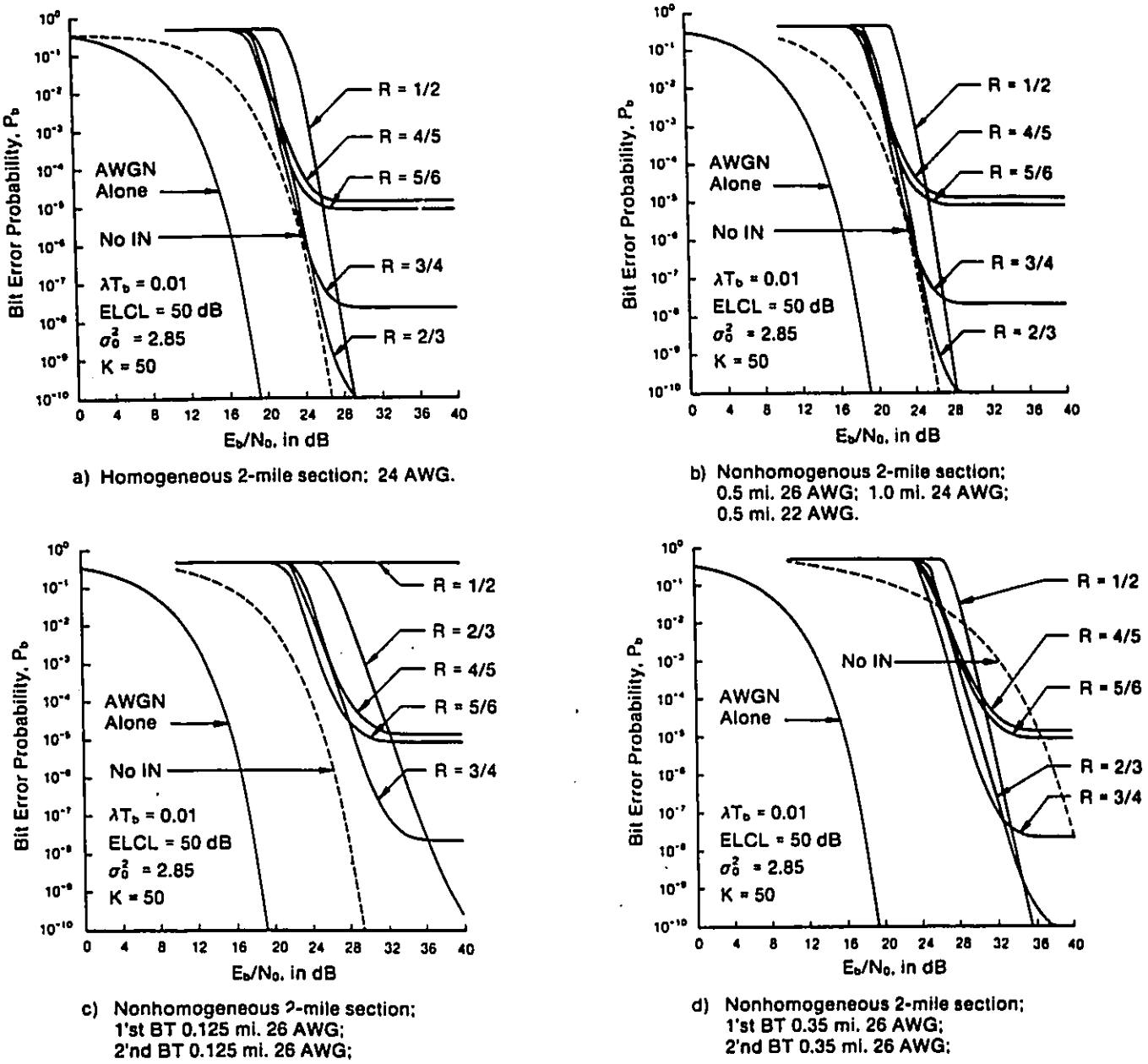

a) Homogeneous 2-mile section: 24 AWG.

b) Nonhomogenous 2-mile section; 0.5 mi. 26 AWG; 1.0 mi. 24 AWG; 0.5 mi. 22 AWG.

c) Nonhomogeneous 2-mile section; 1'st BT 0.125 mi. 26 AWG; 2'nd BT 0.125 mi. 26 AWG;

d) Nonhomogeneous 2-mile section; 1'st BT 0.35 mi. 26 AWG; 2'nd BT 0.35 mi. 26 AWG;

Fig. 7. Coded bit error probability performance using various $K = 8$ convolutional codes at $f_b = 200$ kbits/s.

(taken from Modestino ,Sargrad and Bollen [23])

Figure 5.5.1 Error Rates For "Genie-aided" Erasures Decoding

It can be concluded from these results that:

i) A rate 3/4 should be optimum. Using a convolutional code introduced an error floor, with respect to the signal to AWGN ratio (for FEXT and impulse noise power each fixed). This floor ranged from $P_{bit} = 10^{-5}$ for rate 5/6, down to a minimum of $P_{bit} = 10^{-7}$ for a rate 3/4 code. (It was stated that the error floor could be reduced further by increasing the code constraint length.)

ii) All codes, when operated above their floors, produced a coding gain of approximately 8 dB, compared to the uncoded case. The rate 3/4 code produced a coding gain of 8 dB with a $P_{bit} = 10^{-7}$, the lowest value of floor for all rates tested.

In the 1990 paper [24], the erasure problem was addressed further with the incorporation of the practical erasure identification scheme (described earlier in this section). It was found that the new scheme nearly always increased the immunity of the system to impulse noise. The error floor was reduced to negligible values and was completely eliminated for some code rates. This was explained by the weakness of the ideal erasure model: an erasure was declared whenever an impulse was observed, without regard to its amplitude. Then, for impulses with amplitudes below a certain threshold, useful information was discarded, causing an observable degradation in the decoding process. With the practical erasure declaration process, only essentially worthless bits were discarded. Figure

5.5.2 shows the error performance when the practical erasure criterion is applied to the previously used model.

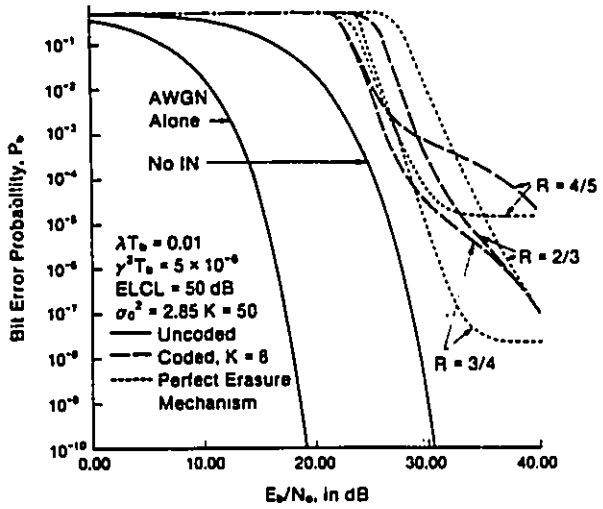

Nonhomogeneous 2-mile section;
1'st BT 0.125 mi. 24 AWG;
2'nd BT 0.125 mi. 24 AWG.

(c)

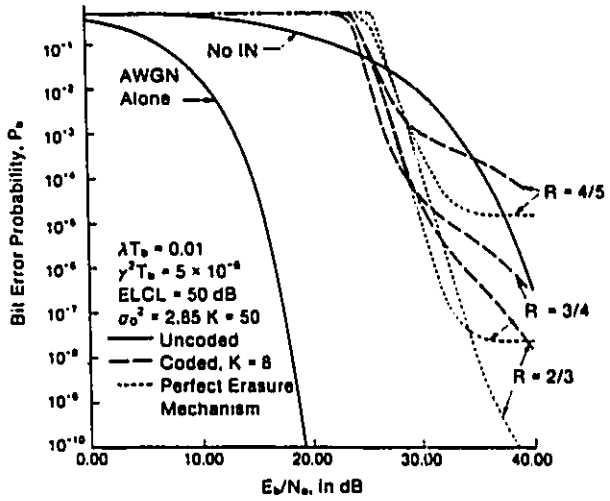

(b)

Nonhomogeneous 2-mile section;
1'st BT 0.35 mi. 24 AWG;
2'nd BT 0.35 mi. 24 AWG.

(d)

Fig. 8. Comparison of coded bit error probability performance of various $K = 8$ convolutional codes on CDSLS at $f_b = 200$ kb/s with $\gamma^2 T_b = 5 \times 10^{-6}$.

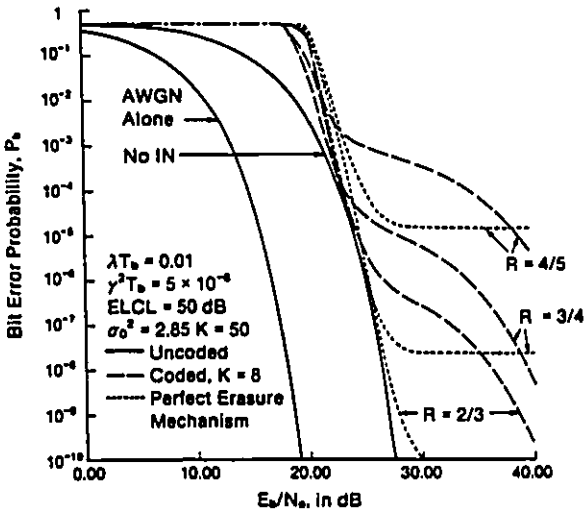

Homogeneous 2-mile section; 24 AWG.

(a)

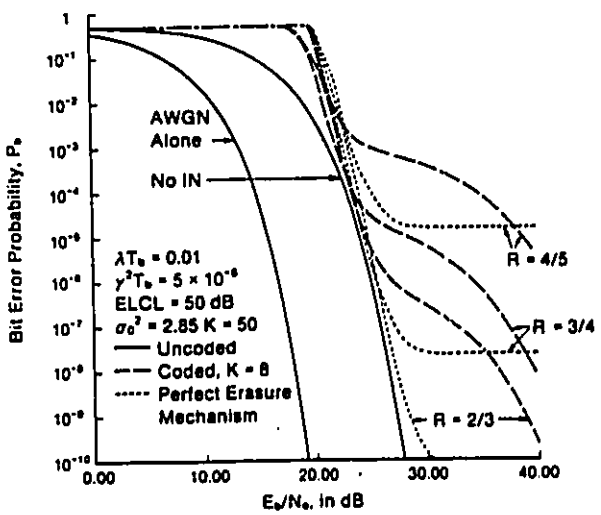

Nonhomogeneous 2-mi. section;
0.5 mi. 26 AWG; 1.0 mi. 24 AWG;
0.5 mi. 22 AWG.

(taken from Sargrad and modestino [24])

Figure 5.5.2 Error Rates For Practical Erasures Decoding

Convolutional coding, with erasures Viterbi decoding, is capable of offering a coding gain in the neighborhood of 8 dB for various combinations of FEXT, AWGN and impulse noise. This is realized only in the absence of NEXT (see Appendix E for the results of a study on the effects of NEXT on error control coding schemes). The presence of NEXT may possibly result in a net coding loss. Otherwise, the erasure decoding technique appears to be of some practical value in most local loop applications.

5.6 PULSE SHARPENING

5.6.1 GENERAL

Pulse sharpening is a proposed technique for reducing the harmful effects of impulse noise. It should be useful for both analog and digital systems, although only the digital will be analyzed.

Pulse sharpening operates in a manner directly opposite to that of pulse smearing, described in Section 5.2. The two techniques achieve similar ends. Pulse sharpening attempts to concentrate the energy of a noise pulse to a small interval of time so that it can be dissipated by a nonlinear device (eg. a clipper). The residual damage to the data signal is then confined to an absolute minimum of time. The smear-desmear technique makes no attempt to dissipate the energy of a noise pulse but merely spreads it over a long time

interval so that its damaging effect on an individual data pulse is minimized.

The pulse sharpening technique operates as follows:

i) Impulse noise is modeled as a random train of ideal delta voltages, routed through a time invariant network to a receiver. The network is used to represent the coupling path from the source of the impulse noise, into the local loop, and along the loop to the receiver. Typically, the impulse noise arrives at the receiver as smeared, wide, low amplitude pulses.

ii) In the receiver, a complement of the impulse coupling network restores the impulse, as near as possible, to its original form.

iii) A ZMNL (per Modestino [18]) device then "kills" the delta voltage by reducing its amplitude to zero, as much as possible, without increasing its width. A hole puncher is used to represent a particular case of such a device, for descriptive purposes.

iv) The bandlimiting pre-detection filter in the receiver (or integrate and dump detector) smooths over the "hole" in the signal without significantly biasing the succeeding decision process.

Figure 5.6.1 is a block diagram of the system.

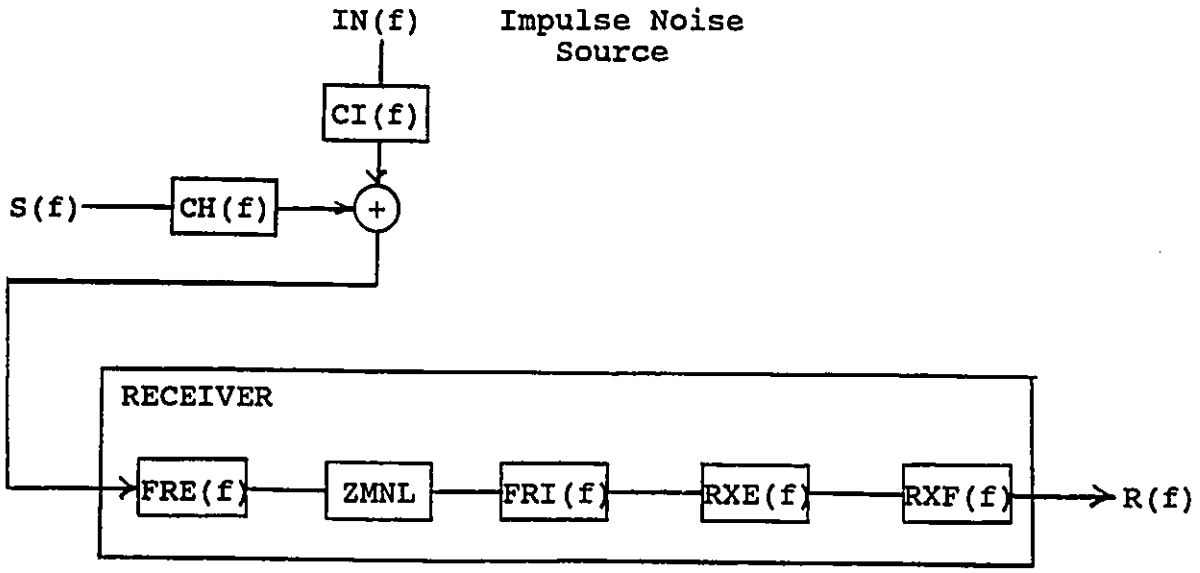

Figure 5.6.1 Impulse Noise Reduction Scheme

S(f) = Fourier transform of the transmit voltage signal, s(t)

CH(f) = Channel transfer function

IN(f) = Fourier transform of the impulse voltage, in(t)

CI(f) = Coupling transfer function, from impulse noise source to receiver input (including part of the local loop)

FRE(f) = Impulse noise sharpening filter transfer function

ZMNL = Zero memory nonlinear device, in particular a hole puncher

FRI(f) = FRE(f) compensating network transfer function

RXE(f) = Local loop post equalizer transfer function

RXF(f) = Receiver pre-detection bandlimiting filter transfer function

R(f) = Fourier transform of the receive voltage signal, r(t), just before detection.

For the noise impulses to be restored to their original delta form and the data signal to be preserved, the following must be met:

i) $FRE(f) = CI(f)^{-1}$

ii) $FRI(f) = FRE(f)^{-1} = CI(f)$

iii) $RXE(f) = CH(f)^{-1}$

iv) RXF(f) is defined by some other requirement (eg. a Wiener filter for Gaussian noise).

How close this can come to completely eliminating the effects of impulse noise depends on many factors. The following are the necessary conditions for the system to operate efficiently.

i) It must be reasonably accurate to model the impulse noise by a random delta generator, coupled to the receiver by a time invariant network. The time invariant network requirement implies that the individual impulses arriving at the receiver must each have the same waveshape, although amplitudes may vary. (This model follows directly from the tentative definition of impulse noise given in Section 3.2.)

ii) The width of the sharpened noise pulse must be as small as possible in order to minimize the size of the "hole" that the ZMNL device punches in the signal. As will be demonstrated, this implies that the bandwidth of the tandem connected networks, CI(f)FRE(f), must be as large as possible. There is a practical upper limit to this bandwidth.

iii) Networks FRE(f) and FRI(f) must be found that meet the conditions already defined. FRI(f) is the complement of FRE(f); finding FRE(f) then becomes the problem. This, and a discussion of the properties of FRE(f), is the topic of the next section.

5.6.2 THE SHARPENING FILTER

At this point one may sense that one is travelling on familiar ground. Network CI(f) may be visualized as the impairment of a communication channel used to transport signals represented by IN(f). Network FRE(f) then takes on the role of a channel equalizer used to restore signal IN(f) by compensating for the frequency and phase distortion introduced by CI(f). Most of the existing channel equalizer technology can be applied to that for the sharpening filter, with some differences. These are now considered.

EFFECTS OF BANDWIDTH CONSTRAINTS:

In practice, we nearly always deal with systems having limited bandwidths. The extraneous noise or the dynamic ranges of analog or digital devices tend to impose these limits. This effect can be modeled, in a somewhat idealized manner, by assuming that a unity gain "brickwall" type of filter has been inserted in the impulse noise path. This situation is shown below in Figure 5.6.2.A. (The dotted portion represents a notch in the passband corresponding to a zero in CI(f). This will be discussed later.) Figure 5.6.2.B represents the waveform of a sharpened noise impulse after passing through a properly compensated sharpening filter with the brickwall filter inserted in the path. This is simply the sinc(t) function for the classical impulse-brickwall situation.

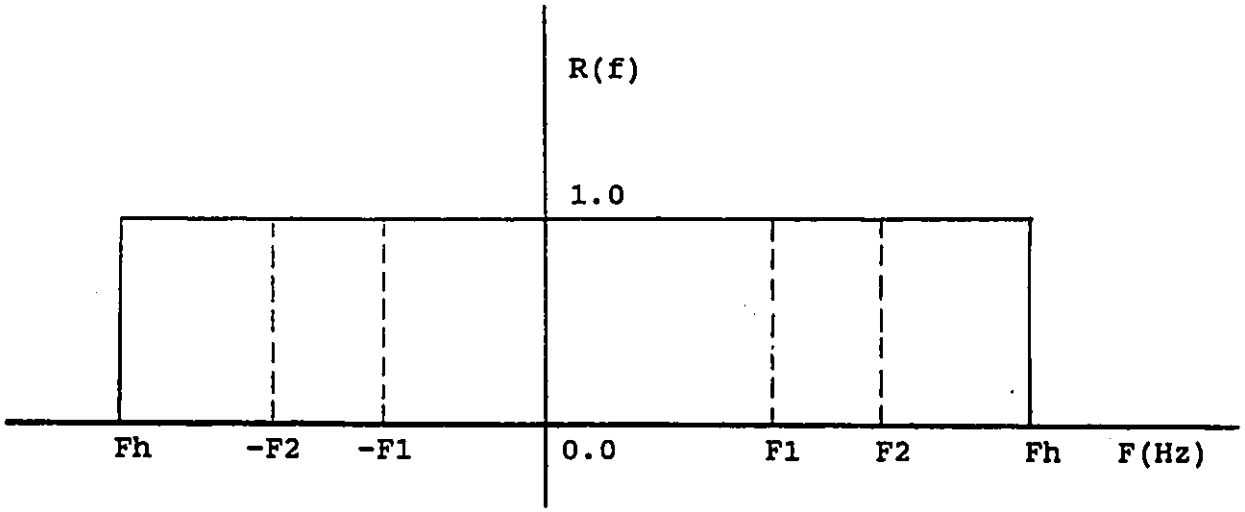

Figure 5.6.2.A Equivalent Bandlimiting Constraint

Figure 5.6.2.C shows a typical sharpened impulse after being treated by the ZMNL. It is immediately apparent that the width of

the "hole" forced into the signal by the ZMNL device is defined by the bandwidth of the brickwall filter. The larger the effective bandwidth of the sharpening path, the thinner is the hole punched into the data signal.

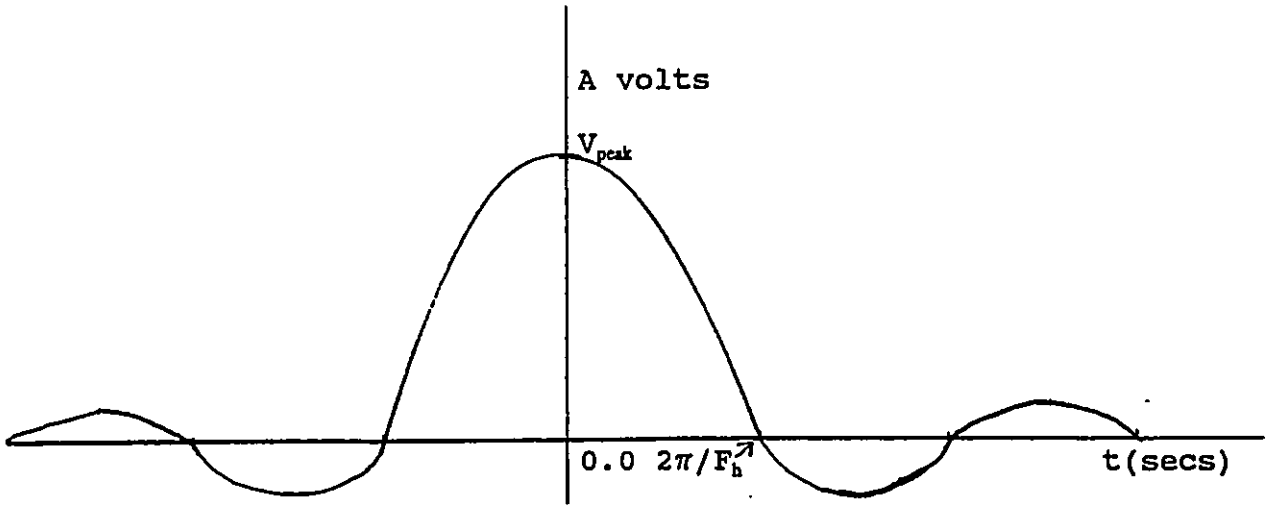

Figure 5.6.2.B Sharpened Impulse

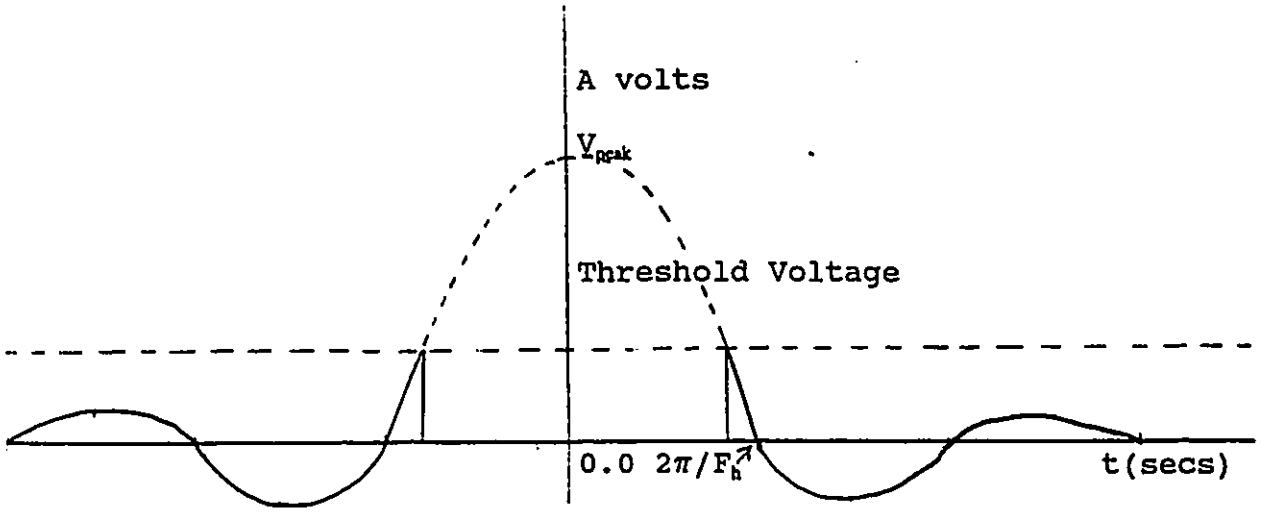

Figure 5.6.2.C ZMNL Processed Impulse

ZEROES IN THE CI(F) NETWORK:

Consider for a moment how the conventional loop system deals with zeroes in the channel transfer function caused by bridged taps. Problems arise when the zeroes are situated within the working passband of the system. This is because the equalizer can remove zeroes in the channel by matching them with poles in the equalizer function. The high equalizer gains required to approximate these poles would seriously degrade the system SNR. In fact, the problem is avoided entirely by applying design limits to the bridged taps.

Zeroes in the crosstalk coupling network, CI(f), can occur in three places: - in the originating circuit of the impulses

- in the electromagnetic coupling mechanism between loops
- in the destination loop.

The electromagnetic coupling element is not likely to contain transmission zeroes. By design, the destination loop should not have in-band zeroes. The originating loop, however, may have in-band zeroes since its design is likely fortuitous. There is then a distinct possibility that CI(f) will have zeroes. Dealing with these will be considered next.

STABILITY OF THE SHARPENING NETWORKS:

CI(f), the NEXT coupling function, being entirely passive, is unconditionally stable [52]. As has been discussed in Section 5.2, its complement is stable only if CI(f) has all poles and zeroes in the left hand complex plane. Since CI(f) can have zeroes in the

working passband of the system then FRE(f) could have poles in the right hand complex plane. To avoid this possibility a notch must be forced into the frequency response of FRE(f) (as shown in figure 5.6.2.A) surrounding the location of each such pole.

The net result of this is to reduce the effectiveness of the sharpening filter. Details on this will not be pursued in this thesis.

THE EFFECTS OF SHARPENING FILTER INACCURACIES:

Inaccuracy can show up in two forms:

- inaccuracy in matching the complementary pairs FRE(f) and FRI(f)
- inaccuracy in matching the complementary pairs CI(f) and FRE(f).

Inaccurate implementation of the filter pair FRE(f) and FRI(f) would introduce distortion in the data transmission path, causing ISI. It would appear that there would be an accuracy problem in implementing the networks FRE)f) and FRI(f) digitally. As Beenker, Claasen and Van Gerwen [41] have pointed out, controlling the data signal distortion produced by mismatching a pair of tandem connected complementary filters is achieved only at the cost of complexity. They considered the use of over a hundred stages in a transversal smearing filter in order to reduce this distortion to acceptable values.

Inaccuracy in matching CI(f) and FRE(f) would decrease the effectiveness of the ZMNL in destroying the energy of the noise impulses. With a matched network pair the ZMNL would see an ideal impulse. With an unmatched pair the ZMNL would see a waveform proportional to their impulse response, when combined. As a result the ZMNL device would remove a larger than necessary part of the output waveform as well as allow impulse sidelobes to pass. This would increase the frequency of data errors at the output of the data detector. Further investigation of this is required.

EFFECTS OF SHARPENING ON DATA SIGNALS:

It is hoped that the filtered data signal at the input to the ZMNL device will be a low, wide, smeared pulse, while the noise pulse will be a narrow high amplitude spike. If the sharpening network also sharpens the data signal, there is a possibility that the ZMNL device will then suppress the data signal, or at least do so partially. Let us now find the conditions for this undesirable event to occur.

Consider a method of generating a binary data signal, in a data transmitter. If we let the source data be represented by a time sequence of delta functions, d_k, then we can use a pulse generating network, with impulse response p_k, to generate the line signal s_k.

Then: $s_k = d_k * p_k$; where * represents the convolution operator.

In the frequency domain this becomes: S(f) = D(f)P(f); where D(f) represents the spectrum of a delta data signal.

At the input to the ZMNL this becomes: D(f)Z(f), where:

Z(f) = P(f)CH(f)FRE(f).

The undesired condition is reached when: Z(f) = CI(f), so that both data signals and impulse noise are ideal impulses, at the input of the ZMNL. Then both data and impulse noise could be "punched out". There is little that can be done to resolve the problem at the receiver; the spectral properties of the far end transmit signal must be changed. The condition causing the problem is not likely to occur in practice, one hopes. In any case, further analysis of the problem is required.

ACQUISITION OF SHARPENING NETWORK CONSTANTS:

The value of the compensating network, FRI(f), would be easy to find, once the value of the sharpening network, FRE(f), has been found. That is, FRI(f) is simply the complement of FRE(f). Finding FRE(f), however, is another matter.

FRE(f) is just the complement of CI(f). Stated another way FRI(f) = CI(f). A single isolated noise impulse arriving at the receiver, bears CI(f), as the frequency spectrum of itself. On the surface it would then appear easy to acquire the constants of CI(f)

by a spectrum analysis routine. Things may not be quite this simple.

A method suggested for adaptively finding CI(f) is as follows:

i) A waveform storage element would be included to capture a complete noise impulse event. Storage would be triggered by sensing a signal with an abnormally high amplitude. Each new impulse would be saved temporarily.

ii) Each sample would have its amplitude normalized (to allow for varying impulse strengths) and polarity set to make the pulse positive going. The captured waveforms would be averaged on a running basis to eliminate the other signals on the loop (eg. digital data, AWGN).

iii) The averaged pulse waveform would be continuously cycled through a programmable digital filter, the constants for which were changed adaptively. A "hill climbing" type of algorithm would be used to find the set of constants giving a maximum amplitude output signal.

iv) The filter constants would be used to derive a set of constants for a the complementary filter. The two sets of constants would be periodically loaded into working filters FRE(f) and FRI(f) respectively.

5.6.3 PROPERTIES OF THE ZMNL DEVICE

For analytical purposes the ZMNL device is treated as an ideal hole puncher. It is ideal in the sense that it is triggered on any noise

pulse strong enough to be harmful and when activated punches out the entire noise pulse. The "bottom of the hole" is set at a neutral level so that it does not bias the following detection process. (The limiter on the other hand leaves a residual that tends to bias detection. Consider the case with logic ONE treated as +1 volt and logic ZERO as -1 volt, with the limiter level set to ±1.2 volts. A strong positive going noise impulse falling on a ZERO would then give a 2.2 volt rise to the +1.2 volt clipping level, thus biasing the subsequent detection process.)

The essential property of the ZMNL device then is that it flags the beginning and ending of the sharpened noise pulse. We can assume that the interval between the start and end of the pulse is not information bearing and reject it from the subsequent decision process. That is, it should act as an erasure interval of time. The detector following the hole puncher then operates in the following manner:

i) A sampled data integrate-and-dump element is used to recover the data. Integration is achieved by adding the samples during a bit interval and dividing the sum by the number of samples, say N. A decision is then made by comparing this result with the threshold and putting out either a ONE or ZERO.

ii) In the presence of a noise impulse, the samples of the N_E pulses between the start and stop flags should be ignored. The sum is then divided by $(N - N_E)$, giving a correct average value that is then presented to the decision device.

iii) The loss in accuracy of the decision process, for Gaussian background noise, is proportional to the quantity $(N - N_B)/N$. This results because the averaging period has been shortened by this factor. This is equivalent to an increase in bandwidth of a matched filter detector given by the factor $N/(N - N_B)$. That is, the background noise power is raised from N_0 to $N_0N/(N - N_B)$, for the original data bandwidth. This indicates that the noise impulses must be sharpened as much as possible in order to minimize decision errors.

5.6.4 COMMENTS

The system was designed to operate efficiently only on pulses that could be modeled by a generator and time invariant coupling network. There are many questions to be asked about its tolerance to impulses that do not conform to this requirement. The following come to mind:

i) Impulse noise in a local loop often comes from many sources, only one of which can be sharpened. How robust is the system for the other non-optimal situations?

ii) Consider the case of a time varying coupling network. Atmospheric disturbances, to a radio receiver, from a distant thunderstorm is a good example of this. The radio wave propagation path is continually changing. How should this case be treated?

There are a number of apparent advantages to the scheme, which are listed below:

i) This scheme should be able to successfully eliminate impulse noise that others cannot. High intensity impulse noise, severely smeared in transmission, is an example.

ii) Since only the data receiver has been modified to incorporate pulse sharpening, it ensures signal compatibility with existing systems. It is then not necessary to establish new line signal standards. (This is a crucial matter for the commercial implementation of any new design.) It also becomes easy to place into service units employing the new design. In an existing network, only those receivers bothered by impulse noise need be replaced.

ii) Combining pulse sharpening with other impulse reducing noise techniques may possibly give superior performance to those others used alone. For example, pulse sharpening could be used as an outer process with pulse smearing-desmearing used as an inner process. Strong impulses that normally would be stretched by smearing into a long burst would be reduced in amplitude by the hole puncher and then further reduced by smearing.

The pulse sharpening technique should be investigated further, both analytically and by computer simulation. It possibly will take a place, as one of the advanced techniques, for dealing with a most serious transmission impairment.

5.7 DESIGN OPTIMIZATION

The following are a number of ways in which system design can be optimized to improve error performance in an impulsive noise environment.

5.7.1 PASSBAND SIGNALLING

Werner [16], in 1990, and Kerpez [43], in 1991, pointed out that most of the energy of impulse noise on local loops is confined to the region below 50 kHz or so. This may not be universally true, because Werner had mentioned that the NYNEX company had found a small number of loops having appreciable impulse noise energy up to a frequency of 200 kHz. They concluded that, in most cases, passband signalling should be less susceptible to impulse noise than baseband.

Sistanizadeh and Kerpez [46], in 1991, reported that QAM was 1.45 times less susceptible to impulse noise than was PAM. Their results were based on a simulation of a loop system using a large number of recorded impulse events, collected by the NYNEX Company, in 1986. The loop was composed of 9 kft of 26 gauge cable. A transmission rate of 200 kbps was used. The PAM system was implemented as a baseband type, using the 2B1Q code, while the QAM was implemented with 16 point QAM on an 87 kHz carrier.

5.7.2 MULTITONE SIGNALLING

Chow, Tu and Cioffi [53] investigated the performance of a multitone HDSL, operating at 1.6 Mbps. 256 single FSK subchannels were used in a computer simulation model. It was stated that such a system has an "inherent tolerance to impulse noise". Also, the system was said to offer optimum tolerance for extremely short noise impulses. (This paper covered the HDSL application of the technique in a general way. Particular aspects, such as impulse noise immunity, were not emphasized.) Why this type of system should have a higher degree of immunity is not clear. Further research will likely be reqired to answer this question.

5.7.3 MODULATION METHOD

In 1965, Engel [14] published his results for a mathematical evaluation of different digital modulation schemes in the presence of impulse noise. He ranked them in order of decreasing immunity as shown in Table 5.7.3.1. The SNR shown is that required to support a P_{bit} of 10^{-5}. A flat channel was assumed with impulse noise represented by the Mertz model.

TABLE 5.7.3.1

Comparison of Digital Modulation Schemes

Modulation Technique	SNR dB
Single-sideband AM with coherent detection	9.4
Double-sideband AM with coherent detection	11.5
Phase shift keying with differentially coherent detection	12.6
Frequency shift keying	15.5
AM with envelope detection.	16.0

(taken from Engel [14])

Engel mentioned that the above order of efficiency also applied to an AWGN environment, implying that it is sufficient to select a modulation technique on the basis of its AWGN performance. There is also a 6.6 dB spread among those systems of digital modulation investigated, making a careful choice of design worthwhile.

5.7.4 DFE OR TOMLINSON PRECODING

Young and Cole [47] studied the use of a DFE in the receiver, or a Tomlinson precoder in the transmitter, in place of a linear equalizer in the receiver. Either type offered an advantage over the linear equalizer in an impulse noise environment. This was because of the absence of the high frequency boost, required with a linear equalizer, to compensate for the frequency roll-off of a

local loop. Because a high level noise impulse can cause error propagation in the DFE, but not in the Tomlinson precoder, there is an advantage in using the Tomlinson precoder, rather than the DFE. The Tomlinson precoder then is to be preferred over either the DFE or the linear equalizer, in an impulse noise environment.

5.7.5 OPTIMAL RECEIVE FILTER

Bennett and Davey [40] showed that the transfer function of an optimal receive filter, for a wideband channel, is of the form:

$$Y(f) = B[\cos \frac{\pi f}{2fs}]^{v};\ 0 < f < fs \text{ where:}$$

B = an arbitrary constant

v = 1 for Gaussian noise

v = 4/3 for impulse noise.

If the filter were optimized for one type of noise a 0.15 dB penalty in SNR would result for the other. Also, a compromise value for v = 7/6 caused a 0.05 dB degradation for either type of noise. There appears little to gain by matching the filter only to impulse noise.

5.7.6 SLICER LEVEL ADJUSTMENT

In 1988 Modestino and associates [23] pointed out, that for an AMI bipolar local loop system, subject to impulse noise, the P_{bit} for a

mark is much less than that for a space. This would suggest that, for a random data pattern, the mark-space threshold voltage could be adjusted upward slightly above the half mark value, to minimize the total occurrence of impulse induced bit errors.

5.7.7 MISCELLANEOUS

Freeman [3] suggested that the effects of impulse noise can be reduced, by configuring loops so as to avoid C.O.'s known to be noisy. He also suggested adding loop repeaters, just before impulse noise sources, so as to increase the SNR. Bender, Kneuer and Lawless [1] followed a similar policy by defining a maximum acceptable cable loss of 31 dB per section at the Nyquist frequency.

Experience indicates that cable pair balance is often disturbed by the terminating arrangement used. Coupling of impulse noise increases tremendously if a pair carrying impulse noise and a nearby pair carrying a data signal are both unbalanced. The method used to couple talk battery into a telephone circuit can cause imbalance for dialing pulses. Also, the method of coupling D.C. sealing current (used to reduce noise caused by corroded splices in the cable pairs) into data pairs, can do the same for the data system.

A brute force approach to improving impulse noise immunity would be to simply increase transmit signal power. Computer simulation

studies (ref. Appendix E) have shown that this step causes no change in the susceptibility to NEXT interference. A 6 dB improvement in impulse noise immunity would result from doubling the transmit signal voltage.

CHAPTER 6

CONCLUSIONS AND RECOMMENDATIONS

CONCLUSIONS:

1) The experimental work of Curtis [11], on the sparking electrical contact, is the primary source of information on the still most common source of impulse noise. It illustrates the complex nature of impulse noise, as corroborated by the experimental observations and data presented in this thesis. The physical events taking place, during contact closing and opening, are far more complex than one would think. This paper should be very revealing to those attempting to model impulse noise.

2) The Mertz [12] probabilistic model of impulse noise is important because it defined the two distribution concept (time of occurrence and amplitude) that all succeeding researchers have used. The Modestino model, however, is the most useful. As Modestino and his associates have shown, it can be used to represent impulse noise when modeling just about any conceivable type of communications system. For example, they analyzed the efficiencies of: amplitude limiting, hole punching, block coding, Viterbi decoding, interleaving, baseband and passband modulation schemes.

3) The burst error model of Gilbert [26] offers many advantages. The use of the two state Markov chain, to represent the error free

and error prone states of a channel, is simple to understand and visualize. As well, the model is convenient to use in practice (easy to fit to experimental data, easy to use for a theoretical analysis). Its accuracy seems to be acceptable.

The Mandelbrot and Mertz models are reasonably uncomplicated to apply and are understood to give acceptable results. However, they are more complex than the Gilbert model. Also, there are slight problems with the mathematical aspects of the Pareto distributions describing the models, that require their users to pay careful attention to details. That is, the values of certain parameters must be cautiously chosen in order to ensure the existence of the distribution mean and standard deviation. Also, a Shannon capacity is undefined for these models.

4) Of the several techniques considered for alleviating the affects of impulse noise, pulse smearing seems to be the most practical for the loop environment. The design of digital smear and desmear filters appears to be straight forward. The smearing and desmearing filters could be built into existing filters in the modem, virtually cost free, if digital filters were used. The remaining techniques do not seem to be commercially feasible, at present. Error control coding and passband signalling could be used but the resulting degradation in signal-to-NEXT ratio, caused by the upward expansion in signal spectra, would likely be considered unacceptable. The use of pulse limiting and hole punching may not be

worthwhile in the local loop, where some of the impulse noise pulses are already amplitude limited to near peak signal values.

5) Pulse sharpening, introduced in Section 5.6 has the potential of offering many of the advantages of the powerful smearing and desmearing method, yet has certain advantages over it. It requires only that the receiver be modified and thus avoids system compatibility problems, resulting when transmitters must also be modified. It should be optimal for high energy noise impulses that have been smeared in transmission to the receiver. Other important advantages may be revealed in the future.

RECOMMENDATIONS:

The following are recommendations for future research:

1) There are still many opportunities open to those wishing to do fundamental research into the nature of impulse noise:

i) Field studies should be brought up to date. The nature of impulse noise itself has changed as a consequence of the changes in the apparatus causing it. Also, the local loop technology has changed tremendously over the past few years, requiring a shift in the emphasis of an investigation. One thorough and universally acceptable study would allow the various candidate models for impulse noise, and schemes for dealing with it, to be compared on a standard basis.

ii) Classifying the types of impulse noise should be considered. This may well reveal that there are distinct families of the phenomena, such that no two members of which can be represented by the same mathematical model.

iii) Computer simulation programs should be written so that any new models for impulse noise could be evaluated.

iv) The connection between impulse noise and burst errors should be investigated further. How a certain kind of impulse noise effects a certain type of loop transmission scheme is an important practical question.

2) Research should be done on the pulse sharpening technique. Its properties are now theoretical and as yet unverified by experimental work. Computer simulation experiments should be performed to provide numerical evidence on the properties of a system employing it. It has the potential for almost completely eliminating the effects of impulse noise, with no known penalties realized. The subject is brand new and presents a wide open field for research.

3) Research should be done on the consequences of combining the techniques, such as:

i) Smearing-desmearing and pulse sharpening

ii) Smearing-desmearing and clipping or hole punching

and so forth.

APPENDIX A

THE COMMERCIAL ENVIRONMENT

The purpose of this section is to review the commercial setting in which impulse noise problems are discovered and solved.

It is a fact of business life that:

i) A customer within a certain distance of the telephone central office will, on demand, be provided with a link that operates virtually error free.

ii) A link, once installed, will always be maintained to this standard.

The financial costs of following such a policy can be, and on occasion are, staggering. The traditional quality control philosophy of manufacturing, that states that it is acceptable to deliver goods with a certain per cent defective, is by comparison an unaffordable luxury.

Time independent troubles are moderately costly to correct. Failures caused by a defective modem or cable pair, for example, are corrected by replacing the defective component. Finding and removing a spurious bridged tap, on a cable pair, may be more time consuming but is a straight forward process.

Solving an impulse noise trouble is extremely time consuming and costly for the following reasons:

i) Impulse noise problems are extremely rare and at the same time are unique. Limited experience at solving them in the past may be of little help in dealing with a new one. One can only guess at how the noise is generated and how it is coupled into the local loop.

ii) The problem cannot usually be solved by changing the cable pairs to the customer's premises. There is rarely more than one cable to the premises and all pairs in it are almost certainly contaminated by the same impulse noise source.

iii) Changing modems, at that point the only alternative, is unlikely to be of benefit, because there is a high degree of uniformity among units of the same make. Trying different designs of modem has been successful, but is bound to be a slow process. Few types of modems are stocked by the communications carrier (an outcome of product standardization and warehouse inventory factors). Even then trial and error is the only way of selecting a preferred unit. The supplier of the standard unit may be willing to make design changes, especially if he wishes to protect his favored status. Testing of the results is a trial and error process, done in the field.

iv) Impulse noise is definitely not a stationary phenomenon. Its intensity varies with time of day, day of week, and maybe day of month or season. It may in fact be largely acyclic; one Wednesday may not resemble any other. Knowing whether or not

changes in the transmission equipment have produced improvements may be uncertain. Apparent improvements, from equipment changes, may in fact be a result of performing field testing on a "good" day; next week the performance may be worse than ever.

v) Field testing of equipment over a lengthy period of time, to obtain stable results, may lead to poor customer relations.

The lesson is clear; better techniques for analyzing and simulating impulse noise are much needed. It would then be a straightforward procedure to select transmission schemes, known to be resistant to the impairment. Accurately ranking commercially available products for impulse noise immunity, as part of the laboratory work of modem standardization, could then be realized.

APPENDIX B

MEASUREMENT OF IMPULSE NOISE

The following description of the procedures used to measure steady noise was taken from Freeman [3]. When noise measurement units were first defined, it was decided that noise power should be given a positive number. The Bell System chose the zero level at minus 90 dBm (or 1 pW) because this was just below the threshold of hearing, for the model 144 telephone handset then in use. This unit of measurement was referred to as the dBrn, decibels, relative, noise. The test sets used to measure noise contained a "weighting network" or filter that duplicated the frequency response of the handset. As different telephone sets were developed, the reference levels were adjusted and new weighting networks were required. In North America ,at present, voice frequency noise measurements are based on the "message C" weighting network with measurements stated in dBrnC. A noise level of -1.5 dBrnC has been defined as the level of a -90 dBm 1000 Hz tone measured through a message C weighting network. (-1.5 rather than 0.0 was used to correct errors in the definitions of earlier schemes, which have not been described in this thesis.) Figure B.1, from Freeman, shows the frequency response curves for the message C network and several others.

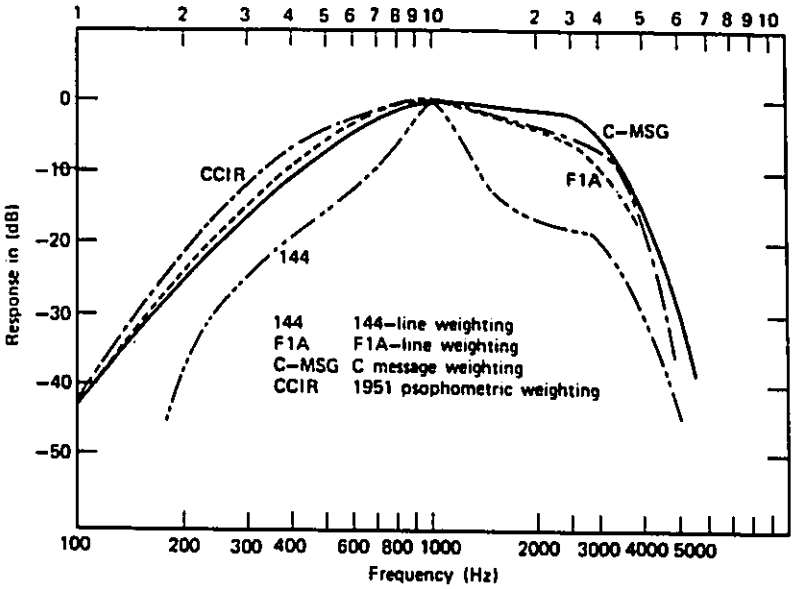

Figure 1.10 Line weightings for telephone (voice) channel noise.

(taken from Freeman [3])

Figure B.1 NMS Weighting Networks

Impulse noise, states Freeman, is measured as the number of "hits" or impulses per interval of time that exceed a threshold given in dBrnC. Thus a digital counter and interval timer are included in an impulse noise measuring set. The measurement is normally stated as the number of hits or "counts", above a specified dBrnC level, in a fifteen minute period of time. However, a fast voltage spike in a bandlimited system, such as a channel or even the weighting network itself, normally causes signal ringing. One spike then becomes a sequence of voltage pulses. To avoid over-counting of the

impulses, AT&T specified a 150 ms dead time after each count. The impulse counter was then limited to a maximum of six or seven counts per second. When a message C weighting network is used, it is stated that this dead band causes a loss of accuracy of 0.9 dB, arising from valid counts missed.

Favin [48] describes the AT&T model 6A noise measuring set, which is representative of this kind of instrument. AT&T [5] has since introduced models 6F and 6G.

The 6F had several useful new features. The weighting network was made plug-in so that others, than message C, could be used (flat frequency response, and 50 kbps which is useful for testing 56 kbps digital loops for example). Four separate threshold detector-counter pairs were added so that impulse counts could be made simultaneously, at four different threshold values.

The 6G is a wideband instrument intended for use from 4 to 560 kHz. Two flat 560 kHz weighting networks are included, one with a fast and the other with a slow roll off above 560 kHz. The 6G lacks much of the versatility of the 6F and is used mainly for testing wideband analog radio channels.

It should be apparent that the structure of the model 6 is very similar to that of a matched filter binary baseband receiver: there is an amplifier, a receive filter and a threshold detector. The

counts of the unit should then be correlated quite well with the errors of a digital receiver.

The AT&T [6] impulse noise objective for local loops is: no more than 15 counts in 15 minutes at a threshold of 59 dBrnC.

Ungar [10] proposed an acceptance limit for ISDN basic access, which operates at 144 kbps, of: no more than 15 counts in fifteen minutes at a threshold of 59 dBrn using a 50 kbps weighting network.

It should be noted, before leaving this section, that although there is a considerable difference of opinion on the causes of impulse noise and how to model it, both mathematically and physically, there is little controversy on how to measure it. The AT&T model 6F impulse counter and equivalents are supreme in this matter.

APPENDIX C

TELEPHONE NETWORK STUDIES

The bulk of the theoretical work on impulse noise and burst errors was done in the early 1960's. Field investigations of these impairments played a critical role in testing and refining the newly created mathematical models. The Bell Laboratories field study of Alexander, Gryb and Nast [27], was by far the principal, if not the only important, study of this time (May 1960). Eight of the keystone theoretical papers ([14], [26], [28], [29], [34], [35], [37], [38]) relied on the results of this study in verifying their conclusions. An obvious benefit of this, was that it made it easy to rank the various models for goodness of fit to the "real world" situation. The Alexander study [27] dealt with end-to-end channels, made up of local loops at the ends and voice frequency carrier systems in the middle. Unfortunately, the inclusion of carrier systems tended to obscure the impulse noise properties of the local loops themselves.

The theoretical models for impulse noise, in the local loops, were simply those for the long haul voice grade channels, adapted to the new situation. No study of the rank of the Alexander study has been performed on the local cable plant. Consequently, many researchers did their own highly specialized studies, of limited extent, as a

necessary part of refining and evaluating their work. (Ten major research papers [7], [8], [9], [13], [15], [25], [32], [39], [41], [49] were in this class.) Many private studies were performed by various organizations for internal use (only condensed reports were released to the outside.) The following are in this class:

"1982 GTE outside plant survey - an analysis of the physical and transmission characteristics," TN83-302.1 GTE Labs. Inc., Waltham, Mass., March 1983 [20],

"The outside plant high frequency test results," GTE Labs. technical note 83-302.8, 1983 [22],

NYNEX Corp., "Characteristics of impulse noise on selected NYNEX metropolitan loops," ECSA Contribution T1D1.3/86-144 [16],

R. A. McDonald, "Report on Bellcore impulse noise study," Contribution T1D1.3/86-256, July 1987 [16].

Some studies involved only the collection of impulse noise waveforms in the local cable plant, using wideband analog tape recorders. It appears that these were to be used to evaluate the robustness of prototype data modems in the laboratory. There have been no attempts, to date, to use these waveforms in the construction of mathematical models. The following are in this class:

Kurland and Molony, "Observations on the effects of pulse noise on digital data transmission systems," Aug. 1967 [49],

R. L. DeWitt and J. P. Forde, unpublished results of a field study, 1968 [29],

Alles, Cuffling, Bertrand and Quintal, "Digital loop system performance prediction using an impulse noise database," 1989 [50].

There is now a need for an intensive study of impulse noise in the local loop environment which may lead to improvements in noise modeling.

APPENDIX D

LOCAL LOOP SYSTEMS

This section of the appendix provides technical details on the various types of data transmission systems used with telephone local loop type cables.

A system is considered to run between two points connected by twisted-pair copper wires. The wires in turn are twisted into groups of 50 pairs, wrapped by a colored tracer cord and called a binder group. A cable is made up of a number of binder groups, ranging in size from 50 to 3000 pairs. Most modern cable pairs are made of 22, 24 or 26 gauge copper wire, with polyvinyl insulation.

The various types of systems using local loops are described as follows:

i) The DDS Access System

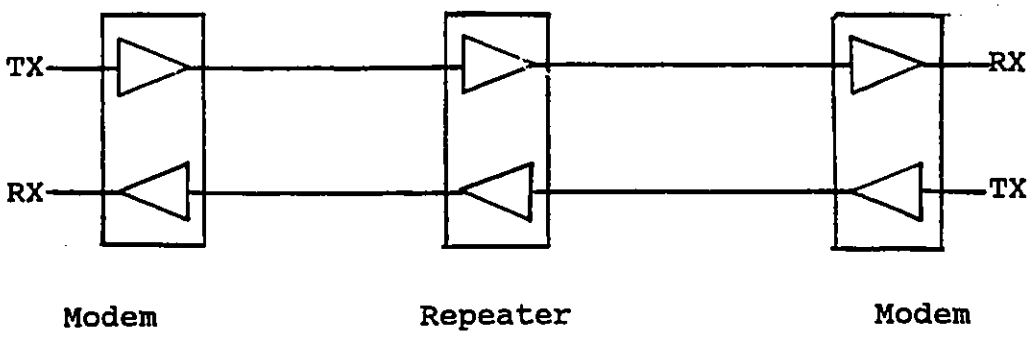

The facility operates synchronously, in a full duplex mode, using two independent local loops.

Standard data rates are: 2.4, 4.8, 9.6 and 56.0 kbps

Cable Requirements: 22, 24 or 26 gauge nonloaded, 31 dB loss at the Nyquist frequency (approx. 13 kft of 26 gauge cable at 56.0 kbps)

Signal format: 50% duty cycle bipolar with 6 zero substitution, substitute words being labelled with bipolar violations.

ii) The T-1 Repeatered Line

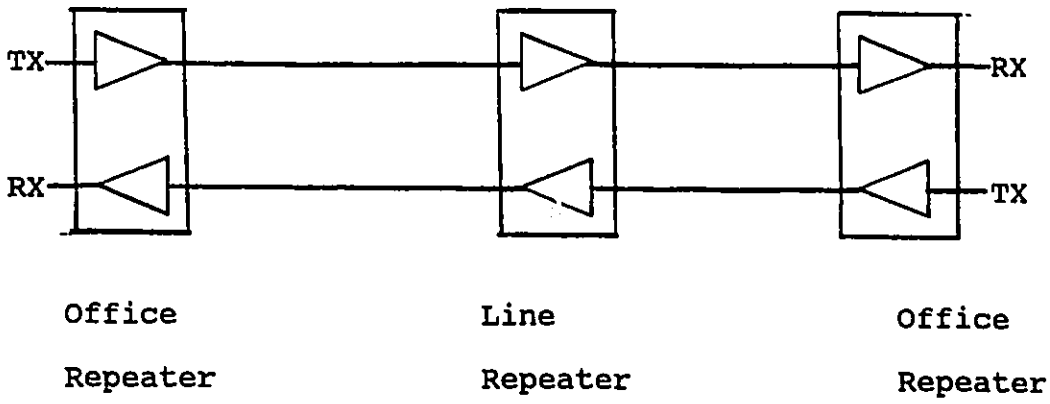

The facility operates synchronously, in a full duplex mode, using two independent local loops.

Data rate is: 1.544 Mbps

Cable requirements: 22 or 24 gauge nonloaded, distance from office to first line repeater is set at 3 kft, distance between line repeaters is set at 6 kft (this is normal manhole spacing for the analog voice service)

Signal format: 50% duty cycle bipolar with 8 zero substitution, substitute words being labelled with bipolar violations

iii) The ISDN Access Line Using TCM

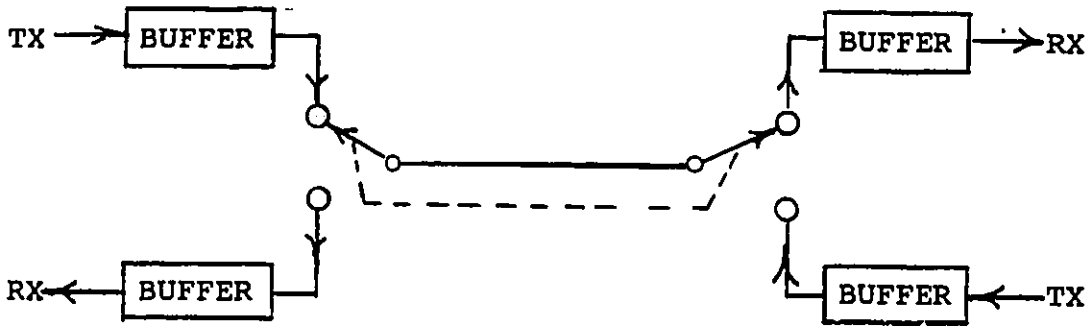

The service operates synchronously, in a full duplex mode. The facility operates in half duplex at double the data rate plus overhead. Full duplex operation is emulated by reversing the direction at a uniform rate, using synchronized switches. (This is also referred to as the ping-pong mode of operation). NEXT vanishes when all systems, using the same cable, are switched simultaneously.

Data rate: 400 kbps (2.5 times 160 kbps) on the facility , 144 kbps externally.

Cable Requirements: not specified

Signal format: not specified

iv) The ISDN Access Line Using Echo Cancelers

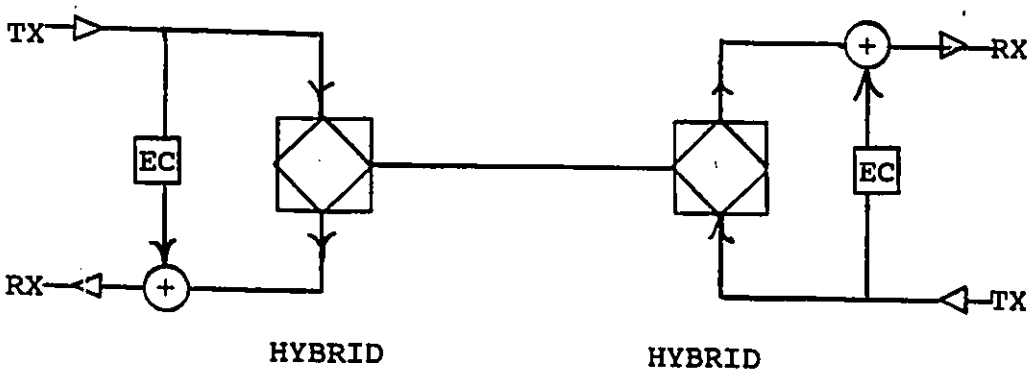

The facility operates synchronously, in a full duplex mode, using a single loop. Hybrid networks are used to isolate the transmit and receive directions. Echo cancellers are used to correct for hybrid unbalance, avoiding the interference caused by far end echo and near end signal leakage across the hybrid.

Data rate: 160 kbps on the facility, 144 kbps externally

Cable requirements: 22, 24 and 26 gauge nonloaded, 35 dB loss at the Nyquist frequency of 80 kHz

Signal Format: 50% duty cycle bipolar with 2B1Q (2 binary to 1 quaternary line code) line coding

v) The HDSL Access Line Using Two 800 kbps Lines

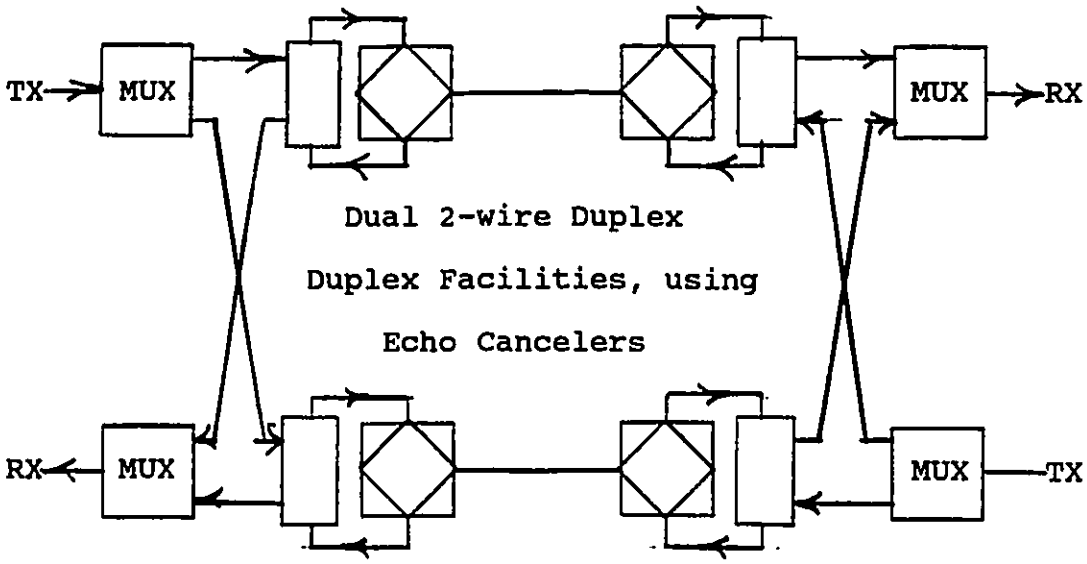

The facility operates synchronously, in a full duplex mode, using a multiplexed combination of 2-wire facilities. Each 2-wire facility operates in full duplex, using hybrid networks and echo cancelers.

Data Rate is: 800 kbps on each 2-wire channel, external at 1.544 Mbps.

Cable Requirements: The system is experimental only. Computer simulations indicate that system should operate up to 12 kft on a 24 gauge nonloaded cable.

Signal Format is: Baseband with 2B1Q coding.

vi) The HDSL Access Line Using 1.544 Mbps Lines

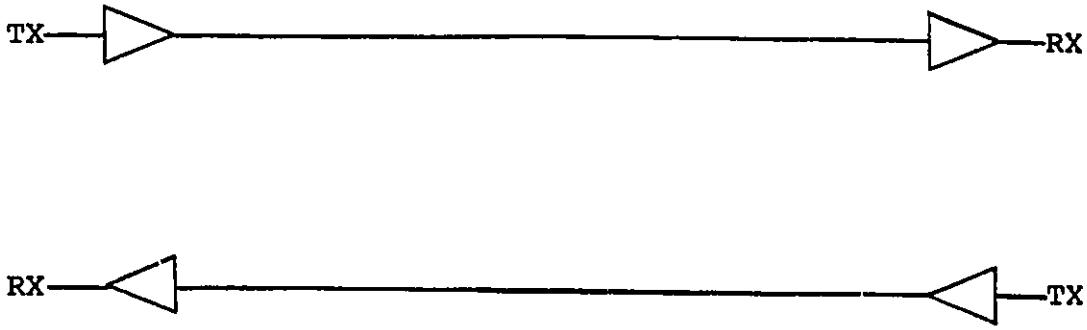

The facility operates synchronously, in a full duplex mode, using two independent local loops. The T-1 signal format is used.

Data Rate is: 1.544 Mbps

Cable Requirements: 24 gauge, up to 12 kft long. Loop repeaters are not used. Range has been extended by employing improved data receivers.

Signal Format: 50% duty cycle bipolar with 8 zero substitution, substitute words being labelled with bipolar violations.

vii) The ADSL Access Line

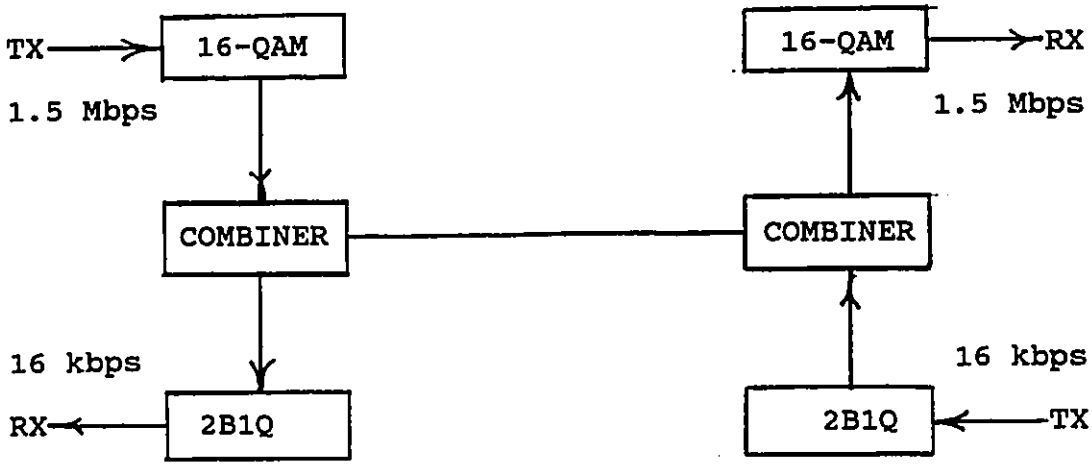

The facility operates synchronously, in a full duplex mode, using one local loop. Transmission in one direction is at a rate of 1.5 Mbps and in the other is at 16 kbps.

Cable Requirements are: Reliable operation is said to be possible with up to 18 kft of 24 gauge cable.

Signal Format: The 1.5 Mbps system uses 16-QAM, or less likely 64-QAM, with a carrier in the range of 297 kHz to 397 kHz. The spectrum does not extend below 40 kHz. The 16 kHz system uses a low pass baseband system. The signal spectra for the two directions are separate from each other. This is an experimental system at this time.

APPENDIX E

COMPUTER SIMULATION OF A LOOP SYSTEM

E.1 ERROR CONTROL CODING IN A NEXT ENVIRONMENT

GENERAL:

The original loop transmission scheme, for which the simulation program was constructed, was found to be ineffective. For its operation the scheme required that the data rate on the loop be increased significantly. Results were positive for a loop model that allowed for signal distortion and AWGN. Unfortunately, when NEXT was added to the model, the weakness of the scheme was revealed: any increase in data rate, caused by increasing data redundancy, invariably lead to an increase in system P_{bit}. It was concluded that any coding scheme that increased the data rate on the loop could not produce any improvement in performance in a strong NEXT environment. This section of Appendix E studies this situation in more detail.

Section E.2 documents version K-16D of the computer simulation program used.

INVESTIGATION 1:

An experiment was performed using NEXT interference only (AWGN was not injected). For a given data rate a local loop length was found

to give a P_{bit} = 0.000258. With the loop length fixed at that value and with a data rate N% higher, a value for P_{bit} was found. This was done for ten values of N, between 1% and 16%. Simulation runs were then done for each of the data rates of 144, 800 and 1544 kbps. The results were plotted in the three curves shown in figure E.1.1.

OBSERVATION 1: The P_{bit} curves were very close together for each of the three initial data rates. It was concluded that further simulation, using 800 kbps, would in fact be representative of the properties of the system for all other data rates.

INVESTIGATION 2:

Using a base data rate of 800 kbps three sets of simulation runs were performed as follows:

Run A: NEXT only environment.

Run B: NEXT and AWGN mixed environment, with the AWGN level set to give the same P_{bit} as was found for the NEXT when used alone.

Run C: AWGN only environment.

The loop lengths were chosen separately in each instance to give a P_{bit} as near as possible to 0.000258, at the base data rate. The loop length was then kept fixed during each run.

The results were plotted in figure E.1.2.

OBSERVATION 2:

Curve C represents the AWGN environment normally used to test the performance of error control codes. For an increase of 18% in

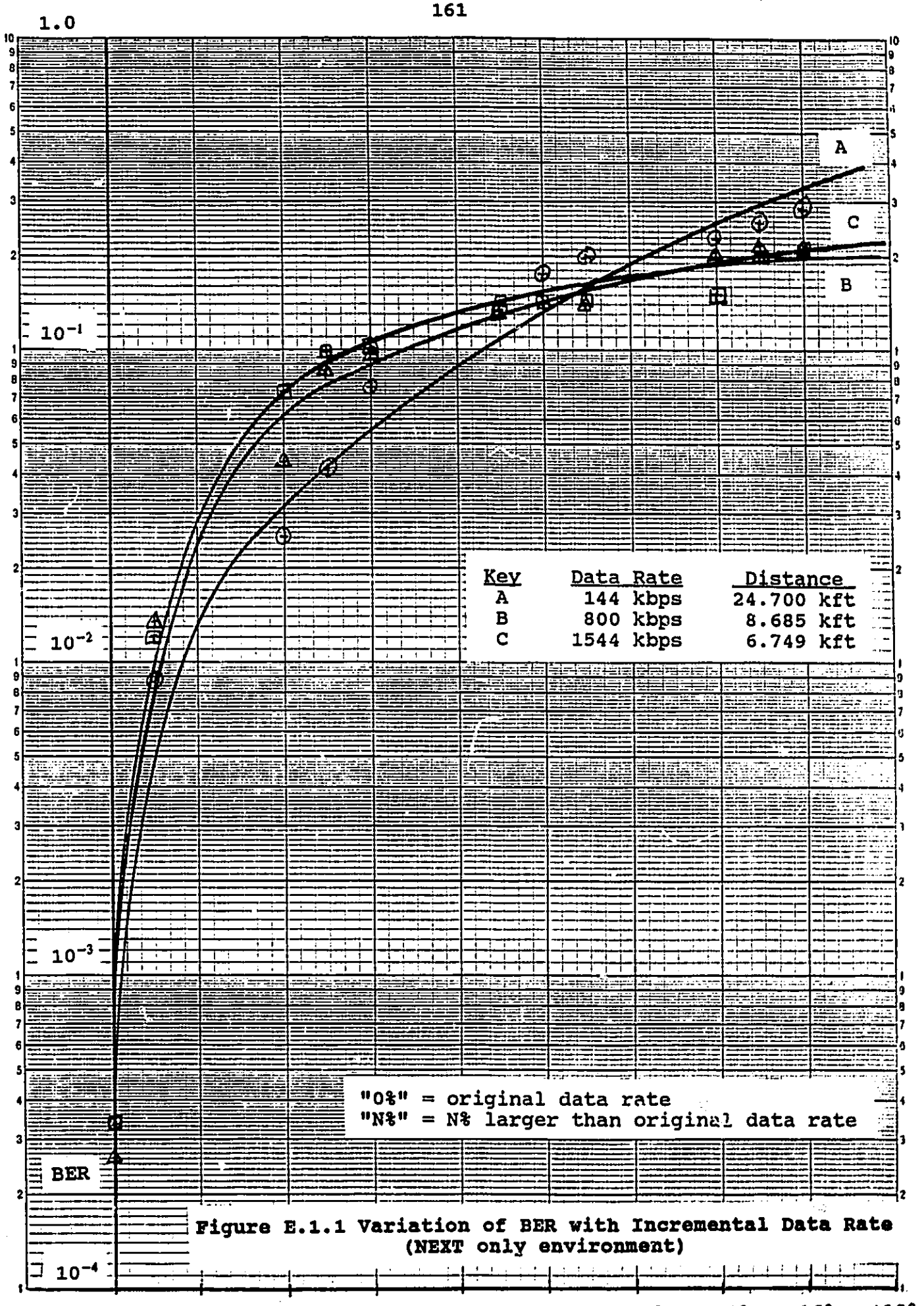

Figure E.1.1 Variation of BER with Incremental Data Rate
(NEXT only environment)

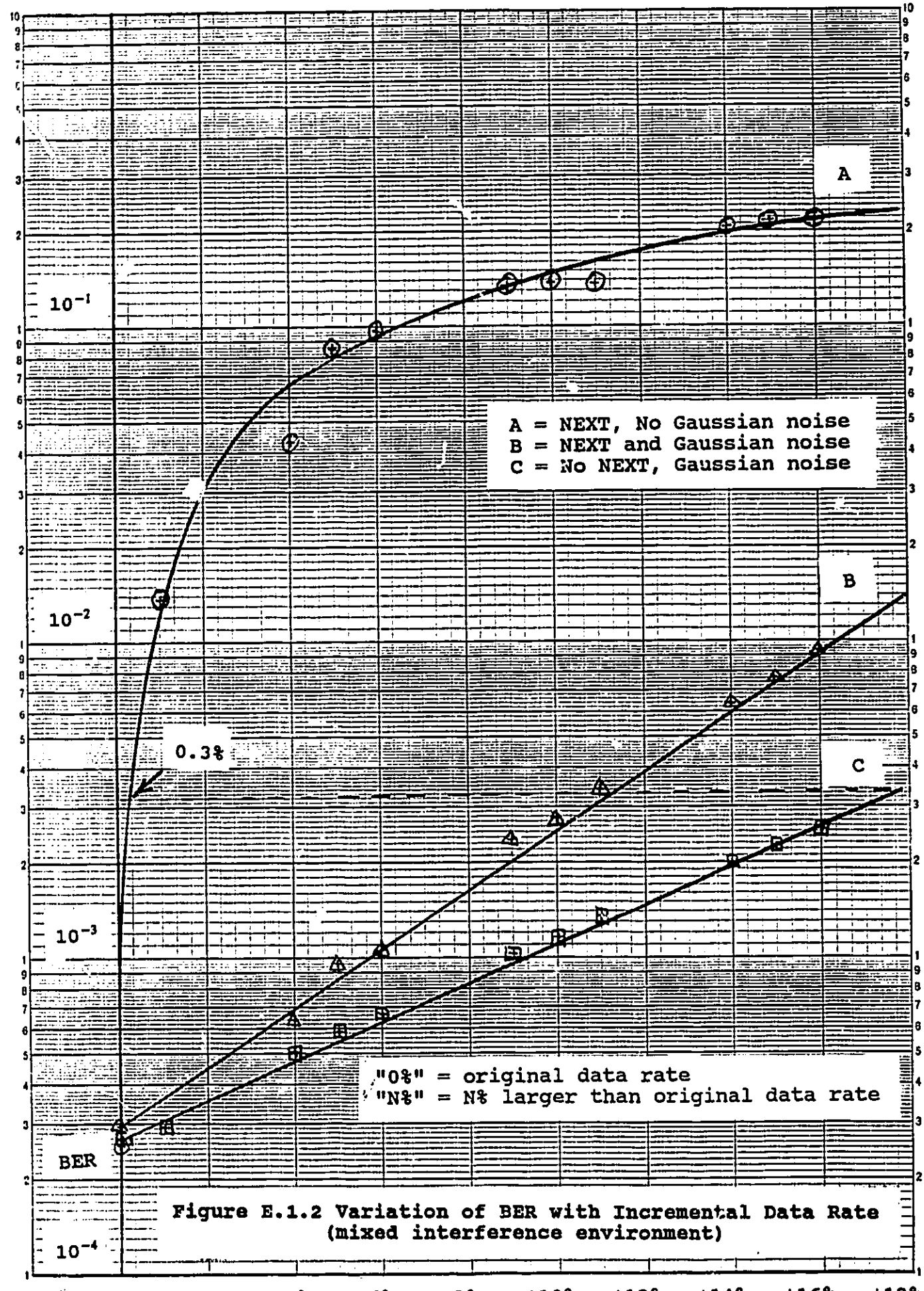

Figure E.1.2 Variation of BER with Incremental Data Rate (mixed interference environment)

SEMI-LOGARITHMIC 46 5890
4 CYCLES X 90 DIVISIONS
KEUFFEL & ESSER CO.

channel data rate, corresponding to a 0.847 rate code, the channel P_{bit} increases only 13 times. Curve represents system performance for the pure NEXT environment. The same increase in loop data rate, as for curve C, caused P_{bit} to be increased 891 times.

ANALYSIS:

It is apparent that the capability of NEXT to impair data transmission is significant. As an aid to studying this further, Table E.1.1 was constructed from the information shown in figure E.1.2.

TABLE E.1.1

Variation of P_{bit} With Data Rate

(for a mixed interference environment)

DATA RATE INCREASE	CODING RATE	P_{bit}		
		NEXT ONLY	AWGN ONLY	NEXT + AWGN
(1)	(2)	(3)	(4)	(5)
0%	1.0000	0.000258	0.000258	0.000258
2%	0.9804	0.030000	0.000350	0.000445
4%	0.9615	0.065000	0.000470	0.000690
6%	0.9434	0.092000	0.000620	0.001050
8%	0.9259	0.120000	0.000830	0.001650
10%	0.9091	0.148000	0.001100	0.002500
12%	0.8929	0.173000	0.001450	0.003850
14%	0.8772	0.197000	0.001950	0.005150
16%	0.8621	0.217000	0.002600	0.009100
18%	0.8475	0.230000	0.003400	0.014000

Col. (1): gives the increase in channel data rate necessary to support channel coding

Col. (2): gives the rate of the code

Cols. (3), (4) and (5): are the values of P_{bit} for each situation.

This data was used to calculate the Shannon capacity of the channel for the three types of interference. The system was modeled as a memoryless binary symmetric channel, using the formula:

$$C = 1 - P\log_2 P - (1-P)\log_2(1-P) \quad [51].$$

This model should represent the computer simulation model quite closely for the following reasons:

i) The local loop should be almost memoryless since it is fully equalized so that ISI is not introduced. The NEXT interference comes from a data source that is uncorrelated with that for the transmit data.

ii) The local loop should be symmetric since the data levels are symmetric (+1, -1) and the NEXT and AWGN signal voltages are also symmetric.

The values of C were then multiplied by the uncoded channel data rate to give the channel capacity, in kbps. The channel capacities were plotted in the three curves shown in figure E.1.3. (The dotted line indicates the break even level for an error control coding scheme.)

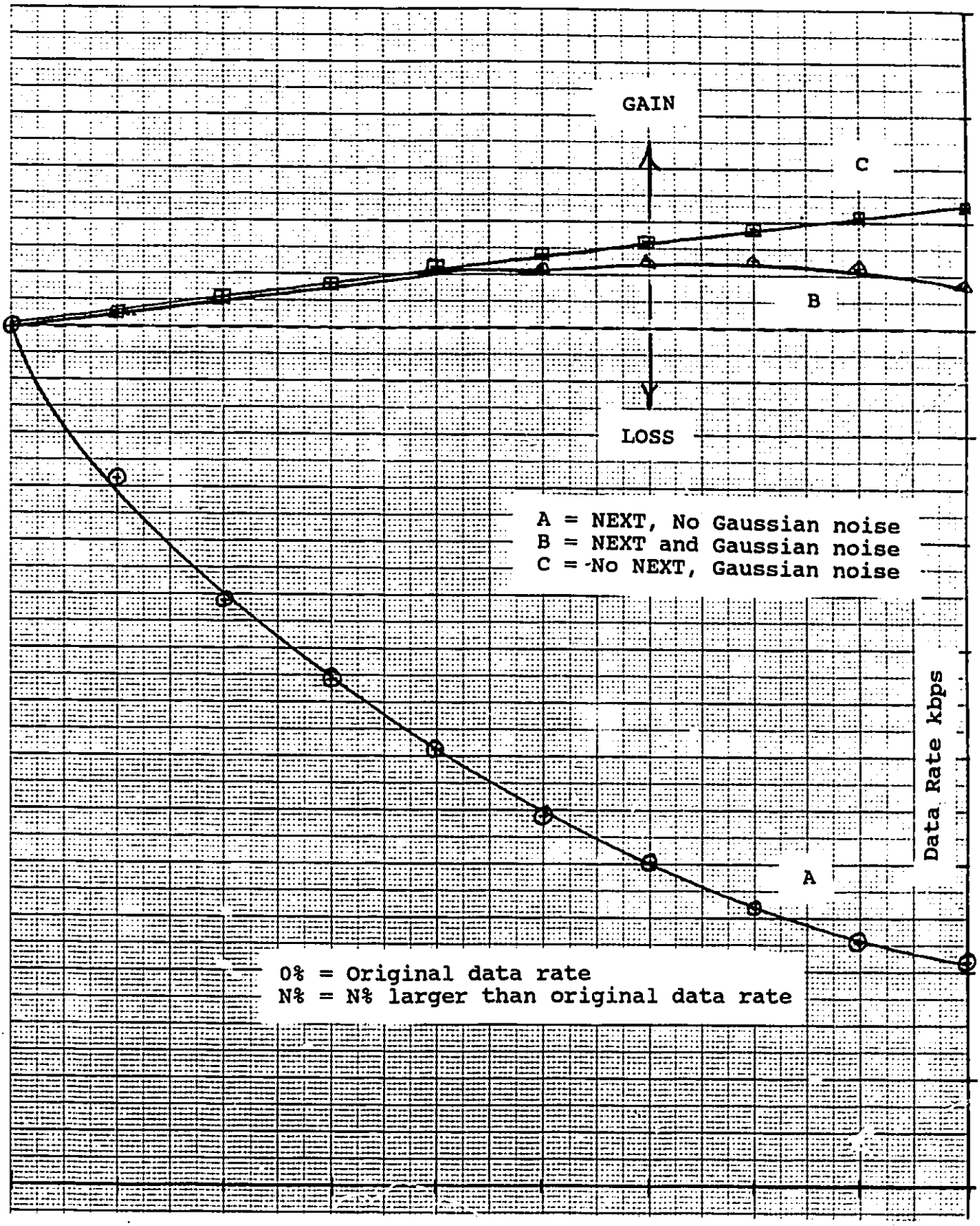

Figure E.1.3 Variation of Channel Capacity with Incremental Data Rate (mixed interference environment)

461510
10 X 10 TO THE CENTIMETER
KEUFFEL & ESSER CO

Curve C, for a pure AWGN interference environment, indicates that it is possible to increase the channel capacity by using error control coding. The capacity tends to increase with increasing channel data rate.

Curve B, for a mixed NEXT and AWGN environment also shows a tendency for the channel capacity to increase with channel data rate. However, at a coding rate of 0.885 (13% data rate increase), the channel capacity reaches a peak value and decreases with decreasing coding rate thereafter.

Curve A, for the pure NEXT environment clearly falls below the dotted line continually as the channel data rate is increased. Error control coding on such a channel is then a wasteful process: as the data rate of the bare channel is increased to accommodate the redundant bits of the code, the channel capacity always decreases.

For a system sensitive to NEXT it is unlikely that the presence of AWGN would moderate the noise environment. This is because nearly all interference in a loop system is caused by outside agencies coupled into the system by crosstalk (AWGN internal to the system itself is not significant, ie loop or amplifier noise temperature is negligibly low).

Crosstalk itself has not been fully investigated; FEXT was not built into the simulation model. However, it is judged that NEXT interference would be dominant over FEXT. Another factor is that NEXT was modeled as being caused by one other similar and phase aligned data system rather from a mixture of sources. From the Central Limit Theorem it would follow that an AWGN source of NEXT would be a suitable choice for modeling more diverse and multiple sources of NEXT interferers. This was not done in the simulation model. However, it is judged that the NEXT coupling mechanism, with its rising frequency response, would be far more important in determining channel P_{bit} rather than the waveform of the source itself.

The computer simulation was based on a baseband 100% duty cycle bipolar signal using hard decision decoding. The results expressed in figure E.1.3 are so strongly decisive that there is little doubt that the results should apply to loop systems in general.

CONCLUSIONS:

Error control coding is not an effective means of combatting transmission errors in a NEXT type local loop channel. For dominant NEXT interference the channel capacity is always decreased by error control coding. For a mixed interference channel, including NEXT, channel capacity may increase for high rate codes, while decreasing for low rate codes.

E.2 SIMULATION PROGRAM VERSION K-16D

Table E.2.1 gives the specifications for the simulation program, version K-16D.

TABLE E.2.1

Product Specification

Mode of Operation:	Monte Carlo based simulation
Platform:	IBM CMS on-line timeshare system
Language:	FORTRAN, WATFOR77 type
Loop Model:	channel loss, in dB, is given by Kalet and Shamai [54] by: Gain dB = -0.279396*DIST*SQRT(f), where DIST = cable length, in kft. f = frequency kHz.
NEXT Model:	coupling transfer function, is given by Kalet and Shamai [54] by: H(f) = 3.1622E-5*LINES*f**0.75, where: LINES = number of interferers f = frequency kHz.
Digital Data Model:	A 17 bit shift register sequence is used to generate the data. Data logic level ONE = +1, integer. Data logic level ZERO = -1, integer. (bipolar with 100% duty cycle.)
AWGN Source:	The system subroutine GGNML is used to generate Gaussian variates.

NEXT Source:	A digital data source, having the same properties as the user data is used.
Structure:	Data is represented by IPF samples per bit, where IPF = 8. Analog data is handled in complex arrays LDIM samples long, where LDIM = 2,048. Binary data is handled in integer arrays LDIM/IPF = 256 symbols long.
Basis:	Voltages are combined arithmetically. Filtering is performed by multiplication in the frequency domain and conversion back to the voltage domain. The system Fast Fourier Transform, FFT2C, is used for both operations.

Program Dynamics:

The block diagram for program version K-16D is shown in figure E.2.1. The program has the following basic components:

i) Input Data section
ii) Build Model section
iii) Initialize System section
iv) Control structure
v) Signal processing section.

The Input Data section serves as the user to process input interface.

INPUT DATA

Input cable length into DIST
Input data rate into DRATE
Input Equalizer distribution factor into EFACTR
Input no. of NEXT interferers into LINES
Input signal-to-AWGN ratio into DB
Input number of runs into JRUN

BUILD MODEL

Build TXT:
 Build transmit bandlimit filter into TXF
 Build local loop into CHE
 Build transmit equalizer into TXE
 Combine TXF, TXE, CHE into TXT.

Build RXT:
 Build receive equalizer into RXE
 Build receive filter into RXF
 Combine RXE, RXF into RXT.

Build TXN:
 Build NEXT coupling into XNF
 Combine TXF, TXE, XNF into TXN.

INITIALIZE SYSTEM

Use srtn PRBS to generate pseudorandom data into JAI

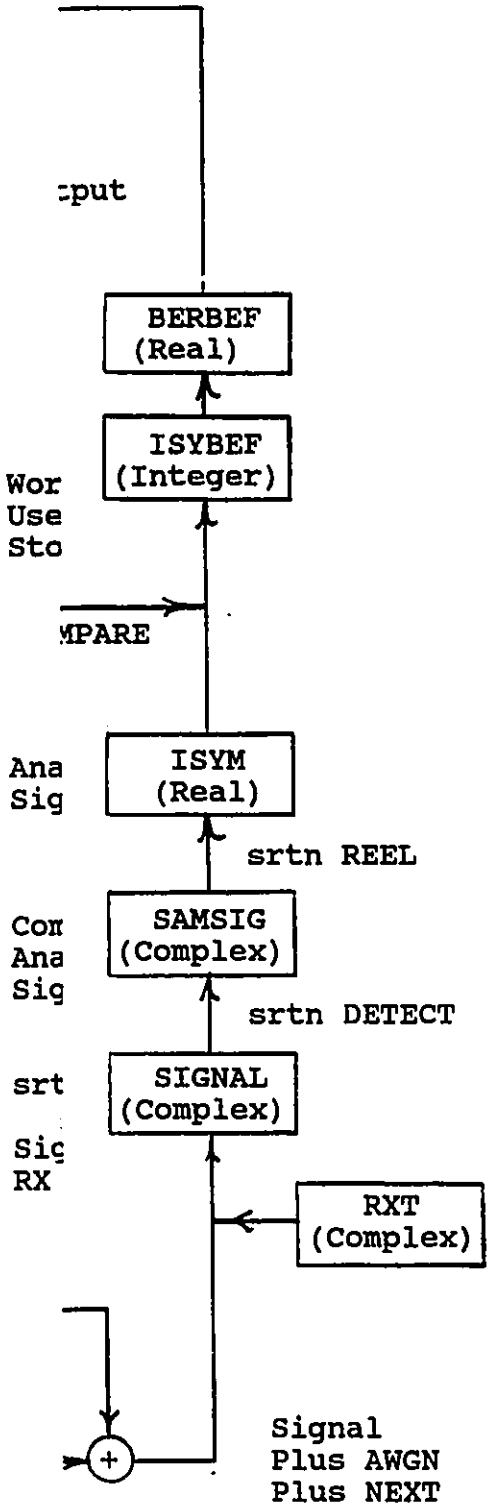

Figure E.2.1 Simulation Program Version K-16D

The Build Model section uses the input data to build the three basic filters in the complex frequency domain. The transmit bandlimiting (raised cosine) filter, transmit channel equalizer and the channel itself are built into filter array TXT. The NEXT coupling transfer function is built into TXN, using the transmit bandlimiting filter, transmit equalizer and NEXT coupling factor. The receiver filter is built into RXT using the receive channel equalizer and the receive bandlimiting (raised cosine) filter.

The Initialize system section generates the pseudorandom data in one step for later use.

The control structure simply allows the signal processing section to start looping, run for a given interval, stop and output error results.

The Signal processing section operates in a loop that processes the data in repeated blocks. (The data blocks are shown within the boxes of the figure. The subroutines, srtn's, are shown between the boxes, indicating a processing of the data from one box to the next.)

Testing Results:

Program testing was performed to ensure that the basic system met the requirements of a bandlimited system contaminated by AWGN. The effects of adding the model local loop were tested and finally that

INPUT DATA

Input cable length into DIST
Input data rate into DRATE
Input Equalizer distribution factor into EFACTR
Input no. of NEXT interferers into LINES
Input signal-to-AWGN ratio into DB
Input number of runs into JRUN

BUILD MODEL

Build TXT:
- Build transmit bandlimit filter into TXF
- Build local loop into CHE
- Build transmit equalizer into TXE
- Combine TXF, TXE, CHE into TXT.

Build RXT:
- Build receive equalizer into RXE
- Build receive filter into RXF
- Combine RXE, RXF into RXT.

Build TXN:
- Build NEXT coupling into XNF
- Combine TXF, TXE, XNF into TXN.

INITIALIZE SYSTEM

Use srtn PRBS to generate pseudorandom data into JAI

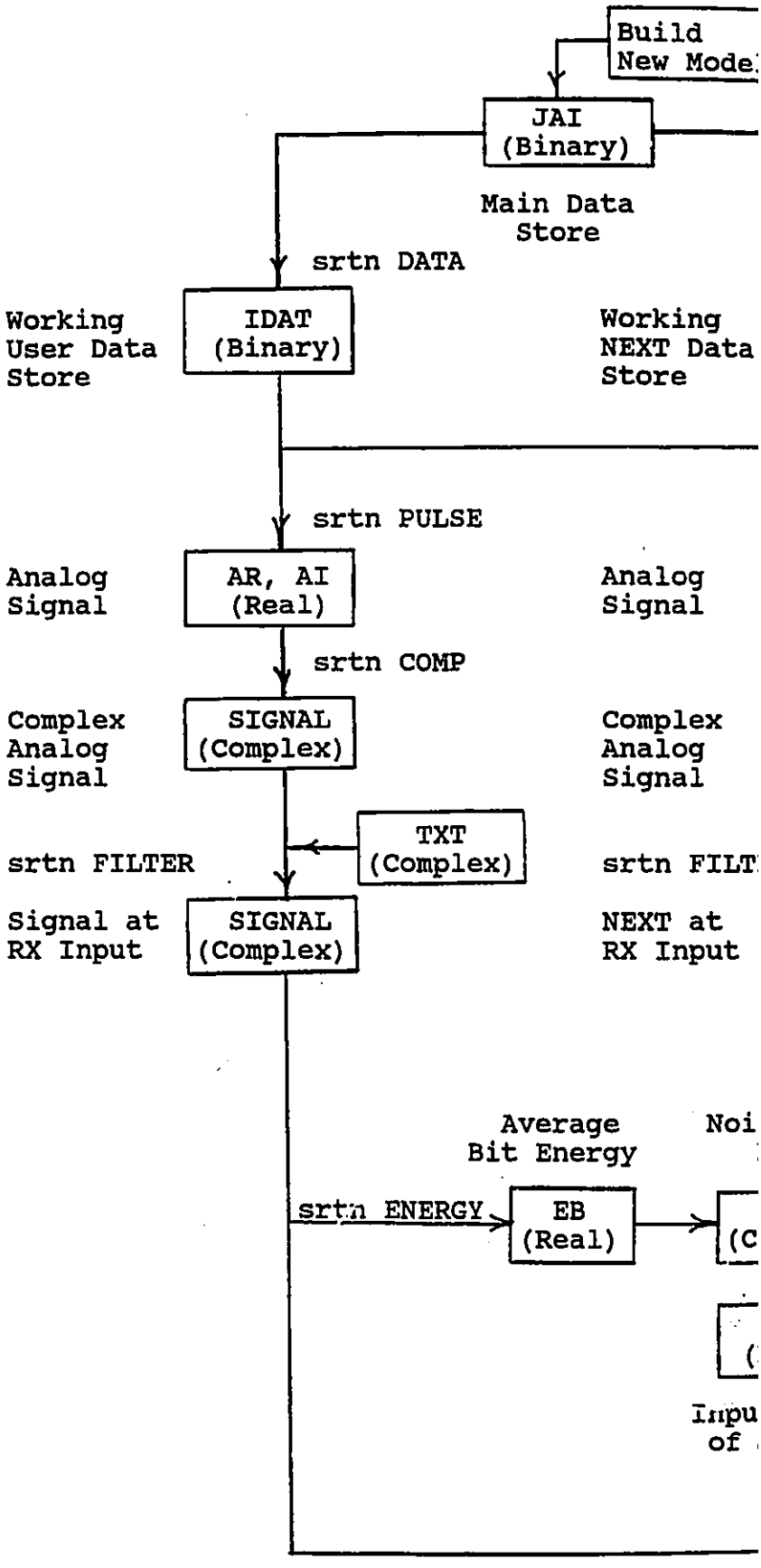

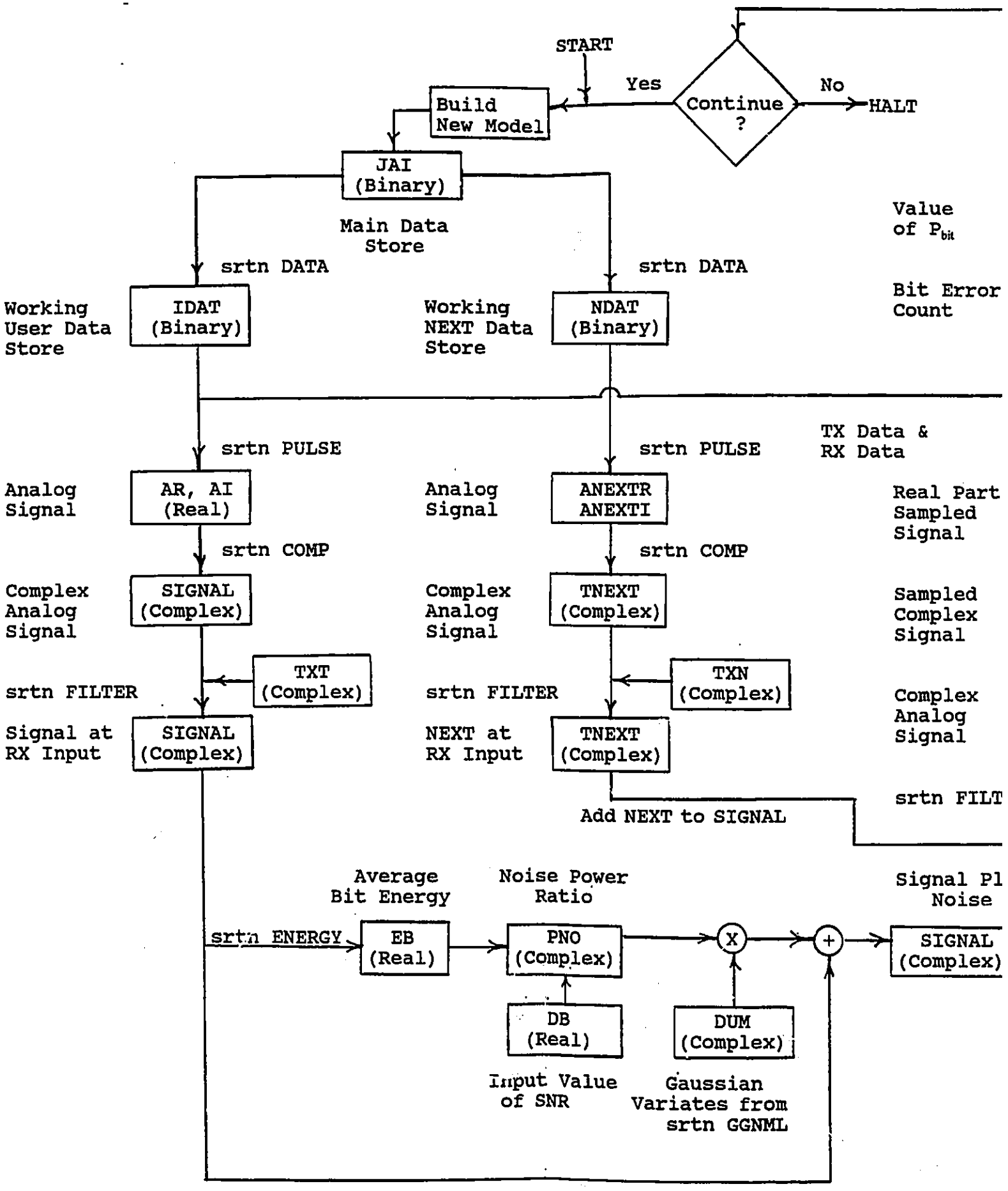
START
Yes
Continue ?
No
HALT
Build New Model
JAI (Binary)
Main Data Store
Value of P_{bit}
srtn DATA
srtn DATA
Working User Data Store
IDAT (Binary)
Working NEXT Data Store
NDAT (Binary)
Bit Error Count
TX Data & RX Data
srtn PULSE
srtn PULSE
Analog Signal
AR, AI (Real)
Analog Signal
ANEXTR ANEXTI
Real Part Sampled Signal
srtn COMP
srtn COMP
Complex Analog Signal
SIGNAL (Complex)
Complex Analog Signal
TNEXT (Complex)
Sampled Complex Signal
TXT (Complex)
TXN (Complex)
srtn FILTER
srtn FILTER
Complex Analog Signal
Signal at RX Input
SIGNAL (Complex)
NEXT at RX Input
TNEXT (Complex)
srtn FILT
Add NEXT to SIGNAL
Average Bit Energy
Noise Power Ratio
Signal Pl Noise
srtn ENERGY
EB (Real)
PNO (Complex)
X
+
SIGNAL (Complex)
DB (Real)
DUM (Complex)
Input Value of SNR
Gaussian Variates from srtn GGNML

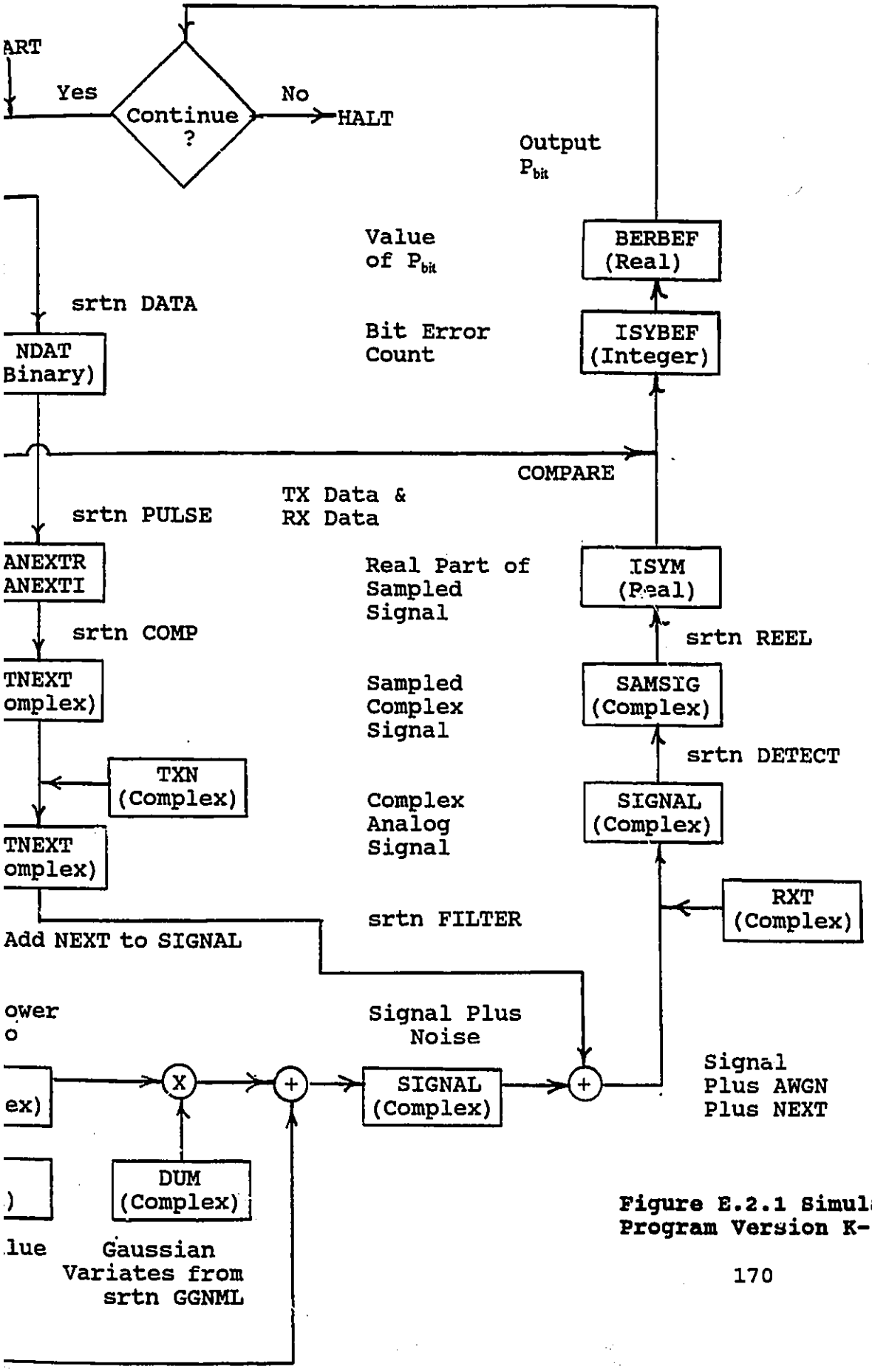

Figure E.2.1 Simulation Program Version K-16D

The Build Model section uses the input data to build the three basic filters in the complex frequency domain. The transmit bandlimiting (raised cosine) filter, transmit channel equalizer and the channel itself are built into filter array TXT. The NEXT coupling transfer function is built into TXN, using the transmit bandlimiting filter, transmit equalizer and NEXT coupling factor. The receiver filter is built into RXT using the receive channel equalizer and the receive bandlimiting (raised cosine) filter.

The Initialize system section generates the pseudorandom data in one step for later use.

The control structure simply allows the signal processing section to start looping, run for a given interval, stop and output error results.

The Signal processing section operates in a loop that processes the data in repeated blocks. (The data blocks are shown within the boxes of the figure. The subroutines, srtn's, are shown between the boxes, indicating a processing of the data from one box to the next.)

Testing Results:

Program testing was performed to ensure that the basic system met the requirements of a bandlimited system contaminated by AWGN. The effects of adding the model local loop were tested and finally that

for adding NEXT were tested. As well as assuring that the system represented the models accurately, the following interesting results were found:

i) The SNR-P_{bit} relationship, for a zero length cable and AWGN only, gave results that agreed with those for the classical antipodal signal system [55].

ii) For AWGN only interference, P_{bit} was a minimum for all transmit end channel equalization and a maximum for all receive end channel equalization (because of AWGN magnification by the receive equalizer).

iii) The P_{bit} for a loop with NEXT interference only, was independent of the location of channel equalization (ie. transmit end or receive end).

iv) P_{bit} was very small for recommended ISDN data rates and loop lengths and AWGN interference only. When NEXT was added to the model P_{bit} rose to nearly 10^{-4}, in each case, which was unacceptable.

The important results, dealing with the use of error control coding on a loop system, are described in Section E.1.

REFERENCES

[1] E. C. Bender, J. G. Kneuer and W. J. Lawless, "Digital data system: local distribution system," B.S.T.J., May-June 1975.

[2] R. W. Lucky, J. Salz and E. J. Weldon, Jr., "principles of Data communication," McGraw-Hill Book Company, 1968.

[3] R. L. Freeman, "Telecommunication Transmission Handbook," 2nd Edition, J. Wiley & Sons, 1981.

[4] American Telephone and Telegraph Company, "Telecommunications Transmission Engineering," Volume 1, Western Electric Company, 1977.

[5] American Telephone and Telegraph Company, "Telecommunications Transmission Engineering," Volume 2, Western Electric Company, 1977.

[6] American Telephone and Telegraph Company, "Telecommunications Transmission Engineering," Volume 3, Western Electric Company, 1977.

[7] H. Cravis and T. V. Crater, "Engineering of T1 carrier system repeatered lines," B.S.T.J., Mar. 1963.

[8] R. Komiya, K. Yoshida and N. Tamaki, "The loop coverage comparison between TCM and echo canceller under various noise considerations," IEEE Trans. Commun., Vol. COM-34 No. 11, Nov. 1986.

[9] J. J. Werner, "The HDSL environment," IEEE J. Select. Areas Commun., Vol. 9 No. 6, Aug. 1991.

[10] S. G. Ungar, "Testing basic access loops for service-affecting impulse noise," IEEE GLOBECOM '89.

[11] A. M. Curtis, "Contact phenomena in telephone switching circuits," B.S.T.J., Jan. 1940.

[12] P. Mertz, "Model of impulsive noise for data transmission," IRE Trans. Commun. Syst., Vol. COM-9, Jun. 1961.

[13] J. H. Fennick, "A report on some characteristics of impulse noise in telephone communication," IEEE Trans. Commun., Vol. 83, Nov. 1964.

[14] J. S. Engel, "Digital transmission in the presence of impulsive noise," B.S.T.J., Oct. 1965.

[15] K. Széchényi, "On the next and impulse noise properties of subscriber loops," IEEE GLOBECOM '89.

[16] J. J. Werner, "Impulse noise in the loop plant," IEEE ICC '90.

[17] J. H. Fennick, "Amplitude distributions of telephone channel noise and a model for impulse noise," B.S.T.J., Dec. 1969.

[18] J. W. Modestino, K. Y. Jung and K. R. Matis, "Modeling, analysis and simulation of receiver performance in impulsive noise," IEEE GLOBECOM '83.

[19] J. W. Modestino, R. E. Bollen and R. P. Prabhu, "Analytical model for evaluation of symbol error probability for digital transmission over the two-wire loop," IEEE GLOBECOM '84.

[20] J. W. Modestino, C. S. Massey, R. E. Bollen and R. P. Prabhu, "Modeling and analysis of error probability performance for digital transmission over the two-wire loop plant," IEEE J. Select. Areas Commun., Vol. SAC-4 No. 8, Nov. 1986.

[21] J. W. Modestino and M. V. Eyuboğlu, "Simulated performance of an adaptive multielement integrated receiver structure in impulse or burst noise," IEEE Trans. Commun., Vol. COM-35 No. 8, Aug. 1987.

[22] R. P. Prabhu, J. H. Drew and T. S. Wallent, "Subscriber loop noise measurements and calibration," IEE Proceedings, Vol. 134 Pt. F. No. 5, Aug. 1987.

[23] J. W. Modestino, D. H. Sargrad and R. E. Bollen, "Use of coding to combat impulse noise on digital subscriber loops," IEEE Trans, Commun., Vol. 36 No. 5, May 1988.

[24] D. H. Sargrad and J. W. Modestino, "Errors-and-erasures coding to combat impulse noise on digital subscriber loops," IEEE Trans. Commun., Vol. 38 No. 8, Aug. 1990.

[25] P. G. Potter and B. M. Smith, "Statistics of impulsive noise crosstalk in digital line systems on multipair cable," IEEE Trans. Commun., Vol. COM-33 No. 3, Mar. 1985.

[26] E. N. Gilbert, "Capacity of a burst-noise channel," B.S.T.J., Sept. 1960.

[27] A. A. Alexander, R. M. Gryb and D. W. Nast, "Capabilities of the telephone network for data transmission," B.S.T.J., May 1960.

[28] E. O. Elliott, "Estimates of error rates for codes on burst-noise channels," B.S.T.J., Sept. 1963.

[29] R. H. McCullough, "The binary regenerative channel," B.S.T.J., Oct. 1968.

[30] M. T. Chao, "Statistical properties of Gilbert's burst noise model," B.S.T.J., Oct. 1973.

[31] W. Turin, "Simulation of error sources in digital channels," IEEE J. Select. Areas Commun., Vol. 6 No. 1., Jan. 1988.

[32] K. Kumozaki, "Error correction performance in digital subscriber loop transmission systems," IEEE Trans. Commun., Vol. 39 No. 8, Aug. 1991.

[33] J. M. Berger and B. Mandelbrot, "A new model for error clustering in telephone circuits," IBM J. Res. & Dev., Vol.7, Jul. 1963.

[34] S. M. Sussman, "Analysis of the Pareto model for error statistics on telephone circuits," IEEE Trans. Commun. Syst., Vol. COM-11 No. 2, Jun. 1963.

[35] E. O. Elliott, "A model of the switched telephone network for data communications," B.S.T.J., Jan. 65.

[36] B. Mandelbrot, "Self-similar error clusters in communication systems and the concept of conditional stationarity," IEEE Trans. Commun. Technol., Vol. COM-13, Mar. 1965.

[37] R. M. Fano, "A theory of impulse noise in telephone networks," IEEE Trans. Commun., Vol. COM-25 No. 6, Jun. 1977.

[38] P. Mertz, "Statistics of hyperbolic error distributions in data transmission," IRE Trans. Commun. Syst., Dec. 1961.

[39] R. A. Wainwright, "On the potential advantage of a smearing-desmearing filter technique in overcoming impulse-noise problems in data systems," IRE Trans. Commun. Syst., Dec. 1961.

[40] W. R. Bennett and J. R. Davey, "Data Transmission," McGraw-Hill Book Company, 1965.

[41] G. F. M. Beenker, T. A. C. M. Claasen and P. J. Van Gerwen, "Design of smearing filters for data transmission systems," IEEE Trans. Commmun. Technol., Vol. COM-33 No. 9, Sept. 1985.

[42] U. L. Rhode and T. T. N. Bucher, "Communications Receivers Principles and Design," McGraw-Hill Book Company, 1988.

[43] K. J. Kerpez, "Forward error correction for asymmetric digital subscriber lines (ADSL)," IEEE GLOBECOM '91.

[44] A. M. Michelson and A. H. Levesque, "Error-Control Techniques for Digital Communication," J. Wiley & Sons, 1985.

[45] J. M. Geist and J. B. Cain, "Viterbi decoder performance in Gaussian noise and periodic erasure bursts," IEEE Trans. Commun., Vol. COM-28 No. 8, Aug. 1980.

[46] K. Sistanizadeh and K. J. Kerpez, "A comparison of passband and baseband transmission schemes for HDSL," IEEE J. Select. Areas Commun., Vol. 9 No. 6, Aug. 1991.

[47] G. Young and N. G. Cole, "Design issues for early high bit-rate digital subscriber lines," IEEE GLOBECOM '90.

[48] D. L. Favin, "The 6A Impulse Counter," Bell Lab. Rec., Mar. 1963.

[49] M. Kurland and D. A. Molony, "Observations on the effects of pulse noise in digital data transmission systems," IEEE Trans. Commun. Technol., Aug. 1967.

[50] L. Alles, K. Cuffling, R. Bertrand and R. Quintal, "Digital loop system performance prediction using an impulse noise database," IEEE GLOBECOM '89.

[51] R. G. Gallager, "Information theory and reliable communication," J. Wiley & Sons, 1968.

[52] M. E. Van Valkenburg, "Network analysis," Prentice-Hall Inc., 1974.

[53] J. S. Chow, J. C. Tu and J. M. Cioffi, "A discrete multitone transceiver system for HDSL applications," IEEE J. Select. Commun., Vol. 9 No. 6, Aug. 1991.

[54] I. Kalet and S. Shamai(Shitz), "On the capacity of a twisted-wire pair: Gaussian model," IEEE Trans. Commun., Vol. COM-38, No. 3, Mar. 1990.

[55] J. G. Proakis, "Digital communications," McGraw-Hill Book Company, 1983.